

UNIVERSITÄT
BAYREUTH

**Sororin and Separase -
An Unexpected Partnership of two Master Regulators
of Mitosis**

DISSERTATION

zur Erlangung des akademischen Grades
- Doktor der Naturwissenschaften (Dr. rer. nat.) -
an der Fakultät für Biologie, Chemie und Geowissenschaften
der Universität Bayreuth

vorgelegt von
Brigitte Neumann
aus Bremen

Bayreuth, 2023

Die vorliegende Arbeit wurde in der Zeit von November 2014 bis Oktober 2020 in Bayreuth am Lehrstuhl für Genetik unter Betreuung von Herrn Prof. Dr. Olaf Stemmann angefertigt.

Art der Dissertation: Monographie

Dissertation eingereicht am: 01.06.2023

Zulassung durch die Promotionskommission: 14.06.2024

Wissenschaftliches Kolloquium: 13.10.2023

Amtierender Dekan: Prof. Dr. Benedikt Westermann

Prüfungsausschuss:

Prof. Dr. Olaf Stemmann	(Gutachter/in)
Prof. Dr. Benedikt Westermann	(Gutachter/in)
Prof. Dr. Stefan Geimer	(Vorsitz)
Prof. Dr. Gerrit Begemann	

for Dad

Abbreviations	I
Abstract	III
Zusammenfassung	V
1 Introduction	1
1.1 The eukaryotic cell cycle – principles and control	1
1.2 Cell cycle regulation and mitotic entry	2
1.3 Mitosis	3
1.4 Cohesin – the mediator of sister chromatid cohesion	4
1.4.1 Cohesin’s basic architecture.....	5
1.4.2 Cohesin loading	8
1.4.3 Establishment of sister chromatid cohesion	9
1.4.4 Resolution of cohesion during mitosis	11
1.5 Separase – the master regulator of mitosis (architecture, functions and regulations)	13
1.5.1 Securin dependent regulation of Separase	16
1.5.2 Securin independent regulation of Separase	18
1.5.3 Non-canonical Separase functions.....	20
1.6 Meiosis	22
1.6.1 General aspects of meiotic divisions	22
1.6.2 Cohesion during meiosis	24
1.7 Aim of this work.....	25
2 Results	26
2.1. Identification of a new Separase interaction partner.....	26
2.1.1 The essential cohesion co-factor Sororin interacts with Separase <i>in vivo</i>	26
2.1.2 Sororin expression seems to assist Separase expression	29
2.1.3 Separase, Sororin and Cohesin form a heterotrimeric complex	29
2.1.4 Separase and Sororin interact in all cell cycle stages.....	31
2.1.5 Separase and Sororin interact during mitotic exit	33
2.2 Mapping Separase-Sororin interaction sites on either protein.....	35
2.2.1 Sororin interacts with all domains of Separase	35
2.2.2 Sororin’s N-terminus interacts with Separase	39
2.3 Functional characterization of the Separase-Sororin complex	41
2.3.1 Sororin re-inhibits active Separase <i>in vitro</i>	41
2.3.2 Separase re-inhibition is mediated by the N-terminus of Sororin	42
2.3.3 Sororin is not a universal inhibitor of Separase	43

2.4 Sororin’s ability to inhibit Separase is dependent on phosphorylation.....	46
2.4.1 Preventing Sororin’s phosphorylation <i>in vivo</i> has no effect on the Sororin-Separase interaction.....	46
2.4.2 Phosphorylation by mitotic kinases render Sororin unable to inhibit Separase <i>in vitro</i>	49
2.4.3 Phosphorylation of Sororin’s N-terminus has no impact on Sororin-Separase complex formation	50
3 Discussion	54
3.1 The Separase-Sororin interaction is likely not conserved in <i>Xenopus</i> and <i>Drosophila</i>	55
3.2 Separase interacts with its inhibitors in a mutually exclusive manner.....	56
3.3 Sororin interacts with Cohesin – independently of Pds5	57
3.4 Mapping Sororin interaction sites on Separase	58
3.5 Mapping Separase-interaction sites on Sororin	61
3.6 Sororin’s function is dependent on phosphorylation	62
3.7 CDK1-Cyclin B1 interacts with Sororin by utilizing a CLD	65
3.8 Separase-Sororin complex formation – a possible role in female meiosis?.....	66
4 Materials and Methods.....	68
4.1 Materials	68
4.1.1 Hard- and Software.....	68
4.1.2 Antibodies	68
4.1.3 Plasmids	70
4.1.4 Buffers and solutions.....	73
4.2 Microbiological techniques	76
4.2.1 <i>E. coli</i> strains and media.....	76
4.2.2 Cultivation of <i>E. coli</i>	77
4.2.3 Preparation of chemically competent <i>E. coli</i> cells	77
4.2.4 Transformation of chemically competent <i>E. coli</i>	77
4.3 Molecular biological techniques	78
4.3.1 Isolation of plasmid DNA from <i>E. coli</i>	78
4.3.2 DNA hydrolysis by restriction endonucleases	78
4.3.3 Dephosphorylation of DNA-fragments.....	79
4.3.4 Separation and analysis of DNA fragments by agarose gel electrophoresis.....	79
4.3.5 Gel extraction of DNA fragments.....	80
4.3.6 Polymerase chain reaction (PCR).....	80
4.3.7 Ligation of DNA fragments	81
4.3.8 DNA sequencing.....	82
4.3.9 Determination of mRNA, DNA and protein concentrations in solutions	82

4.4 Protein biochemical methods	82
4.4.1 SDS-Polyacrylamide gel electrophoresis (SDS-PAGE)	82
4.4.2 Immunoblotting (Western blot)	83
4.4.3 Coomassie staining	83
4.4.4 Protein expression in <i>E. coli</i>	83
4.4.5 Ni ²⁺ -NTA affinity purification of His ₆ -SUMO3-tagged proteins	84
4.4.6 Non-covalent coupling of antibodies to sepharose beads	85
4.4.7 Immunoprecipitation (IP)	85
4.4.8 Tandem affinity purification (TAP)	86
4.4.8 Preparation of protein-coupled NHS-activated sepharose	86
4.4.9 Testelution of antigen coupled NHS-activated sepharose	87
4.4.9 Affinity chromatography for antibody purification	87
4.4.10 Purification of active human Separase	88
4.4.11 Coupled <i>in vitro</i> transcription and translation (IVTT)	88
4.4.12 <i>in vitro</i> kinase assay	89
4.4.13 <i>in vitro</i> cleavage assay	89
4.5 Cell biological methods.....	90
4.5.1 Cell lines	90
4.5.2 Cultivation of mammalian cells	90
4.5.3 Cultivation of <i>Xenopus</i> and <i>Drosophila</i> cells	91
4.5.4 Storage of cells.....	91
4.5.5 Transfection of cultured cells.....	91
4.5.6 Synchronization of mammalian cells	92
4.5.7 Taxol-ZM-override	93
4.5.8 Quantitative analysis of cell cycle stages by flow cytometry	93
5 Supplement.....	95
6 References	105
7 Danksagung.....	127
8 (Eidesstattliche) Versicherungen und Erklärungen	128

Abbreviations

Δ	delta (marks deletion of mentioned section)
aa	amino acids
ABC-like	ATP binding cassette-like
Ac	active (Separase)
AFM	atomic force microscopy
APC/C	anaphase promoting complex/cyclosome
APD	active protease domain
AurB	Aurora B
BI	BI-2536 (Plk1 inhibitor)
BSA	bovine serum albumin
CD	caspase-like catalytic domain
CDK	cyclin dependent kinase
CIM	cyclin interaction motif
CLD	Cdc6-like domain
co-IP	co-immunoprecipitation
CV	column volume
D-box	destruction-box (motif)
DIC	differential interference contrast
DMEM	Dulbecco's modified Eagle Medium
Dmt	Dalmatian (hybrid protein - Sgo1 and Sororin - in <i>Drosophila</i>)
DMSO	Dimethyl sulfoxide
Dox	Doxycycline
DTT	Dithiothreitol
eGFP	enhanced green fluorescent protein
EM	electron microscopy
EV	empty vector
FL	full length
GFP	green fluorescent protein
h	(as prefix) human
hc	heavy chain
IgG	Immunoglobulin G
IP	immunoprecipitation
IPTG	Isopropyl β-d-1-thiogalactopyranoside
IVTT	<i>in vitro</i> transcription and translation
LB	lysogeny broth
LP2	lysis buffer
m	(as prefix) mouse
MTOC	microtubule-organizing centre
MWCO	molecular weight cut-off
NBD	nucleotide binding domain
NEBD	nuclear envelope breakdown
NES	nuclear export signal
NF	Nieuwkoop Faber
NHS	N-hydroxysuccinimide

Abbreviations

o/n	over night
PAGE	polyacrylamide gel electrophoresis
PBE	polar body extrusion
PCR	polymerase chain reaction
PD	protease dead
PEI	polyethylenimine
pHH3	phosphohistone H3
PI	propidium iodide
PIM	pimples (<i>Drosophila securin</i>)
PPD	pseudo-protease domain
pre-RC	pre-replicative Complex
PSCS	premature sister chromatid separation
rb	(as prefix) rabbit
RC	Roscovitine (CDK1-inhibitor)
RNAi	RNA interference
rpm	rounds per minute
RO	RO-3306 (CDK1-inhibitor)
RT	room temperature
SAC	spindle assembly checkpoint
SD	substrate-binding domain
SDS	sodium dodecyl sulfate
siRNA	small interfering RNA
SMC	structural maintenance of chromosomes
Sor	Sororin
SPD	Separase protease domain
SSE	<i>Drosophila</i> Separase
SUMO	small ubiquitin like modifier
TAP	tandem affinity purification
Tax	Taxol
TEV	tobacco etch virus
THR	three rows (second part of <i>Drosophila</i> Separase)
TM	transmembrane
TPR	tetratricopeptide repeat
WCE	whole cell extract
w/o	wash out
WT	wildtype
xS3	<i>Xenopus laevis</i> cells
ZM	ZM447439 (aurora kinase inhibitor)

Abstract

In order to accurately distribute a cell's genetic information to generate two genetically identical daughter cells the two copies of each chromosome must be held together from their generation in S-phase until their separation in anaphase. This so-called cohesion is mediated (Luo und Tong 2017) by a ring-shaped multi-protein complex called Cohesin, which encircles DNA and is composed of the three core-subunits Smc3, Smc1 and Scc1. Cohesin rings are removed from chromatin in a stepwise manner. First, Cohesin is removed from chromosome arms by the Wapl-dependent non-proteolytic prophase pathway signaling. Cohesin at centromeres is protected by the Wapl antagonists Sororin and Sgo1-PP2A, the latter keeping Sororin in a dephosphorylated "active" state, thereby preserving centromeric cohesion. Separase finally triggers sister chromatid separation by proteolytically cleaving Scc1 of centromeric Cohesin at the metaphase to anaphase transition. Separase becomes active only upon liberation from its (mutually exclusive) inhibitors Securin, Cdk1-cyclin B1 and Sgo2-Mad2. Apart from triggering all eukaryotic anaphases, Separase also regulates a variety of other processes: Separase inhibits residual Cdk1-cyclin B1 in late M-phase, chiefly contributes to centriole disengagement in early G1, and facilitates homology directed repair of DNA double strand breaks in G2-phase. Whether the timely execution of these diverse cellular functions requires interaction of Separase with yet additional binding partners remains unresolved.

In this study, Sororin was identified as an unexpected interactor of Separase and provide further insight, which domains of either protein mediate the interaction. Importantly, bacterially expressed Sororin specifically re-inhibits active Separase *in vitro*. The Separase-interacting, N-terminal part of Sororin is thereby necessary and sufficient for Separase inhibition. Moreover, cleavage of Scc1, its meiotic counterpart Rec8 and Separase auto-cleavage is more efficiently inhibited by Sororin than cleavage of other Separase substrates. Interestingly, phosphorylation of full-length (FL) Sororin by Aurora B (AurB) and Cdk1-Cyclin B1 (but not by Plk1) renders it unable to protect Scc1 from Separase *in vitro*. Phosphorylation of Sororin's N-terminus by corresponding kinases, however, has no such effect on re-inhibition of Separase, arguing for a more complex mode of inhibition, possibly by phosphorylation of Sororin's C-terminus. Sgo1-PP2A keeps centromeric Sororin dephosphorylated until the

former relocalizes to kinetochores. In view of this known mechanism, our findings suggest that Sororin might shield centromeric Cohesin in early mitosis not only from Wapl but also from prematurely activated Separase.

Zusammenfassung

Um die genetische Information einer Zelle exakt zu verteilen und zwei genetisch identische Tochterzellen zu erzeugen, müssen die beiden Kopien jedes Chromosoms von ihrer Entstehung in der S-Phase bis zu ihrer Trennung in der Anaphase zusammengehalten werden. Diese sogenannte Kohäsion wird durch den ringförmigen Multiproteinkomplex Cohesin vermittelt, der die DNA umschließt und aus den drei (Kern-)Untereinheiten Smc3, Smc1 und Scc1 besteht. Der Cohesin-Ring wird schrittweise vom Chromatin entfernt. Zunächst wird Cohesin von den Chromosomenarmen mit Hilfe des Wapl-abhängigen, nicht-proteolytischen Prophaseweges entfernt. Das Cohesin an den Zentromeren wird durch die Wapl-Antagonisten Sororin und Sgo1-PP2A geschützt, wobei letzteres Sororin in einem dephosphorylierten „aktiven“ Zustand hält, wodurch die zentromerische Cohesion erhalten bleibt. Separase löst schließlich die Schwesterchromatidentrennung aus, indem sie Scc1 des zentromerischen Cohesins am Metaphase-Anaphase Übergang proteolytisch spaltet. Separase wird erst nach Entfernung von ihren Inhibitoren Securin, Cdk1-Cyclin B1 und Sgo2-Mad2 aktiv. Diese Inhibitoren können nicht gleichzeitig mit Separase interagieren. Separase löst nicht nur alle eukaryotischen Anaphasen aus, das Enzym reguliert auch eine Reihe anderer Prozesse: Separase hemmt verbliebenes Cdk1-Cyclin B1 in der späten M-Phase, trägt maßgeblich zu Zentriolen-Trennung in der frühen G1-Phase bei und ermöglicht in der G2-Phase die Reparatur von DNA-Doppelstrangbrüchen durch homologe Rekombination. Inwieweit die rechtzeitige Ausführung dieser verschiedenen zellulären Funktionen die Interaktion von Separase mit weiteren Bindungspartnern erfordert, ist noch nicht vollständig geklärt.

In dieser Studie wurde Sororin als ein unerwarteter Interaktor von Separase identifiziert. Weiterhin werden Erkenntnisse darüber geliefert, welche Domänen beider Proteine die Interaktion vermitteln. Es wird gezeigt, dass bakteriell exprimiertes Sororin die aktive Separase *in vitro* spezifisch reinhibiert. Der Separase-interagierende, N-terminale Teil von Sororin ist dabei notwendig und hinreichend für die Separase-Inhibition. Darüber hinaus wird die Spaltung von Scc1, dem meiotischen Gegenstück Rec8 und die Separase-Selbstspaltung durch Sororin effizienter gehemmt als die Spaltung anderer Separase-Substrate. Interessanterweise führt die Phosphorylierung von Vollängen-Sororin durch AurB und Cdk1-Cyclin B1 (aber nicht durch Plk1) dazu, dass Sororin Scc1 *in vitro* nicht mehr vor Separase

beschützen kann. Die Phosphorylierung des N-Terminus von Sororin durch die entsprechenden Kinasen

hat jedoch keinen solchen Effekt auf die Inhibition von Separase, was für einen komplexeren Mechanismus der Inhibition spricht, der möglicherweise in Phosphorylierung des C-Terminus von Sororin besteht. Sgo1-PP2A hält zentromerisches Sororin in einem dephosphorylierten Zustand, bis ersteres zu den Kinetochoren relokalisiert wird. In Anbetracht dieses bekannten Mechanismus deuten die hier präsentierten Ergebnisse darauf hin, dass Sororin das zentromerische Cohesin in der frühen Mitose nicht nur vor Wapl, sondern auch vor vorzeitig aktivierter Separase schützen könnte.

1 Introduction

1.1 The eukaryotic cell cycle – principles and control

The series of highly regulated events that enable the reproduction of a eukaryotic cell is called the cell cycle. One of the most important functions of the cell cycle is to accurately duplicate a cell's genetic information and distribute it evenly between the two newly formed and thus genetically identical daughter cells. The cell cycle is divided into four main phases: in S ("synthesis")-phase DNA is replicated which results in duplication of the chromatids. In M-phase (M) the previously duplicated genetic information is evenly distributed between the two future daughter cells. Therefore, a nuclear division – mitosis – is followed by subsequent division of the cytoplasm (cytokinesis). S- phase and mitosis are often separated from each other by so called "gap"-phases in which, for example, protein biosynthesis and cell growth take place. The first gap-phase (G1) is arranged before S-phase, the second (G2) before mitosis. The period from the end of one mitosis to the beginning of the next, which includes the gap-phases and S-phase, is summarized as interphase (Fig. 1) (summarized in Morgan, 2007).

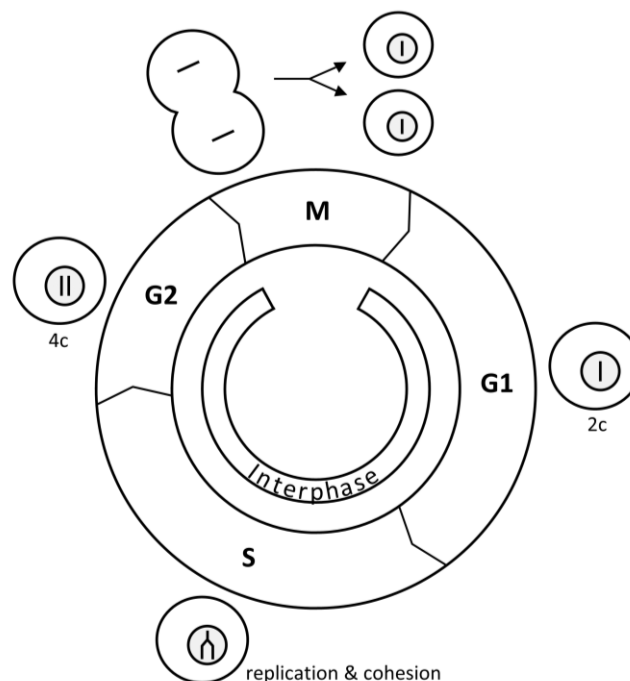


Figure 1 | The eukaryotic cell cycle. The period between two cell divisions, which generates two genetically identical daughter cells (M-phase, which) is also called interphase. In interphase the gap phases, G1 and G2, flank S-phase, where DNA is replicated. DNA replication results in duplication of a cell's DNA content (2c/4c: chromatid copy number, see text for details.)

1.2 Cell cycle regulation and mitotic entry

A complex network of regulatory proteins governs progression through the cell cycle phases to obtain genetically identical daughter cells. Several intermediate control points ensure this. Thus, a cell is only able to enter the next cell cycle phase when all necessary conditions, such as correct DNA replication or segregation, are fulfilled. These control points are tightly regulated mainly by phosphorylation and ubiquitin-dependent proteasomal degradation of specific proteins (summarized in Murray, 2004 and Morgan, 2007).

The central component of the cell cycle control system is the enzyme family of cyclin-dependent kinases (CDKs). CDKs are activated by binding to so-called cyclins and controlled by attachment of activating and inhibiting phosphorylation groups (Lindqvist et al., 2009, Murray et al., 2004). Different types of these cyclins are present in different cell cycle phases, some of them oscillate in their abundance due to periodic transcription and degradation. This leads to the phase-dependent formation of specific Cyclin-CDK complexes and, thus, corresponding phase-dependent CDK activities, which drive different cell cycle events (summarized in Murray, 2004 and Morgan, 2007).

Mitotic entry is driven by the CDK1-Cyclin B1 complex, also known as MPF (mitosis or maturation promoting factor) (Gautier et al., 1990; Lindqvist et al., 2009, Masui and Markert, 1971). Cyclin B1 levels are kept low in G1- and S-phase by the activity of the anaphase promoting complex/cyclosome (APC/C) in the previous M- and G1-phase. The APC/C is a ubiquitin E3 ligase, which labels Cyclin B1, among other substrates, for proteasomal degradation. Levels of Cyclin B1 rise at the end of S-phase after DNA replication is completed but CDK1 remains inactive due to the inhibitory phosphorylation of CDK1 by Wee1 kinase. The Cyclin B1-CDK1 complex is activated by dephosphorylation of CDK1 resulting in further CDK1-activation and thus CDK1-mediated inhibition of Wee1. This self-amplifying and switch-like feature allows an abrupt and irreversible entry into mitosis. Cyclin B1-CDK1 then triggers various mitotic events, such as chromosome condensation, nuclear envelope breakdown and mitotic spindle formation (Crasta et al., 2006; Heald and McKeon, 1990; Shintomi et al., 2015; Ward and Kirschner, 1990).

1.3 Mitosis

M-phase generates two genetically identical daughter cells originating from one mother cell and is generally subdivided into five different phases (Fig. 2). In prophase chromosomes start to condense to a more compact structure. At the same time, the paired centrosomes of each cell, consisting of two centrioles and duplicated in the previous S-phase, migrate to opposite poles of the cell and act as microtubule-organizing centers (MTOCs). This is the basis for the construction of a bipolar mitotic spindle by polymerization of microtubules, a highly dynamic polymer of α - and β -tubulin, emanating from each MTOC. Different types of microtubules ensure the correct positioning of the mitotic spindle in the cell. Astral microtubule fibers anchor the spindle poles to the cell cortex. Whereas both poles are connected by opposing and overlapping so-called interpolar microtubules that connect the two poles and interact with each other via motor proteins in an anti-parallel manner. This ensures bipolarity of the spindle. During late prophase, the construction of the spindle apparatus is accompanied by the disassembly of the nuclear membrane (nuclear envelope breakdown/NEBD). A subset of spindle fibers called kinetochore microtubules (or K-fibers) penetrate into the area of the former nucleus and interact with the kinetochores of the chromosomes, a large protein structure assembled onto the centromeric region of the DNA (Fukagawa and Earnshaw, 2014; Georgatos et al., 1997). In metaphase sister chromatids are now attached to the spindle apparatus and are arranged in the equatorial plate of the cell. Only if this step is performed correctly and all chromosomes are connected in a bipolar manner to the microtubules of the spindle (amphitelic attachment), the separation of sister chromatids can take place in the following anaphase (Fig. 2).

In case of incorrect attachment of chromosomes to the mitotic spindle the APC/C associated with its essential co-activator Cdc20 (APC/C^{Cdc20}) (Hwang et al., 1998) is inhibited by the spindle assembly checkpoint (SAC). This essential mitotic surveillance pathway senses improperly or unattached kinetochores to the mitotic spindle. Only after proper attachment of all chromosomes to the mitotic spindle is achieved, the APC/C^{Cdc20} is activated triggering mitotic exit (reviewed in Musacchio, 2015).

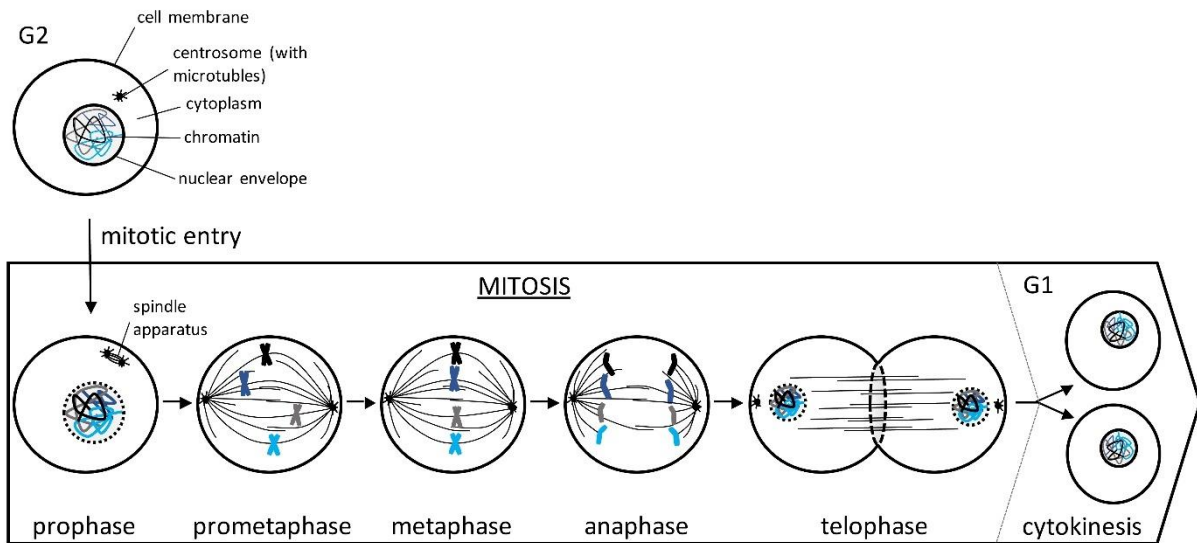


Figure 2 | The eukaryotic cell cycle. After G2-phase the cell enters mitosis, which is characterized by five intermediate steps. After mitotic exit and completion of cytokinesis, the cells enters G1-phase. See text for details.

By shortening of the microtubules attached to the kinetochore, the now separated sister chromatids are drawn to opposite poles of the cell. At the same time spindle poles are pushed further apart, mediated by the motor proteins on the interpolar microtubules. In the final phase of mitosis (telophase) the spindle apparatus disassembles, nuclear envelope reformation occurs and the chromosomes – each consisting of only one chromatid - decondense again and the nuclear division of the cell is completed. Mitosis is followed by division of the cytoplasm, which is called cytokinesis. This is mediated by a contractile ring of actin and myosin fibers, which constrict the cell locally between the two newly formed nuclei. Another set of proteins (ESCRT - endosomal sorting complexes required for transport) are recruited to and assist in fusion of opposite areas of the cell's plasma membrane (abscission) (Guizetti et al., 2011). The two genetically identical daughter cells can separate from each other, and the cell cycle can start anew (summarized in Morgan, 2007; Alberts et al., 2008, Fig. 2).

1.4 Cohesin – the mediator of sister chromatid cohesion

From the time of their generation in S-phase until their separation in anaphase, the sister chromatids of each chromosome must be held together. Only by physically linking sister

chromatids the correct division of DNA into the newly emerging daughter cells and the resulting genetic stability can be ensured. This physical connection is referred to as cohesion and is achieved by two events. One is the so-called catenation of DNA, which occurs naturally during replication and describes physical intertwinement of DNA. This catenation is largely removed until metaphase by the constitutively active enzyme topoisomerase II in conjunction with condensation (Sundin and Varshavsky, 1981; DiNardo et al., 1984; Koshland and Hartwell, 1987; Nasmyth and Haering, 2009). This has been demonstrated in yeast: here, replicated circular minichromosomes are still physically connected after topoisomerase II activity. Accordingly, an additional mechanism mediating cohesion besides catenation was proposed (Koshland and Hartwell, 1987). The current, widely accepted model regarding said second mechanism suggests that the multiprotein ring complex Cohesin holds sister chromatids together by topologically embracing both copies of each chromosome (Gruber et al., 2003).

1.4.1 Cohesin's basic architecture

Cohesin is a multimeric protein complex consisting of three core subunits. The two elongated SMC (structural maintenance of chromosomes) proteins – Smc1 and Smc3 – form 45 nm long, rod-shaped, anti-parallel and intramolecular coiled-coil structures by folding back onto themselves in their central “hinge” region (Fig. 3A). Both proteins strongly interact with each other via this hinge domain forming a V-shaped heterodimer (Anderson et al., 2002; Haering et al., 2002; Melby et al., 1998). The N- and C-termini (so-called head domains) of Smc1 and Smc3, respectively, form an ATP nucleotide binding domain (NBD). Interaction of Smc1 and Smc3 enables the association of both NBDs, leading to the formation of a globular, ABC-like ATPase domain with two asymmetric ATP interaction sites (Arumugam et al., 2003; Haering et al., 2002; Haering et al., 2004; Hopfner, 2016; Lammens et al., 2004). Upon binding of two ATP molecules to the walker box motif of one head and the ABC signature motif of the respective other head, both NBDs are firmly engaged. Consequently, a single head domain is not able to hydrolyze ATP independently but rather must do so by engaging with the opposing head domain (Hirano et al., 2001; Vasquez Nunez et al., 2019) (Fig. 3A). ATPase activity is thereby dependent on head engagement and interaction with DNA (Hirano et al., 2001; Lammens et al., 2004). The third Cohesin core subunit Scc1/Mdc1 (also known as Rad21), a protein of the α -Kleisin super-family, bridges the Smc NBDs (Haering et al., 2002; Haering et al., 2004;

Schleiffer et al., 2003). The N-terminal domain of Scc1 forms a four helix bundle and interacts with the coiled-coil emerging from the region of the NBD of Smc3 (its "neck"). The C-terminal domain of Scc1, with its winged helix interacts with the base of the Smc1 NBD, thus closing the tripartite ring (Fig. 3A) (Gligoris et al., 2014; Haering et al., 2004; Huis in't Veld et al., 2014). The fairly unstructured middle region of Scc1 provides a landing platform for a variety of regulatory proteins. One integral and peripheral associated protein is Scc3 in *Saccharomyces cerevisiae* and essential for Cohesin's structure and function (Haering et al., 2002; Orgil et al., 2015; Roig et al., 2014). Scc3 is expressed in two variants in somatic mammalian cells: SA1 and SA2 (Losada et al., 2000). An additional peripheral protein is Pds5 (Panizza et al., 2000). Depending on the cell cycle phase Pds5 mediates the interaction with the cohesion-regulatory proteins Eco1 (an acetyl transferase), Wapl or Sororin, respectively in a mutually exclusive manner (Boavida et al., 2021; Minamino et al., 2015; Nishiyama et al., 2010; Vaur et al., 2012)

According to the widely accepted "ring model" it is assumed that a single Cohesin molecule embraces sister chromatids in its lumen in a topological manner (hence the alternatively used term "embrace model") (Gruber et al., 2003; Haering et al., 2008). In line with this model, natural or artificial cleavage of Cohesin core subunits lead to precocious sister chromatid separation due to dissociation of Cohesin from chromatin (Gruber et al., 2003; Pauli et al., 2008; Uhlmann et al., 1999; 2000). Consistently, Cohesin associated with replicated small circular minichromosomes purified from yeast cells remain tightly bound. Cleavage of either the Cohesin ring or the entrapped circular DNA abolishes this association. Fusing Cohesin subunits chemically by crosslinking and thereby rendering Cohesin resistant against detachment of subunits *in vitro* additionally supports this model, since circular minichromosomes remain tightly bound to these artificially glued Cohesin molecules. Taken together, these experiments suggest a topological interaction of Cohesin and DNA (Ivanov and Nasmyth, 2005; 2007; Haering et al., 2008). Additionally, *in vitro* experiments using a purified Cohesin core complex from *Schizosaccharomyces pombe* and circular plasmid DNA demonstrated that Cohesin bound DNA in a topological fashion. This was achieved by adding the Cohesin loader (see below) to Cohesin and DNA (Murayama and Uhlmann, 2014). Furthermore, the Cohesin ring model suggests movement of the protein complexes along

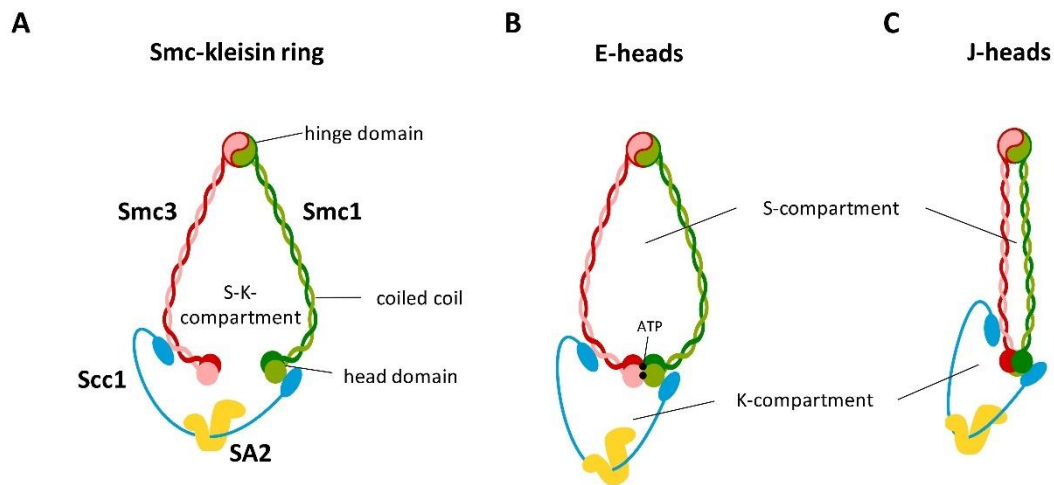


Figure 3 | Cohesin architecture. (A) Cohesins basic architecture with non-engaged head domains of the respective Cohesin subunits, forming the SK-compartment. (B) Upon ATP binding the Smc head domains engage (E-heads), whereas arms (coiled-coils) remain open and two compartments form: S (Smc) and K (kleisin). (C) In the absence of ATP rotation of the respective head domains occurs (juxtaposed/J-state), creating alternative S- and K-compartments with co-aligned arms. Modified from Chapard et al., 2019.

entrapped DNA, which can indeed be observed *in vivo* and *in vitro* (Davidson et al., 2016; Lengronne et al., 2004). Very recently, the current understanding of the ring model was enhanced using yeast and bacterial SMC complexes. Cohesin ring complexes consisting of the core subunits come in various shapes as visualized by electron microscopy (EM) and atomic force microscopy (AFM): V-shaped, O-shaped, bent and also complexes with a more rod-like closed structure are observed, suggesting a dynamic conformation of the holo-complex (Anderson et al., 2002; Hons et al., 2016; Huis in't Veld et al., 2014; Lee et al., 2020). Upon ATP binding, the SMC head domains are in an engaged configuration (E-state) with open arms of the respective proteins. This results in two compartments: one large SMC-ring (S-compartment) and a second ring between the engaged SMC-heads and the connecting kleisin (K-compartment) (Bürmann et al., 2019; Chapard et al., 2019; Collier et al., 2020; Fig. 3B). In the absence of ATP, the SMC head domains rotate into a different conformation, thereby adopting a juxtaposed state (J-state), creating alternative S- and K-compartments with co-aligned arms (Chapard et al., 2019; Collier et al., 2020; Diebold-Durand et al., 2017, Fig. 3C). The significance of these conformational changes is not yet completely understood. However, it was shown that different K-compartment configurations are able to entrap either single DNA

molecules (with the head domains in an E- or J-state) or sister DNAs (J-state) *in vitro* and *in vivo*, suggesting that the latter might be a feature of sister chromatid cohesion (Chapard et al., 2019; Diebold-Durand et al., 2017; Vasquez Nunez et al., 2019, Fig. 3).

1.4.2 Cohesin loading

In higher eukaryotes soluble Cohesin is loaded back onto single chromatids already in telophase using intact Cohesin complexes from earlier mitotic events. In yeast, however, reloading occurs later (late G1) because Cohesin is fully cleaved and Scc1 needs to be resynthesized (Ciosk et al., 2000; Sun et al., 2009; Waizenegger et al., 2000, see below). Although Cohesin can load onto DNA throughout the cell cycle, Cohesion is established in a co-replicative manner (Moldovan et al., 2006; Skibbens et al., 2009, Srinivasan et al., 2020; see below for details).

Cohesin loading onto chromatids is mediated by the Cohesin loading complex (also termed kollerin (Nasmyth, 2011)) consisting of the essential proteins Scc2 and Scc4 (NIPBL and Mau2 in humans) (Ciosk et al., 2000; Gillespie and Hirano, 2004; Michaelis et al., 1997; Tóth et al., 1999; reviewed in Wendt, 2017). The Scc2-Scc4 complex makes multiple *in vivo* contacts with Cohesin and Cohesin loading sites on centromeric DNA and promoters of actively transcribed genes (Kagey et al., 2010; Lopez-Serra et al., 2014; Petela et al., 2018). In order to load DNA into the Cohesin ring, the ring must be opened for DNA entrapment, which requires transient dissociation of one of Cohesin's interfaces. By artificially locking different interfaces of the core complex, it was previously proposed that DNA enters the ring through the hinge interface, formed by Smc1 and Smc3 (Buheitel and Stemmann, 2013; Gruber et al., 2006; Fig. 3). More recent data in fission yeast and bacteria – by analyzing corresponding cohesin-like proteins - challenge this view by suggesting that actual loading into the ring occurs by opening of the Scc1-Smc3 interface. This initial loading reaction is mediated by two events: first Scc2 of the kollerin complex transiently displaces Pds5 from Cohesin (Petela et al., 2017) and secondly by the conformational change of a dynamic coiled-coil discontinuity (so-called “elbows”) in each Smc- protein (Bürmann et al., 2019; Collier et al., 2020; Murayama and Uhlmann, 2015). Interaction of Scc2 and SA1/2 with both the hinge domain, as well as the coiled coil arms, induces bending of the elbows of each Smc subunit. This folding reaction exposes K105 and K106 of Smc3, serving as a DNA-sensor for the Cohesin ring. Upon contact between DNA with

the top of the ATPase, DNA passes through the Scc1-Smc3 interface (“kleisin gate”), which only opens upon head engagement due to ATP binding but not hydrolysis (Higashi et al., 2020; Murayama and Uhlmann, 2015; Petela et al., 2018). The kleisin gate is then sealed again after DNA entered the K-compartment. Closing of the kleisin gate thereby is achieved by a conformational change of the Scc2 subunit, which locks DNA against a shut Smc1-Smc3 interface (Higashi et al., 2020). Scc2 and the DNA-sensor bound to DNA ultimately stimulate ATP hydrolysis resulting in the disengagement of the NBDs of Smc1 and Smc3 (Arumugam et al., 2003; Murayama and Uhlmann, 2015; Petela et al., 2018; Weitzer et al., 2003). Head disengagement then releases DNA trapped in the K-compartment into the S-K compartment and DNA entry into the Cohesin ring is completed. (Diebold-Durand et al., 2017; Higashi et al., 2020; Murayama and Uhlmann, 2015). While Cohesin remains bound to chromosomes after loading, the kollerin complex dissociates from DNA and Pds5 replaces Scc2 again on Scc1 (Higashi et al., 2020; Hu et al., 2011; Kikuchi et al., 2016; Murayama and Uhlmann, 2015; Petela et al., 2017; Petela et al., 2018)

1.4.3 Establishment of sister chromatid cohesion

Cohesins association with DNA is highly dynamic until S-phase (see above) as the loading reaction is constantly counteracted by Wapl. This “releasing factor” interacts stoichiometrically with Cohesin via three conserved FGF-motifs. Whereas the middle and C-terminal motif interact with Scc1/SA2, the N-terminal FGF-motif interacts with Pds5 (Kueng et al., 2006; Ouyang et al., 2013; Shintomi and Hirano, 2009; Fig. 4A). Release of the Cohesin ring from DNA - independent of any proteolytic activity - is achieved by opening of the kleisin-gate and requires the interaction of Pds5 and Wapl. (Beckouët et al., 2016; Buheitel and Stemmann, 2013; Chan et al., 2012; Chatterjee et al., 2013; Gandhi et al., 2006; Gerlich et al., 2006; Hara et al., 2014; Higashi et al., 2020; Murayama and Uhlmann, 2015; Ouyang et al., 2013; Sutani et al., 2009). The Wapl-Pds5 dimer requires Cohesin in an ATP-bound state in order to open the ring and promote an outward trajectory of DNA, consistently it does not stimulate Cohesins ATPase activity (Elbatsh et al., 2016; Murayama and Uhlmann, 2015). As mentioned above ATP hydrolysis enables opening of the Smc1-Smc3 head-interface, which facilitates DNA to exit the S-compartment, into the K-compartment. Finally, Wapl bound to Pds5 opens the kleisin gate and DNA can exit the Cohesin ring (Murayama and Uhlmann, 2015; Beckouët

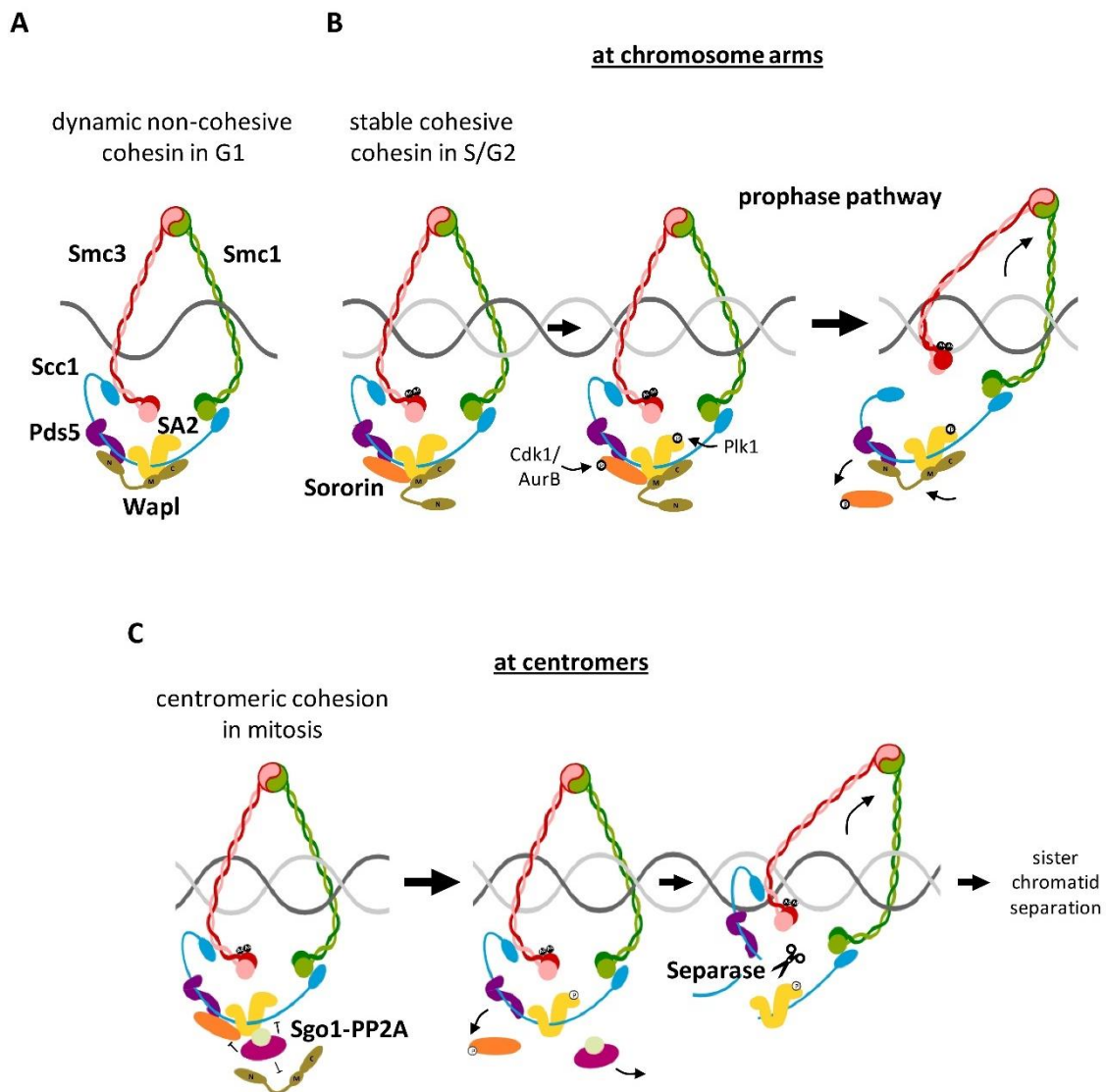


Figure 4 | Cohesin cycle in mammalian cells. (A) During telophase and G1 Cohesin's association with chromatin is highly dynamic due to Wapl's association with Pds5 and hence, release of Cohesin. (B) Acetylation of Smc3 during S-phase results in association of Sororin with Pds5 and subsequent displacement of Wapl from Pds5. This stabilizes Cohesin on chromatin and establishes cohesion. During prophase mitotic kinases, such as Cdk1, AurB (AurB) and Plk1 phosphorylate Sororin and SA2. Phosphorylation of Sororin leads to the displacement from Pds5. Wapl re-associates with Pds5 and displaces Cohesin from chromatin (the so-called prophase pathway). (C) at centromeres cohesion is protected against the prophase pathway by Sgo1-PP2A, which keeps Sororin in a dephosphorylated state and competes with SA2 for Wapl association. At the metaphase to anaphase transition Sgo1-PP2A relocates to kinetochores, which finally allows for active Separase to cleave Scc1 at centromeres and hence enable sister chromatid separation (inspired by Boavida et al., 2021; Hara et al., 2014; modified)

et al., 2016). However, the exact mechanism of this opening activity is not yet completely understood.

Stable cohesion of sister chromatids is established in a co-replicative manner. This is first established by acetylation of the two conserved DNA-sensor residues (K105/6) within Smc3's

NBD by the acetyltransferase Eco1 in S-phase (Ivanov et al., 2002; Minamino et al., 2015; Rolef Ben-Shahar et al., 2008; Rowland et al., 2009; Skibbens et al., 1999; Tóth et al., 1999; Unal et al., 2008; Zhang et al., 2008). In humans two isoforms are expressed, Esco 1 and Esco2 (Hou and Zou, 2005). It is currently believed that Esco1, which is expressed throughout the cell cycle, is ultimately responsible for cohesion establishment. This is supported by the notion that Pds5 and Esco1 directly interact, depending on an Esco1 specific domain. Furthermore, this interaction is essential for enzyme localization to Cohesin, suggesting that Esco1 is recruited to Cohesin by Pds5 in order to establish cohesion and displace Scc2 at the same time (Kikuchi et al., 2016; Minamino et al., 2015). The acetylation of Cohesin weakens DNA binding, blocks ATPase activity and is further associated with Cohesin ring complexes in the J-state, which are able to mediate the stable entrapment of sisters (Beckouët et al., 2016; Chapard et al., 2019; Heidinger-Pauli et al., 2010; Minamino et al., 2015). In yeast, the acetylation of Smc3 is sufficient to establish stable sister chromatid cohesion. In vertebrates, however, Cohesin association with DNA is additionally stabilized by the recruitment of Sororin through Pds5 to acetylated Cohesin (Ladurner et al., 2016; Lafont et al., 2010; Liu et al., 2013; Nishiyama et al., 2010; Nishiyama et al., 2013; Rankin et al., 2005; Schmitz et al., 2007). Sororin competes with Wapl for interaction with Pds5 via its own FGF motif. This results in Wapl's displacement from Pds5 (but not Cohesin). As a result, stable Cohesin-DNA interaction along chromosomes in post replicative cells is established, since ring opening and the subsequent release of DNA is prevented (Kuong et al., 2006; Liu et al., 2013; Nishiyama et al., 2010; Nishiyama et al., 2013; Schmitz et al., 2007; Fig. 4). So far Sororin has only been identified in metazoans, but it seems to be missing in yeast (Nishiyama et al., 2010; Rankin et al., 2005; Yang et al., 2019; Yamada et al., 2017). In the latter the acetylation of Smc3 is thought to be sufficient to prevent Wapl from ring opening (Beckouët et al., 2010; Beckouët et al., 2016; Camdere et al., 2015; Elbatsh et al., 2016).

1.4.4 Resolution of cohesion during mitosis

Upon entry into mitosis Cohesin in many eukaryotes is removed in a stepwise manner to ensure proper segregation of sisters. In the first step, which is also called the prophase pathway, the majority of Cohesin along chromosome arms is non-proteolytically released (reviewed in Morales and Losada; 2018; Sumara et al., 2000; Waizenegger et al., 2000; Fig. 4).

In order to accomplish this process, Wapl's association with Pds5 and, hence, its ring opening function has to be up regulated. This is achieved by the activity of mitotic kinases such as AurB, Cdk1 and Plk1, that phosphorylate SA2 and Sororin. The phosphorylation of SA2 by Plk1 is necessary for the removal of Cohesin, although not sufficient (Hauf et al., 2005). Once phosphorylated, Sororin loses its ability to interact with Pds5 and therefore can be replaced by Wapl, which then results in ring opening and the subsequent release of DNA (Gandhi et al., 2006; Hauf et al., 2005; Kueng et al., 2006; Liu et al., 2013, Nishiyama et al., 2013; Fig. 4B).

Cohesin at centromeres is protected against the prophase pathway in order to ensure sister chromatid cohesion until anaphase. Therefore, a protein complex comprising of Shugoshin 1 (Sgo1) and protein phosphatase 2A (PP2A) is recruited mainly to centromeres. To achieve this, Bub1 kinase first phosphorylates centromeric histone 2A (H2A), which creates the initial binding site for Sgo1 at kinetochores (Kawashima et al., 2010; Liu et al., 2013; Tang et al., 2004; Tang et al., 2006; Yamagishi et al., 2010). Upon entry into mitosis, Sgo1 is redirected from H2A to Cohesin at the inner centromere as a result of centromeric transcription and CDK1-dependent phosphorylation of Sgo1 at Thr346 (Zhang and Liu, 2020). Thereby, Sgo1 brings PP2A in close proximity to Cohesin. The Sgo1-PP2A complex constantly dephosphorylates SA2 and Sororin, thereby antagonizing the activity of mitotic kinases, and hence, prophase pathway (Hara et al., 2014; Kitajima et al., 2004; Kitajima et al., 2006 Liu et al., 2013; McGuinness et al., 2005; Shintomi and Hirano, 2009; Riedel et al., 2006; Fig. 4C). Consistently, the knockdown of endogenous Sororin or Sgo1 leads to premature sister chromatid separation in mitosis (McGuinness et al., 2005; Nishiyama et al., 2010; Schmitz et al., 2007; Tang et al., 2004). Furthermore, the Sgo1 interaction with the Cohesin subunit SA2 prevents Wapl from interaction with SA2 and Scc1, thereby adding another layer of protection to centromeric cohesion (Hara et al., 2014; Fig. 4). When cells reach metaphase and bi-oriented sister kinetochores are under tension, Sgo1 is removed from centromeres and localizes back to kinetochores (Liu et al., 2013). Upon tension at the metaphase to anaphase transition Sgo1 dissociates from centromeres in a Bub1 dependent manner. This detachment triggers the dissociation of AurB from centromeres, thereby stabilizing biorientation (Llano et al., 2008; McGuinness et al., 2005; Nerusheva et al., 2014).

Sister chromatid separation is completed at the metaphase to anaphase transition, once the large cysteine protease Separase is activated by the APC/C^{Cdc20}. Separase proteolytically

removes residual (peri)centromeric Cohesin by cleavage of the Scc1 subunit. This irreversible molecular process finally triggers anaphase and, hence, chromosome segregation (Uhlmann et al., 1999; Fig. 4C).

1.5 Separase – the master regulator of mitosis (architecture, functions and regulations)

Separase is a large (140-250 kDa, depending on the organism) and essential Cys-endopeptidase that acts as the universal trigger of all eukaryotic anaphases. Human Separase is one of the largest representatives, consisting of 2120 amino acids (aa) and a molecular mass of 233 kDa (Uhlmann et al., 1999; Uhlmann et al., 2000; Wirth et al., 2006). Separase homologs from in different species vary significantly in length and sequence. However, due to their well conserved C-terminal catalytic domain, which is very similar to caspases and gingipains, Separase's belong to the CD clan of cysteine peptidases (Nasmyth, 2002; Uhlmann et al., 2000; Winter et al., 2015). Consistently highly conserved cysteine and histidine residues were shown to form the catalytic dyad (His2003 and Cys2029 in human Separase) and are, hence, an essential part of Separase's active site and, secondly, essential for the enzyme's proteolytic activity. Substrate recognition is further ensured by several conserved residues in this domain (Luo and Tong, 2021; Uhlmann et al., 2000; Winter et al., 2015).

A detailed crystal structure of Separase in complex with Securin was first resolved using a smaller part of Separase from the thermophilic fungus *Chaetomium thermophilum* (Lin et al., 2016). Recently the structure of full length *Caenorhabditis elegans* (*C. elegans*) Separase in complex with Securin was determined at near-atomic resolution (3.8-Å) using single-particle cryo-electron microscopy (EM) confirming Separase's previously demonstrated triangular-shaped and bilobed architecture (Boland et al., 2017; Viadiu et al., 2005). Separase harbors a large N-terminal tetratricopeptide repeat (TPR)-like α -solenoid domain, comprising of a bundle of α -helices, which docks onto the well conserved C-terminal protease domain (Boland et al., 2017, Luo and Tong, 2017; Viadiu et al., 2005; Winter et al., 2015). However, these TPR-repeats are missing in yeast Separase (Luo and Tong, 2017).

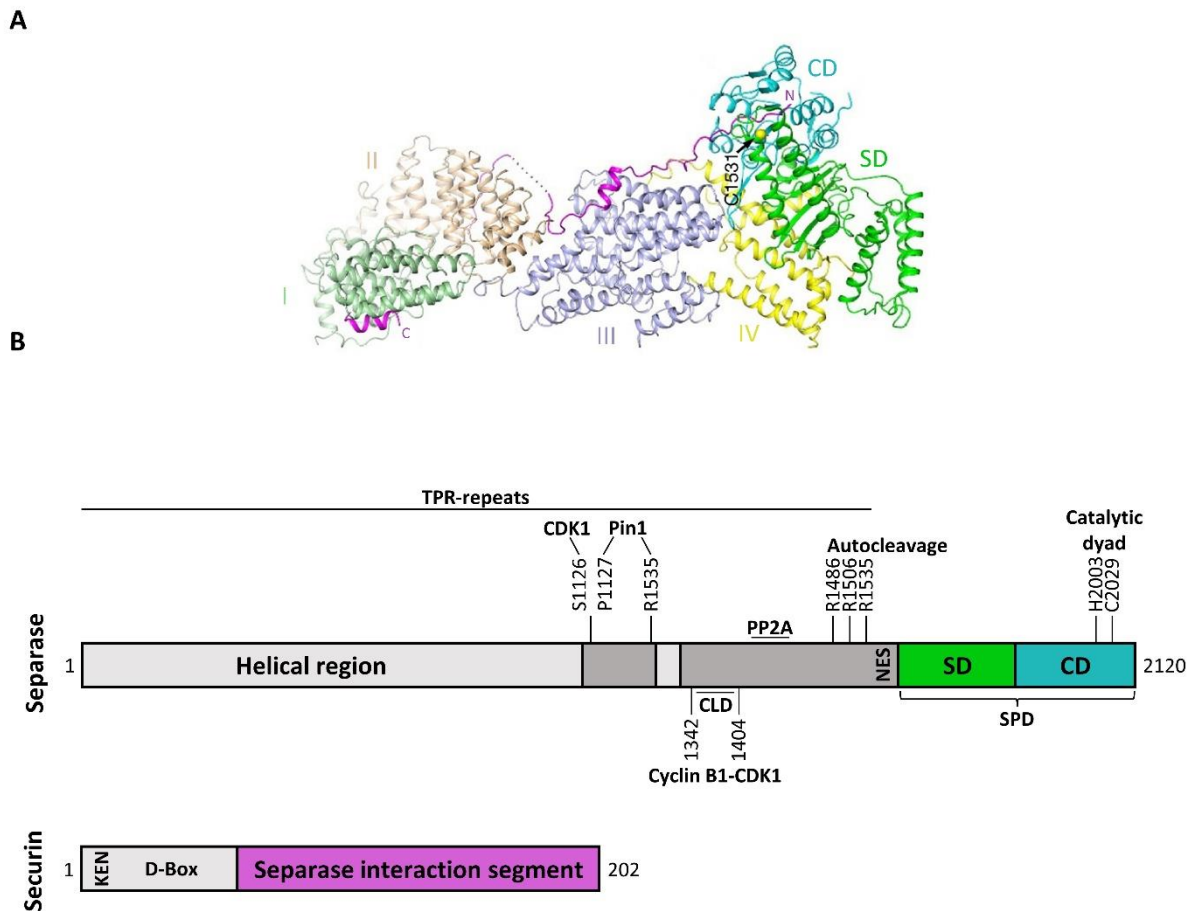


Figure 5 | Architecture of mammalian Separase. (A) Crystal structure of the Separase-Securin complex of *S. cerevisiae* (modified from Luo and Tong, 2017, used with permission by Springer nature). (B) Overview of the domain organization of human Separase and Securin, respectively. Important regulatory motifs are highlighted (TPR: tetratricopeptide repeat; CLD: Cyclin B1 interacting Cdc6-like domain, NES: nuclear export signal, SD: substrate-binding domain; CD: catalytic domain; modified from Luo and Tong, 2021). See text for details.

Both main domains of Separase are separated by a clearly defined cleft at their interface containing a nuclear export sequence (NES). Moreover, the α -solenoid domain contains two intrinsically disordered insertions that project towards Separase's catalytic site and possess important modification and protein interaction motifs for regulation of the protease (see below, Fig. 5). The N-terminal region is the most poorly conserved. Hence, a detailed structure of this region is not available for the human protein. However, human Separase is most likely composed in a similar fashion as demonstrated for *C. elegans* and *S. cerevisiae* (Boland et al., 2017; Luo and Tong, 2018; Rosen et al., 2019).

The C-terminal protease domain of Separase can be subdivided into a caspase-like catalytic domain (CD, aa1935-2120) containing the catalytic dyad and a substrate-binding domain (SD, aa1622-1934). The CD and SD are also referred to as the active protease domain (APD, aa1891-

2120) and the pseudo-protease domain (PPD, aa1755-1890), respectively (In the following work the abbreviations CD and SD will be used for APD and PPD). Together they are also named the Separase protease domain (SPD) (Lin et al., 2016; Luo and Tong, 2018; Fig. 5). The SPD of Separase is covered by additional β -strands provided by the α -solenoid domain, which are thought to further stabilize the SPD and therefore assist in mediating the protease activity of Separase by also contributing to substrate binding (Lin et al., 2016; Luo and Tong, 2018).

Caspases are typically expressed as inactive pro-enzymes and possess a nearly identical substrate binding groove, which is shaped by four surrounding loops (L1-L4). In order to get activated, the critical loop L4 needs to reorganize by either homo-dimerization or cleavage of an internal linker or both (Chai et al., 2001; Lin et al., 2016; reviewed in Shi, 2002). The CD of Separase has a very similar fold to caspases and also contains an L4, whose conformation is structurally similar to those in active caspase 9, even when in complex with its main inhibitor Securin (Boland et al., 2017; Uhlmann et al., 1999; Lin et al., 2016). Consistently, once the interaction of the Separase-Securin complex is resolved by APC/C dependent degradation of Securin's N-terminal KEN/D-boxes and degraded by the proteasome, no further processing of Separase is needed in order for the protease to become an active enzyme (Ciosk et al., 1998; Cohen-Fix et al., 1996; Funabiki et al., 1996; Kumada et al., 1998; Uhlmann et al., 1999; Zou et al., 1999). The association of Separase and Securin, as well as the inhibition of Separase by Securin is conserved in all eukaryotes studied so far in this respect, including fungi, plants and animals (Cromer et al., 2019; Funabiki et al., 1996; Yamamoto et al., 1996; Zou et al., 1999).

Separase cleaves its substrates after the arginine residue (P1) of the consensus motif (S/D)xExxR (x, any residue) (Hauf et al., 2001; Lin et al., 2016; Uhlmann et al., 1999; Stemmann et al., 2001; Sullivan et al., 2004). Scc1 contains eight respective motifs, cleavage of two of them results in the metaphase to anaphase transition, which ultimately triggers mitotic exit (Hauf et al., 2001). Importantly, the central disordered region of human Separase contains four ExxR sites, three of which (at position 1486, 1506 and 1535) are cleaved by Separase itself upon activation of the enzyme (Waizenegger et al., 2002; Zou et al., 2002). After auto-cleavage, the respective fragments remain associated. Furthermore, the CD of Separase remains intact and no apparent loss of proteolytic activity is detectable upon auto-cleavage (Waizenegger et al., 2002; Zou et al., 2002). Auto-cleavage of Separase is important for mitotic progression and

interaction with additional accessory proteins (Holland et al., 2007; Papi et al., 2005; Waizenegger et al., 2002).

1.5.1 Securin dependent regulation of Separase

Since premature separation of sisters is fatal for genome stability, anaphase must be induced with the right timing (Kops et al., 2005). Therefore, the potentially dangerous Separase needs to be kept inactive throughout most of the cell cycle, which is achieved by a variety of tightly regulated mechanisms. First of all, Separase is largely excluded from the nucleus, during interphase in mammals and, thus, Cohesin is spatially separated from Separase (Holland and Taylor, 2006; Sun et al., 2006). Due to the enzyme's large physical mass, Separase is unable to pass the nuclear envelope. However, even if a small amount of Separase is retained in the nuclear space after nuclear envelope reassembly in telophase, a nuclear export sequence (NES) further ensures the active Crm1/exportin-mediated transport out of the nucleus (Stade et al., 1997; Sun et al., 2006).

Most importantly, the activation of Separase is regulated by the tightly controlled APC/C-dependent proteolysis of Separase's main inhibitor Securin. Orthologs of Securin are poorly conserved across species and were identified based on their conserved function as a Separase inhibitor and presence of at least one destruction (D)-box motif in the coding sequence. Thereby, making Securin an APC/C^{Cdc20} substrate, rather than by sequence homology (Jäger et al. 2001; Kitagawa et al., 2002; Leismann et al., 2000; Zou et al., 1999).

Interestingly, Securin inhibits Separase by utilizing a non-cleavable pseudo-substrate cleavage site. Substrate binding is blocked due to the bound Securin segment to Separase's active site. In the peptide sequence of Securin the arginine at P1 is missing and replaced by a hydrophobic residue, which makes it incompatible with catalysis. Creating a consensus motif for Separase cleavage by mutating said proline residue to an arginine residue consistently transforms Securin into a Separase substrate. This demonstrates that Securin acts as a pseudo-substrate, which inhibits Separase competitively and is not cleaved under normal conditions (Boland et al., 2017; Lin et al., 2016; Nagao and Yanagida, 2006; Waizenegger et al., 2002). Securin, a mostly intrinsically disordered protein, binds Separase in an anti-parallel fashion along the entire length of the protease, thereby interacting with all domains (Boland et al., 2017; Csizmok et al., 2008; Holland et al., 2007; Jäger et al., 2004; Luo and Tong, 2018; Viadiu et al.,

2005, Fig. 5). Interestingly, Securin has not only an inhibitory but also an activating effect on Separase. For instance, Securin is essential in *S. pombe* and *D. melanogaster*. Depleting Securin in those organisms results in the same phenotype as the depletion of Separase, i.e., the inability to separate sister chromatids and defective chromosome disjunction (Funabiki et al., 1996; Pflieger et al., 2005; Stratmann and Lehner, 1996). In contrast, Securin is not essential in budding yeast and mammals (including human cell lines). Its deletion does not cause any drastic effect, i.e., cells do neither suffer from non-disjunction, nor from premature separation of sisters. Deletion of Securin rather reduces the overall amount of a cell's Separase pool and the activity of the enzyme present (Alexandru et al., 1999; Hellmuth et al., 2015a; Jallepalli et al., 2001; Mei et al., 2001; Pflieger et al., 2005; Yamamoto et al., 1996; Wang et al., 2001). The association of Securin with Separase occurs in a co-translational manner, which serves two main purposes: the interaction with Separase, as the enzyme is being translated (nascent Separase). This not only assists proper folding and thereby solubility of the protease, but also ensures its immediate co-translational inhibition, making Securin an unconventional "chaperone" of Separase (Hellmuth et al., 2015a; Hornig et al., 2002). Consistently, depletion of endogenous Securin results in the aggregation/misfolding of Separase, as judged by precipitation assays in respectively treated human cells (Hellmuth et al., 2015a). In addition, overexpression of Separase also leads to aggregation/misfolding of the enzyme, determined by the same assay, if the amount of produced Separase exceeds the amount of Securin present. The aggregation of excess Separase can be repressed by simultaneous overexpression of Securin further confirming Securin's positive effect on Separase (Hellmuth et al., 2015a).

Once established, the Separase-Securin complex is additionally regulated by association of PP2A with a conserved motif of Separase (Hellmuth et al., 2014; Hertz et al., 2016; Holland et al., 2007; Fig. 5). The pool of Securin not bound to Separase is phosphorylated, boosting its efficient APC/C-dependent degradation. Securin associated with Separase, on the other hand, is kept in a dephosphorylated state, due to the simultaneous interaction with PP2A, which stabilizes the Separase-Securin complex by delaying APC/C-mediated degradation of Securin (Gil-Bernabé et al., 2006; Hellmuth et al., 2014; Holland et al., 2007). This mechanism ensures rapid and timely Separase-activation and, thus, abrupt segregation of sisters at the metaphase

to anaphase transition. As a result, Separase is activated only when most free Securin has already been destroyed (Hellmuth et al., 2014).

1.5.2 Securin independent regulation of Separase

Since Securin deficient cells are viable and undergo a largely normal anaphase without significant defects in chromosome segregation, there is reason to suspect an additional way of Separase regulation (Pfleghaar et al., 2005). Indeed, using *Xenopus* egg extracts, CDK1-CyclinB1 was identified to be a Securin-independent interactor and inhibitor of Separase (Gorr et al., 2005). This inhibition depends on the essential phosphorylation of Separase on Ser1126 (in humans) and additional residues (Thr1346/Ser1399) within a Cdc6-like domain (CLD, aa1340-1400) by CDK1-CyclinB1 (Boos et al., 2008; Gorr et al., 2005). The phosphorylation of Ser1153 results in the recruitment of the peptidyl-prolyl *cis-trans* isomerase Pin1 to Separase (Hellmuth et al., 2015b). Pin1 then catalyzes Separase's isomerization at the phosphorylated Ser1126-Pro1127 peptide bond. This induces a conformational change of Separase (most likely *trans* to *cis*), which in turn enables the stable interaction of CDK1-CyclinB1 (via Cyclin B1) with the CLD of Separase. This CDK1-CyclinB1 interaction has, similar to Securin, a stabilizing effect on Separase. However, association of Securin and CDK1-CyclinB1 with Separase, is mutually exclusive (Boos et al., 2008; Gorr et al., 2005; Hellmuth et al., 2015b). Whereby Securin exclusively binds to the *trans* conformer of Separase, CDK1-CyclinB1 exclusively binds to the *cis* conformer (Hellmuth et al., 2015b). This exclusive interaction pattern (dependent on Pin1-mediated isomerization) also ensures that Separase, liberated from Securin due to APC/C^{Cdc20} dependent degradation, cannot be re-inhibited by residual free Securin (Hellmuth et al., 2014; see above). Here, CDK1-CyclinB1 is able to take over and interact with Separase as well as inhibit the protease (Hellmuth et al., 2015a). But since CyclinB1 is phosphorylated, and therefore rapidly degraded by the APC/C^{Cdc20}, Separase is active and cleaves Cohesin (Hagting et al., 2002; King et al., 1995; Stemmann et al., 2001).

Once the majority of CyclinB1 is degraded and Scc1 is cleaved, the remaining pool of CyclinB1 is sufficiently dephosphorylated by phosphatase activity. At this time Separase interaction with the remaining CDK1-CyclinB1 complex peaks again (Hellmuth et al., 2015b; Shindo et al., 2012; Toyoshima-Morimoto et al., 2001). This so-called "second wave" of CDK1-CyclinB1-Separase complex formation, at a time when the overall level of CyclinB1 is already very low,

results in residual active Separase inhibition (and interestingly also *vice versa* (Gorr et al., 2005)). Association of CDK1-Cyclin B1 with Securin-resistant Separase in late mitosis probably serves multiple purposes. For one the *cis* conformer of Separase is aggregation prone, which results in inactivation of the enzyme. Therefore, interaction with CDK1-CyclinB1 stabilizes the protease, possibly until early G1-phase, where Separase's proteolytic activity is required for centriole disengagement (Tsou and Stearns, 2006; Tsou et al., 2009; Nakamura et al., 2009; Schöckel et al., 2011, Hellmuth et al., 2015). Centriole disengagement is essential for centriole duplication later in the cell cycle, ensuring the formation of a bipolar mitotic spindle and hence, ensuring genomic stability (reviewed in Agircan et al., 2014). By degradation of the remaining CyclinB1 in the CDK1-CyclinB1-Separase complex, active Separase once again would be liberated for a brief pulse of activity. This in turn allows cleavage of centrosomal Cohesin and Pericentrin-B, which is promoting centriole disengagement (Hellmuth et al., 2015; Kahlen and Stemmann, unpublished data; Lee and Rhee, 2012; Matsuo et al., 2012; Schöckel et al., 2011). At that time, the nuclear envelope already reassembled, thereby protecting newly loaded Cohesin on DNA.

This mutually exclusive but dual inhibition mechanism by Securin and CDK1-cyclinB1 limits Separase's proteolytic activity to ensure proper regulation of late mitotic events (Hellmuth et al., 2014; Hellmuth et al., 2015b; Shindo et al., 2012).

As already mentioned above mammalian cells lacking Securin (*Securin*^{-/-}) are viable, which can be partially explained by the regulation of Separase by CDK1-cyclin B1 (Gorr et al., 2005; Jallepalli et al., 2001). Additionally, mice with a heterozygous knock-in of a CDK1-CyclinB1 resistant Separase allele (*Separase*^{+/S1121A}) or both defects combined (*Securin*^{-/-} *Separase*^{+/S1121A}) lead to embryonic lethality (Huang et al., 2008). Embryonic stem cells of *Securin*^{-/-} *Separase*^{+/S1121A} mice, however, appear relatively normal, suggesting yet another possible mechanism in Separase regulation (Mei et al., 2001; Wang et al., 2001). Additionally, mouse embryos lacking the SAC component and APC/C co-activator Cdc20 (*Cdc20*^{-/-}) arrest in mitosis. These cells are not able to degrade either Securin or Cdk1-Cyclin B1, therefore Separase cannot be activated, even if all chromosomes are properly aligned and the SAC is satisfied. Interestingly embryos of *Securin*^{-/-} *Cdc20*^{-/-} double knockout mice arrest in metaphase as well but with scattered chromosomes, suggesting that separation of sisters can

occur in these cells (Li et al., 2007). The loss of sister chromatid cohesion is rescued upon SAC activation by treatment with nocodazole (Li et al., 2007). These results initially lead to the speculation of a putative Separase inhibitor that is dependent on the SAC but independent of Securin. In that context it was previously shown that Sgo2, a protein with to this point no known essential function in mammalian mitosis, interacts with the SAC component Mad2 in a Cdc20-like manner (Lee et al., 2008; Llano et al., 2008; Orth et al., 2011). Surprisingly, a specific Separase-Sgo2-Mad2 interaction could be demonstrated by co-immunoprecipitation (co-IP) experiments in mammalian cells, alongside the known interaction partners Securin and CDK1-cyclin B1 (Gorr et al., 2005; Hellmuth et al., 2020). Re-inhibition assays of *in vitro* activated human Separase also showed, that Sgo2-Mad2 not only serves as a new interaction partner of Separase but is also able to block the enzymes activity (Hellmuth et al., 2020). Further experiments demonstrated that all three inhibitors interact with Separase in a mutually exclusive manner, thereby adding a previously unknown and APC/C^{Cdc20}-independent branch of Separase regulation (Hellmuth et al., 2020). Taken together: while Separase-Securin and Separase-CDK1-Cyclin B1 complexes rely on APC/C-mediated degradation of the inhibitor, the removal of Sgo2-Mad2 occurs independently of APC/C. It happens through the disassembly of the Separase-Sgo2-Mad2 complex, which is facilitated by the AAA+ ATPase TRIP13 and the co-factor p31Comet (Hellmuth et al., 2020).

1.5.3 Non-canonical Separase functions

The canonical function – as outlined above – is cleavage of Cohesin. One non-canonical function – centriole disengagement - has already been mentioned above. Beyond its essential role in regulating mitosis (and meiosis, see below) by Cohesin cleavage, Separase is required for several additional mechanisms.

In *C. elegans* for example, it was demonstrated that Separase regulates the trafficking of vesicles (in meiosis and mitosis), which might be important for cytokinesis (Bai and Bembenek, 2017; Bembenek et al., 2007; Bembenek et al., 2010). In that context, polar body extrusion (PBE) at the end of female meiosis I (PBE I) is compromised, causing female sterility, if Separase is deleted specifically in mouse oocytes (Gorr et al., 2006; Kudo et al., 2006). However, PBE I can be restored upon injection of mRNA encoding wildtype Separase and interestingly, also

by mRNA encoding catalytically inactive Separase, possibly because inhibition of CDK1 is needed for PBEI, rather than Separase activity (Gorr, et al., 2006; Kudo et al., 2006).

A rather widespread role for Separase was described in yeast cells, where Separase was identified as a Ty1 integrase- interaction partner and may be required for Ty1 element retrotransposition into the genome (Ho et al., 2015). In *Drosophila* as well as human fibroblasts, Separase might be important for telomere fusion, possibly by capping telomeres (Cipressa et al., 2016). Furthermore, in early *C. elegans* embryos reduced APC/C^{Cdc20} and hence, reduced Separase activity, disrupts the asymmetric localization of the mitotic spindle, which is important for unequal cytokinesis and anterior-posterior axis formation (Rappleye et al., 2002).

A role for Separase aside from mitosis/meiosis was recently demonstrated for interphase. A common initial cause of cancer is DNA damage, often inflicted by DNA double-strand breaks (DSBs). In order to protect the genomic integrity, cells trigger a DNA damage response to mediate a checkpoint-dependent cell cycle arrest. If attempts to repair DSBs fail, cells will ultimately induce apoptosis (reviewed in Ciccia and Elledge, 2010). In yeast and in human cells it was previously shown that Cohesin is enriched at DNA is upon DNA damage, especially in the vicinity of DSBs. This *de-novo* loading of Cohesin in a replication-independent manner is required for efficient DNA damage repair (Kim et al., 2002; Ström et al., 2004; Ström et al., 2007; Unal et al., 2004; Unal et al., 2007). Consistently, if the synthesis of Scc1 was inhibited, the recruitment of Cohesin DSBs decreased. This observation coincided with the increase in abundance of Scc1 cleavage fragments, suggesting a correlation between the two events. Also, DSB repair efficiency decreased upon expression of a Separase-resistant Scc1-allele (Nagao et al., 2004; McAleenan et al., 2013). Taken together these observations suggested a role of Separase in the DNA damage response in interphase. In fact, it was recently demonstrated, that mammalian Separase is recruited to DSBs in post replicative cells, where the enzyme is activated to locally cleave Scc1 (Hellmuth et al., 2018). Cohesin cleavage, thereby enables DNA damage repair (Hellmuth et al., 2018).

Finally, a new role for Separase recently emerged in regulating the apoptotic machinery: If a cell enters mitosis with prematurely activated Separase, anti-apoptotic factors become

Separase substrates upon phosphorylation by Nek2A, a kinase that is only active very early in mitosis and already degraded by the APC/C^{Cdc20} in prometaphase. Upon phosphorylation by Nek2A, corresponding substrates are then cleaved by the protease (Boekhout and Wolthuis; 2015; Hayes et al., 2006; Hellmuth and Stemmann, 2020). Cleavage of these anti-apoptotic factors by Separase early in mitosis converts the respective fragments into pro-apoptotic factors, thereby initiating cell death and hence, eliminating cells that lost the integrity of the SAC (Hellmuth and Stemmann, 2020).

1.6 Meiosis

Eukaryotic sexual reproduction is considered to be an important driver of evolution since it increases genetic diversity and therefore facilitates the development of complex life. The ploidy of any organism must be kept constant to avoid a doubling of the chromosome content in each subsequent generation. Therefore, a reduction of the number of chromosomes is required during the development of germ cells. This reduction takes place during the generation of haploid gametes (i.e., sperm cells and oocytes) – from a diploid precursor cell - in the process of meiosis.

1.6.1 General aspects of meiotic divisions

During meiosis, one round of DNA replication is followed by two consecutive rounds of chromosome segregation and cell division, without an intervening S-phase: meiosis I and II. (Fig. 6). During the first meiotic reductional division (meiosis I) homologous chromosomes, each consisting of two sisters, pair and become physically linked by chiasmata (reviewed in Morgan, 2007). In anaphase I, in stark contrast to mitosis, homologs rather than sisters are separated. Since sister chromatids are still held together, a second meiotic division resembling mitotic divisions must occur. This “equatorial division” is called meiosis II. Sister chromatids bi-orient during meiosis II, are separated from each other and distributed into two newly forming daughter cells. Thus, four haploid germ cells are generated (summarized in Morgan, 2007; Fig. 6). There are, however, significant differences in male and female meiosis in mammalian cells. Whereas male meiosis (spermatogenesis) is symmetrical and generates four haploid sperm cells in a continuous process throughout the entire life span, female meiosis (oogenesis) is highly asymmetric.

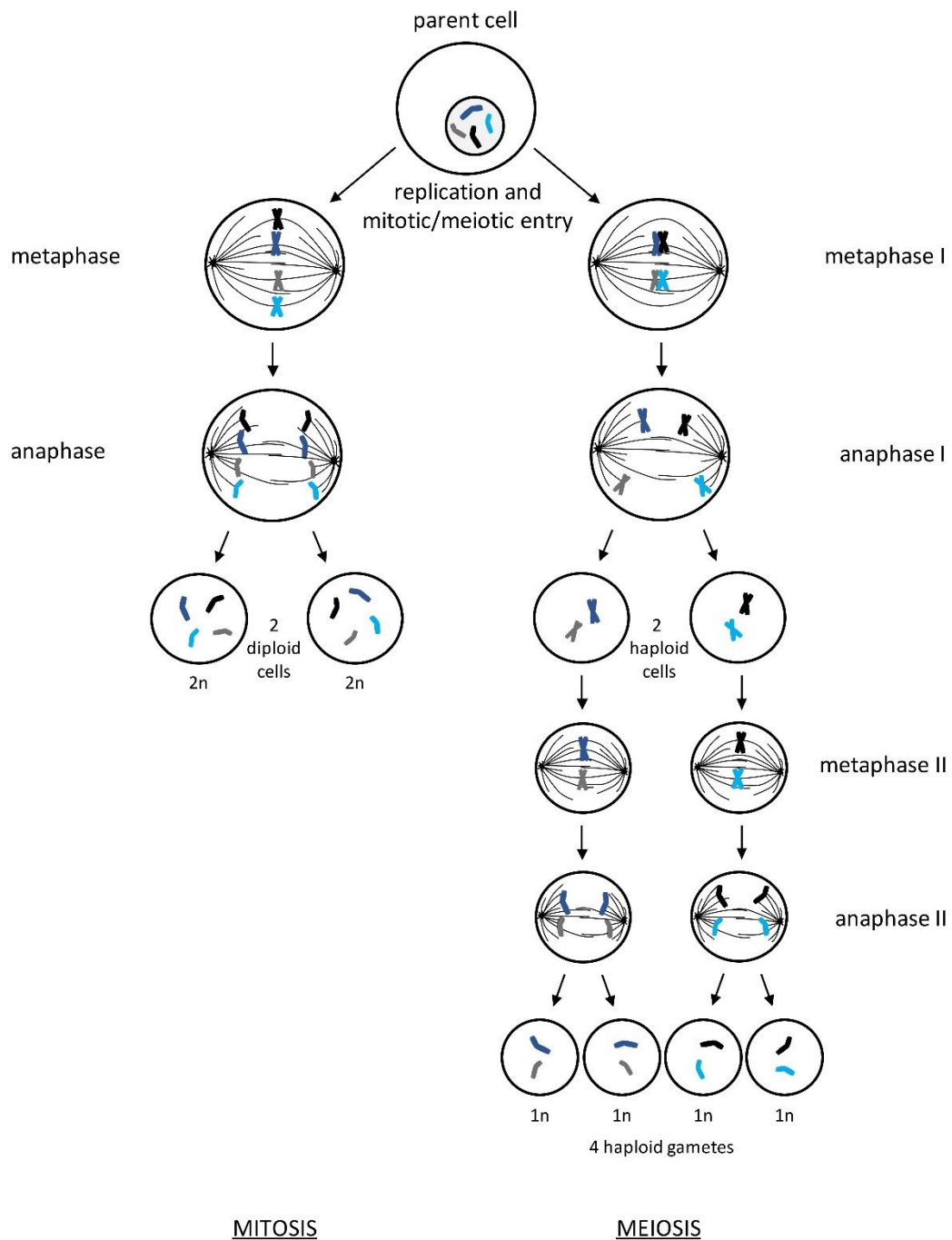


Figure 6 | Overview of mitotic and meiotic cell divisions. During mitosis chromosomes, duplicated from a parental cell by replication, are evenly segregated to generate two identical daughter cells. In meiosis two rounds of chromosome segregation (segregation of homologs during meiosis I, segregation of sisters during meiosis II) without an intervening S-phase evenly distribute the chromosomal content between four haploid gametes (sperm and egg, respectively). For details see text.

During female gamete formation two polar bodies are extruded, i.e., two small haploid cells containing a small amount of cytoplasm and half of the chromosomal content during each meiotic division, destined for apoptosis. This results in the formation of a single haploid oocyte. This process starts during embryogenesis; however, oocytes arrest in prophase of meiosis I until puberty. Oocytes exit from this meiotic arrest upon hormonal stimulation and progress further through meiosis and arrest in metaphase II, which is only completed upon fertilization (reviewed in Morgan, 2007).

1.6.2 Cohesion during meiosis

Like in mitosis, sister chromatid cohesion during meiosis is mediated by Cohesin. However, the ring complex in meiotic cells is composed of meiosis-specific paralogs of the Cohesin subunits: Smc1, Scc1, and SA1/2 of mitotic Cohesin are functionally replaced by Smc1 β , Rec8, and Stag3, respectively (Biswas et al., 2013; Hopkins et al., 2014; Nasmyth and Hearing, 2009; Peters et al., 2008; Revenkova et al., 2004; Tachibana-Konwalski et al., 2010). During meiosis I, homologous chromosomes, come together and undergo recombination through a process called crossing-over. This exchange of genetic material between homologous chromosomes increases genetic diversity. After homologous recombination homologs are tethered together by Cohesin distal from crossovers (Brar et al., 2009). Removal of Cohesin in meiosis requires solely the activity of Separase, probably instead of a prophase-pathway, to allow the separation of homologous chromosomes in meiosis I and the separation of sisters in meiosis II (Buonomo et al., 2000; Keating et al., 2020; Kitajima et al., 2003; Kudo et al., 2009; Terret et al., 2013).

During meiosis I, centromeric Cohesin is protected against active Separase to keep sisters together by two mechanisms: (1) Rec8 - in contrast to Scc1- must be phosphorylated to become a substrate of Separase (Hauf et al., 2005; Katis et al., 2010; Kudo et al., 2009; Riedel et al., 2006) and (2) PP2A is recruited to centromeres by Sgo2, the meiotic counterpart of Sgo1. PP2A keeps Rec8 in a dephosphorylated state and, thus, prevents Rec8 cleavage at centromeres. This allows preservation of centromeric sister chromatid cohesion in meiosis I (Lee et al., 2008; Llano et al., 2008). After successful execution of meiosis I and hence segregation of homologous chromosomes, Sgo2-PP2A relocates from centromeric Cohesin to kinetochores upon bi-orientation (i.e., tension) of sisters in meiosis II (Gomez et al., 2007;

Lee et al., 2008). However, a definite answer for this key question of how “de-protection” of meiotic centromeres in meiosis II occurs is still to be elucidated (Keating et al., 2020). At anaphase of meiosis II the now deprotected and phosphorylated centromeric Cohesin is cleaved by Separase, triggering the segregation of sister chromatids, thereby generating four haploid cells (Chambon et al., 2013; Llano et al., 2008; Terret et al., 2003; Wassmann, 2013).

1.7 Aim of this work

One of the key factors ensuring genome stability is correctly timed chromosome segregation during mitosis. For proper chromosome segregation it is crucial that Separase, responsible for triggering anaphase by cleaving the Cohesin-subunit Scc1, is kept inactive throughout most of the cell cycle. Accordingly, Separase is regulated via a variety of mechanisms such as phosphorylation and inhibition by various proteins. Said inhibitors interact with Separase, thereby creating a layer of safety mechanisms to prevent premature sister chromatid separation. Moreover, Separase has additional functions beyond the cleavage of Cohesin. A yet unknown, Separase-regulated process, corresponding regulators, interactors, and substrates might exist and remain to be discovered. Recently, the protein Sororin was proposed to be another interactor of Separase by Zhang and Pati, 2012. As discussed above Sororin is an accessory Cohesin subunit, which is essential for the maintenance of cohesion until anaphase. The aim of the present work was to investigate this surprising interaction of Sororin and Separase in order to generate further insights into the corresponding mode of action and relevance. Biochemical and cell biological characterization of said interaction should be implemented. To this end, the interaction sites on both proteins with either protein or possible additional proteins should be identified as precisely as possible. In addition, the regulatory function of Sororin on the proteolytic activity of Separase and the corresponding physiological relevance should be investigated.

2 Results

2.1. Identification of a new Separase interaction partner

2.1.1 The essential cohesion co-factor Sororin interacts with Separase *in vivo*

The vast number of processes, regulated by the essential master regulator of the cell cycle Separase, as extensively outlined above, suggest that there are other processes and substrates of the protease waiting to be discovered.

Screening data published by Zhang et al. suggest that the essential Cohesin co-factor Sororin forms a complex with Separase (Zhang and Pati, 2012, unpublished data). Intrigued by this report, we tried to reproduce this interaction. To this end, human cell culture was used and HEK293T cells were transfected with plasmid DNA coding for human Sororin (hSororin, hereafter the term Sororin is used for hSororin, if not otherwise stated) with a C-terminal eGFP (enhanced green fluorescent protein)-tag. Upon mitotic entry most chromatin associated proteins, such as Sororin, relocalize from the nucleus/chromatin to the cytoplasm, due to various reasons i.e., the prophase pathway (Holzmann et al., 2019). To obtain a high concentration of soluble protein, cells were arrested in prometaphase using the spindle poison taxol. Taxol suppresses the dynamic behavior of microtubule plus-ends, which activates the SAC and hence, arrests cells in mitosis with a static bipolar spindle (summarized in Hornick et al., 2008). To be able to differentiate between early and late mitosis, two different time points were analyzed: "0" as the first cell harvest point after a 14h taxol incubation. At this time, the AurB inhibitor ZM447439 (hereafter called ZM) was added to already harvested cells. AurB inhibition silences the SAC and drives cell synchronously from prometaphase through an anaphase-like state and finally into G1-phase, mimicking mitotic exit (Ditchfield et al., 2003; Hauf et al., 2003; Shindo et al., 2012). The final sample was harvested 55 minutes ("55") after ZM-addition to obtain late mitotic cells. Successful mitotic exit was analyzed by Separase auto-cleavage and Securin degradation.

By immunoprecipitation (IP) experiments using beads covalently coupled to a GFP-binding protein/nanobody (Rothbauer et al., 2008) the Sororin-Separase interaction could be verified using western blot analysis during early mitosis as well as late mitosis (Fig. 7). A control GFP-non-binding protein, with the necessary interaction sites mutated (Fig. S1, based on Kirchhofer et al., 2010) was used as a control and did not show any comparable interaction. A corresponding opposite IP experiment, wherein endogenous wildtype (WT) Separase was

precipitated also demonstrated an interaction between Separase and Sororin (Fig. 7C). In a similar experiment, chromatin from the same cell-pool was isolated, washed, DNA was digested using Benzonase (DNase) and finally chromatin-associated proteins were analyzed as described before. Even though much weaker (probably due to a lower abundance of proteins), the same Separase-Sororin-interaction could be demonstrate using only these chromatin-bound proteins (data not shown).

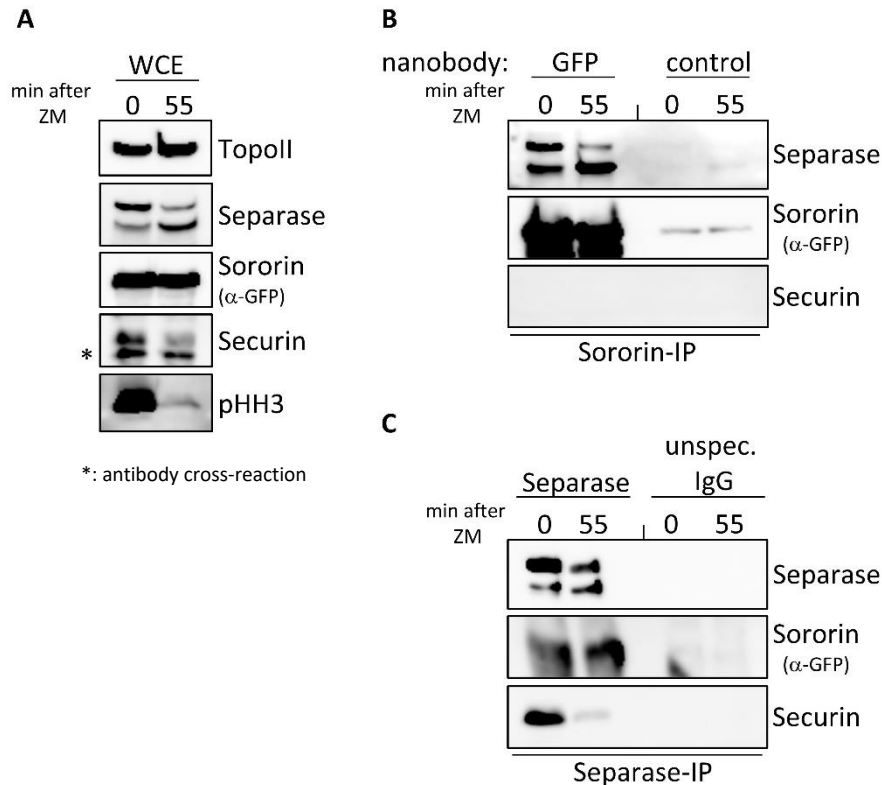


Figure 7 | Sororin is a newly identified interaction partner of human Separase. (A) HEK293T cells were transfected with a plasmid encoding Sororin-eGFP. Cells were arrested in mitosis approximately 36h after transfection by taxol treatment. Additional 14h later cells were either harvested ("0") or further treated with ZM for 55 min ("55"). Whole cell extracts were boiled with SDS sample buffer and analysed by immunoblotting using the indicated antibodies. (B, C) Subsequently, cleared cell lysates were prepared and incubated with (B) GFP nanobody coupled beads, or respective beads coupled to a GFP nanobody no longer capable to interact with GFP. (C) Additionally, lysates were incubated with beads coupled to either Separase antibody or unpecific IgG's as a control. Beads were eluted by boiling with SDS sample buffer, eluates were analysed by immunoblotting using indicated antibodies (antibodies against tags are indicated in brackets). *: nonspecific binding of the Securin antibody.

To exclude artificial interaction of Sororin and Separase, due to unphysiological levels of the ectopically expressed protein, interaction of the endogenous proteins should also be demonstrated. Therefore, two polyclonal rabbit antibodies, raised against an *E. coli*-expressed, purified (His₆-SUMO-tagged) full length (FL) Sororin, were characterized and found

to work in western blot analysis and IP-experiments (Fig. S2). This Sororin antibody, a respective Separase antibody as well as unspecific Immunoglobulin Gs (IgGs) as controls, were coupled to sepharose beads. Those coupled beads were incubated with cell lysates as indicated and analyzed by immunoblot. Reciprocal co-IP-experiments confirmed the Sororin-Separase interaction to be very specific, since Sororin or Separase, respectively, did only very weakly bind to unspecific IgG coupled sepharose beads (Fig. 8).

Unfortunately, we found that the Sororin antibody, which can be successfully coupled to sepharose beads and used for IP, sometimes precipitates a non-specific background protein that can be detected just below Separase with the common Separase antibody used in the lab. Further tests with different antibodies directed against Separase showed that this is not a modified form of Separase, but rather unspecific background (data not shown). To prevent false results and still be able to use the well-characterized Separase antibody, eGFP-tagged Sororin was used after this proof of principle.

Nevertheless, an interaction between Separase and Sororin could be validated on an endogenous level in mitotic cells (Fig. 8).

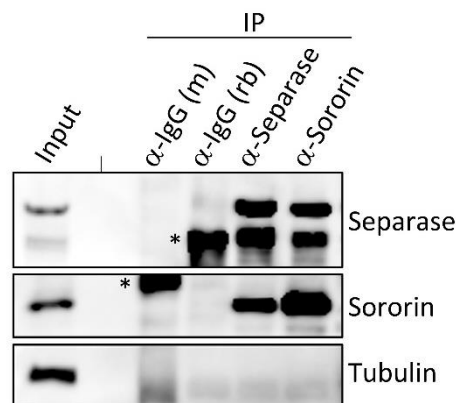


Figure 8 | Endogenous Separase and Sororin interact in human cell culture. HeLa K cells were arrested in prometaphase using taxol. Cleared cell lysates (Input) were incubated with beads coupled to α -Separase or α -Sororin antibody, respectively. Corresponding unspecific IgG's were used as a control (m: mouse, control for the Separase antibody; rb: rabbit, control for the Sororin antibody). Input and beads after IP were boiled in SDS sample buffer and subjected to immunoblotting using the indicated antibodies. Note that both unspecific IgGs precipitate unspecific background (marked by a *). Tubulin serves as a loading control.

2.1.2 Sororin expression seems to assist Separase expression

Encouraged by the identification of Sororin as a new interaction partner of human Separase, we sought to further analyze the Sororin-Separase interaction. In our initial interaction studies of Sororin and Separase in human cells, we noticed better expression of Separase if Sororin was also transiently overexpressed (Fig. 9). It was previously demonstrated that Securin acts as a “chaperone” of Separase by association in a co-translational manner, thereby assisting proper folding of Separase and ensuring its immediate inhibition at the same time. This can be demonstrated by overexpression of Separase with or without co-expression of higher amounts of Separase, when Securin is co-expressed in cultured cells followed by pelleting assays (Hellmuth et al., 2015a; Hornig et al., 2002). We propose a less pronounced but similar effect for Sororin, as evident by individual and co-expression of both proteins in human cells (Fig. 9).

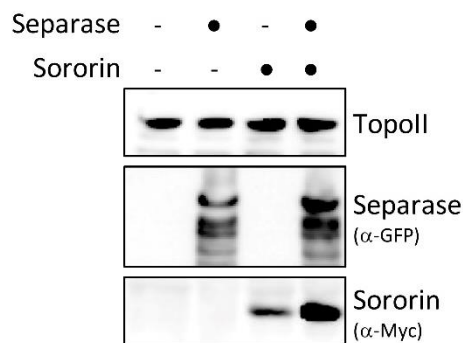


Fig. 9 | Transient overexpression of Sororin boosts Separase expression and *vice versa*. HEK293T cells were transfected with a plasmid encoding Myc-Sororin or GFP-Separase (•: transient transfection of the corresponding plasmid, -: empty vector was transfected to a corresponding total amount of plasmid-DNA). Cells were arrested in mitosis approximately 36h after transfection by taxol treatment. Additional 14h later cells were harvested, centrifuged at 16.000 g and boiled in SDS sample buffer and subjected to immunoblotting using the indicated antibodies (antibodies against tags are indicated in brackets). Topoisomerase II serves as a loading control.

2.1.3 Separase, Sororin and Cohesin form a heterotrimeric complex

To test if Sororin, Separase and other Separase interaction partners can form a multimeric complex, a tandem affinity purification (TAP) was performed using HEK293T cells expressing

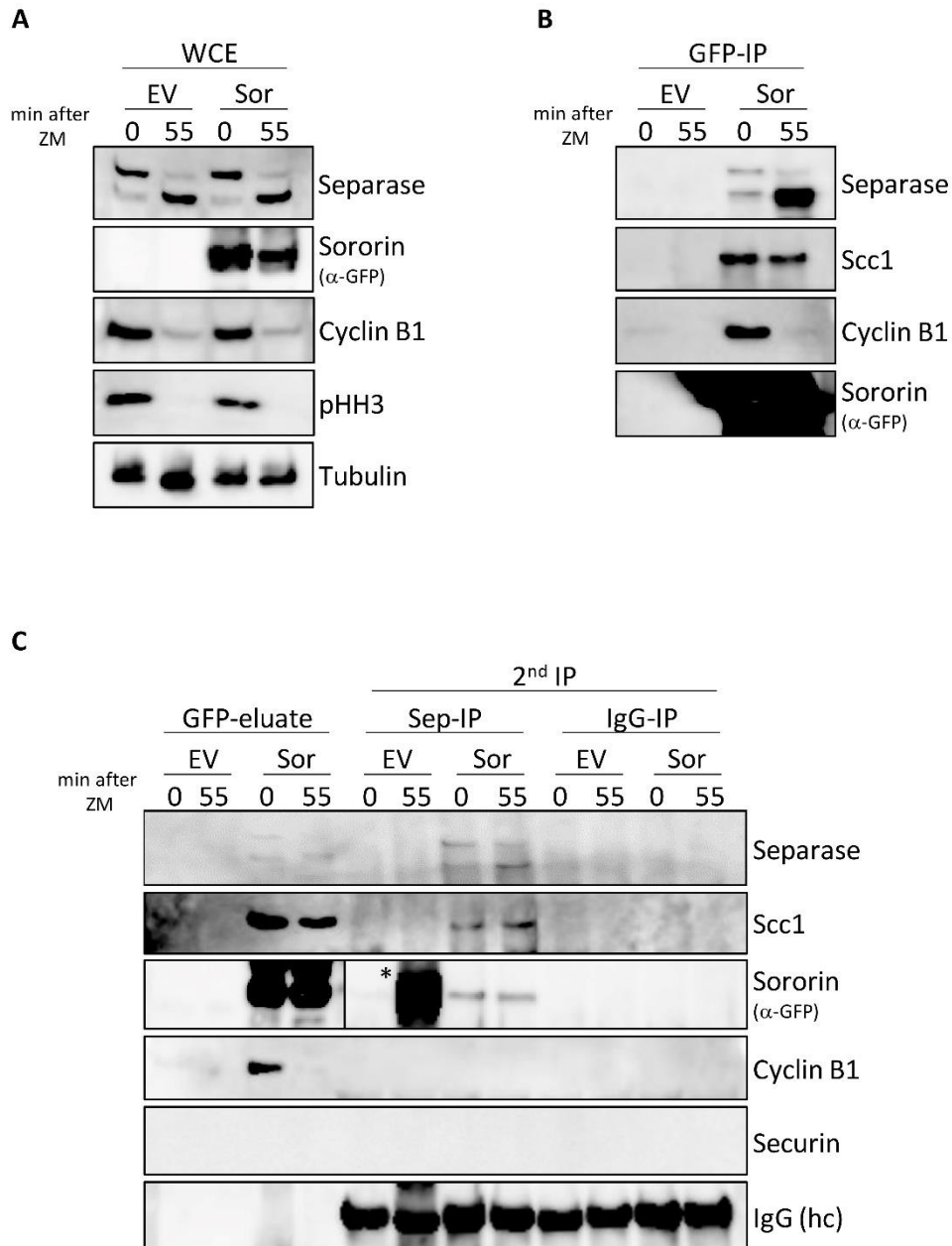


Figure 10 | Sororin, Securin and Cyclin B1 interact with Separase in a mutually exclusive manner. HEK293T cells were transiently transfected with plasmid DNA encoding Sororin-TEV-eGFP (Sor), an empty vector was used as a control (EV). Cells were arrested in mitosis approximately 36h after transfection by taxol treatment. Additional 14h later cells were either harvested (“0”) or further treated with ZM for 55 min (“55”). (A) Whole cell extracts were boiled with SDS sample buffer and analysed by immunoblotting using the indicated antibodies. (B) Subsequently, cleared cell lysates were prepared and incubated with GFP nanobody coupled beads. A fraction of the beads were boiled in SDS sample buffer and analysed as described. (C) The majority of beads was treated with TEV-protease and the resulting GFP-eluate was used for a 2nd IP using either Separase antibody coupled beads (Sep-IP), or IgG coupled beads as a control (IgG-IP). Corresponding beads were finally eluted by boiling in SDS sample buffer and analysed by immunoblotting using the indicated antibodies (antibodies against tags are indicated in brackets). Tubulin was used as a loading control for WCE samples, the heavy chain (hc) of the coupled antibodies was used as a loading control for the 2nd IP. Due to very high amounts of protein the Sororin immunoblot was edited for better illustration, indicated by a straight line. Note however, that all samples were analysed as described on the same blot. A strong background band is marked with an asterisk (*).

Sororin-TEV-eGFP. The additional tobacco etch virus (TEV) protease cleavage site of the transgenic Sororin allows for protein-complex elution in the first purification step. Cells transfected with an empty vector (EV) were used as a control. Since all currently known inhibitors interact with Separase in a mutually exclusive manner (Boos et al., 2008; Gorr et al., 2005; Hellmuth et al., 2020; Uhlmann et al., 1999), their interaction pattern with regard to Sororin were analyzed. Cells were harvested in prometaphase (taxol arrest "0") and in a late mitotic stage, i.e., 55 minutes after ZM-addition ("55"). Whole cell lysates were treated with Benzonase and then subjected to a first IP using GFP nanobody coupled beads (GFP-IP, Fig 10B). Proteins precipitated by this first purification step were analyzed by immunoblotting, either by boiling the beads (Fig. 10B) or following elution with TEV-proteas (Fig. 10C). This revealed that Sororin interacts with Separase and surprisingly also with Cyclin B1 in prometaphase. However, no Sororin-Securin interaction was detectable (Fig. 10B, C). Remarkably Sororin interacts mostly with auto-cleaved Separase in late mitosis, and the Sororin-Cyclin B1 interaction can no longer be detected (Fig. 10).

These eluate-samples from the first TAP-step were further processed by using them as input for a second purification step utilizing Separase-antibody coupled sepharose beads (Fig 10C). Interestingly the simultaneous precipitation of all three proteins - Sororin, Separase and Cyclin B1, respectively - can no longer be observed. However, concurrent interaction of Sororin, Separase and the Cohesin subunit Scc1 is evident (Fig. 10C). Indicating that the Interaction of Separase and Sororin, Securin, or Cyclin B1, respectively, is mutually exclusive. However, a heterotrimeric complex of Separase, Sororin and Scc1, i.e., Cohesin, seems to form.

2.1.4 Separase and Sororin interact in all cell cycle stages

To further analyze the Separase-Sororin interaction, HeLa cells were transiently transfected with plasmids encoding C-terminally GFP-tagged Sororin, and samples of all cell cycle stages (G1/S, G2, G2/M, early and late mitosis) were prepared. Samples were taken from cells synchronized at the G1/S-boundary by a double-thymidine-block using the DNA synthesis inhibitor thymidine (Chen et al., 2018; Schwartzman et al., 1984). To arrest cells in G2, cells were treated with RO3306, a small-molecule inhibitor of CDK1 (Vassilev et al., 2006). This treatment was administered after releasing the cell population from a previous thymidine

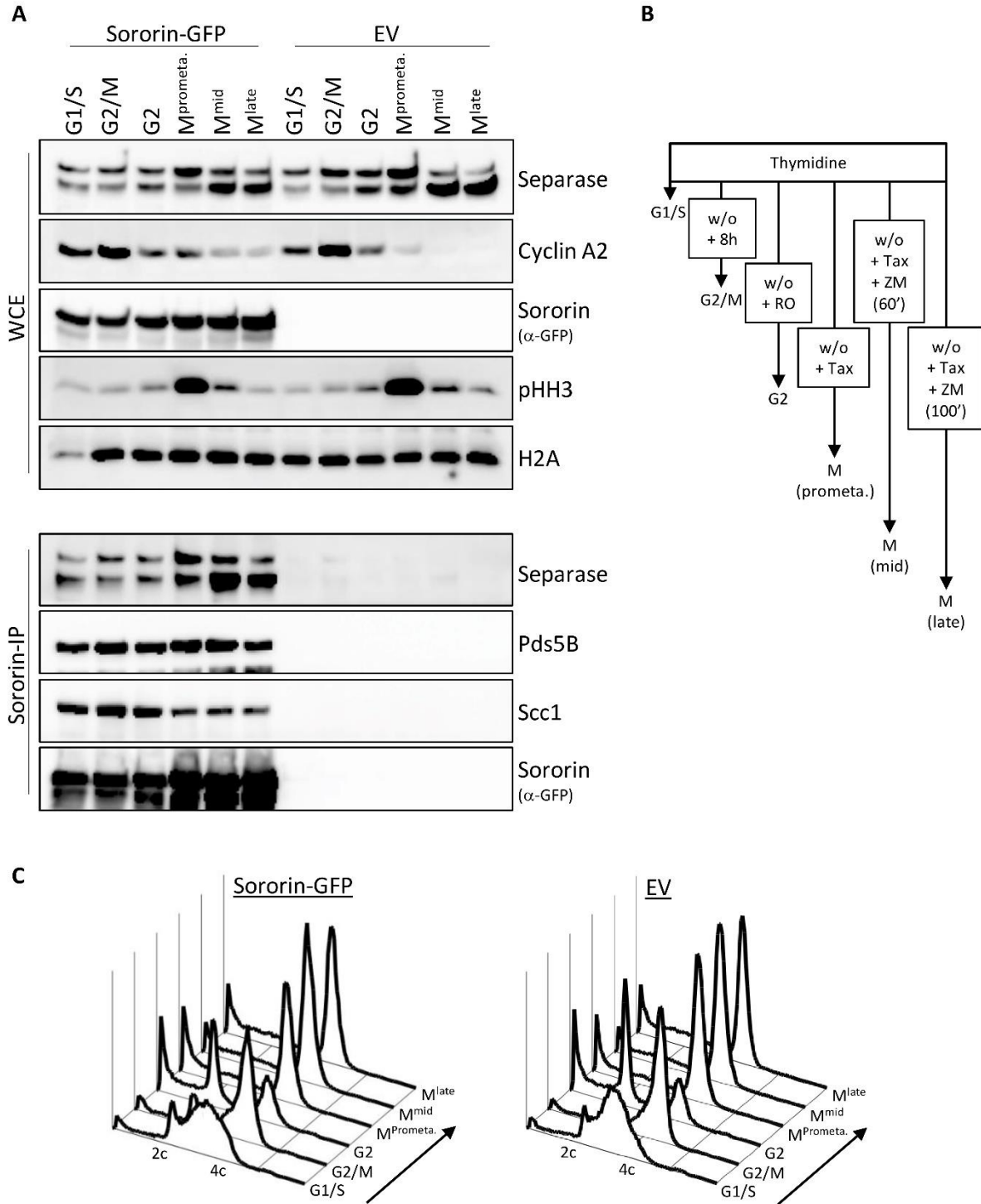


Figure 11 | The Sororin-Separase complex persists throughout the cell cycle. See next page for legend.

Figure 11| The Sororin-Separase complex persists throughout the cell cycle. HeLa K cells were transiently transfected with plasmid DNA encoding Sororin-eGFP, an empty vector was used as a control (EV). Cells were subjected to a double thymidine-block to synchronize cells at the G1/S boundary. Following washout (w/o) cells were divided equally and treated according to the desired cell cycle stage to be analysed. For G2-cells the CDK1-inhibitor RO-3306 (RO) was supplemented after washout. For mitotic cells taxol was added (early mitotic cells: “prometa.”). For middle and late mitotic cells taxol arrested cells were treated with ZM for 60min (mid) and 100 min (late), respectively. (A) WCE’s were prepared, samples were boiled in SDS sample buffer and analysed by immunoblotting using the indicated antibodies. H2A serves as a loading control for WCE. Sororin was precipitated by incubation with GFP-nanobody coupled beads. Beads were subsequently eluted by boiling in SDS sample buffer und analysed by immunoblotting using the indicated antibodies (antibodies against tags are indicated in brackets). (B) Experimental procedure. (C) a subset of corresponding cells from (A) were analysed by flow cytometry. Therefore, cells were fixed, and DNA was stained by PI. Direction of the cell cycle indicated by an arrow (c: chromosome copy number, Tax: taxol, M: mitosis).

treatment. G2 cells were collected eight hours after releasing from a thymidine-block. Mitotic cells were obtained as described.

Sororin-eGFP was isolated via its affinity tag, and the interaction pattern of endogenous Separase was analyzed by immunoblotting. Mock transfected cells were used as a control and treated accordingly (see EV, Fig. 11). The respective cell cycle stage was verified by propidium iodide (PI)-staining and flow cytometry (Fig. 11C). The mitotic stage of corresponding samples was further verified by analysis of the mitosis specific phosphorylation of histone H3 at Ser10. The G2 phase was verified via abundance of Cyclin A (Juan et al., 1998, Fig. 11). Surprisingly the Separase-Sororin interaction seems to exist throughout the cell cycle, wherein the interaction appears to be strongest in mitosis (Fig. 11).

2.1.5 Separase and Sororin interact during mitotic exit

The interaction of Separase-Cyclin B1 transiently decreases during metaphase to anaphase transition to than form for a second time in late mitosis/G1-phase. This so-called “second wave” occurs at a time where the total amount of Cyclin B1 in the cell is already very low, due to APC/C^{Cdc20} dependent degradation (Hellmuth et al., 2015b; Toyoshima-Morimoto et al., 2001; Fig. 12 C). This repeated strong interaction of both binding partners is thought to inhibit residual active Separase in late mitosis (Gorr et al., 2006; Hellmuth et al., 2015b).

To test how Sororin and Separase interact during mitosis and mitotic exit and whether a similar “second wave” of interaction occurs between Separase-Sororin, HeLa cells expressing Sororin-eGFP by transient transfection were synchronized at the G1/S-boundary using thymidine. After release from this arrest, cells were arrested in prometaphase using taxol and harvested by mitotic shake-off. Finally, ZM was added to drive all cells synchronously through

anaphase into a G1-like state. Samples were taken before ZM-addition and at various timepoints over the course of 180 minutes after ZM-addition. Mock transfected control cells were treated accordingly and sampled before ZM-addition and at the final time-point after 180 min (Fig. 12). Finally, all samples were lysed, divided equally and Sororin-GFP was isolated via its affinity tag. Furthermore, endogenous Separase was isolated by corresponding antibodies coupled to sepharose beads. Accordingly, beads coupled to unspecific IgG's were

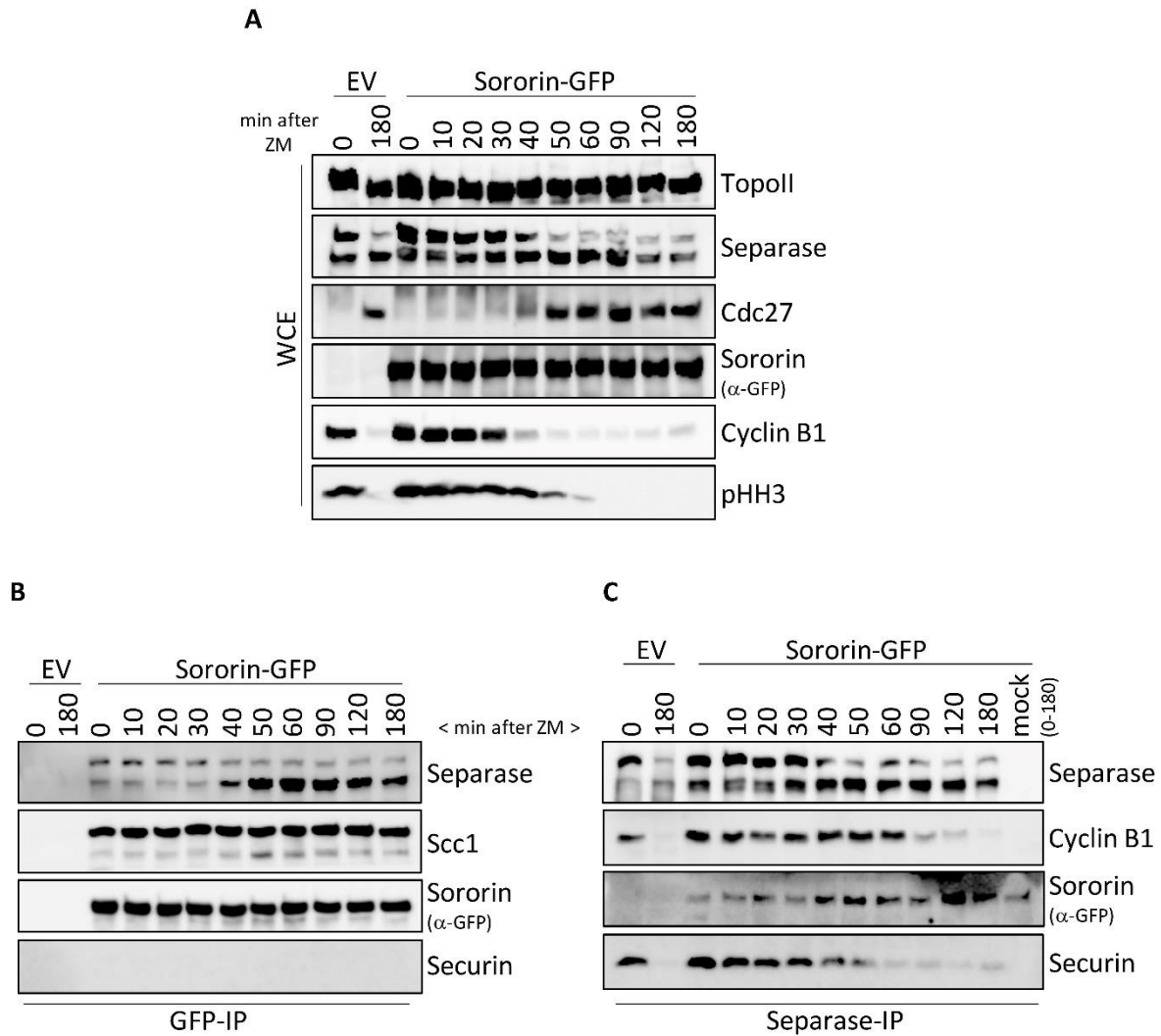


Figure 12 | Sororin and Separase interact, particularly in mitosis. HeLa K cells were transiently transfected with plasmid DNA encoding Sororin-eGFP, an empty vector was used as a control (EV). Cells were blocked at the G1/S boundary using thymidine, subsequently released by washout of thymidine and treated with taxol to synchronize cells in early mitosis. Mitotic cells were harvested by mitotic shake-off and treated with ZM to simultaneously release cells into mitosis. Samples were taken at the indicated time points. (A) WCE samples were boiled with SDS sample buffer and subjected to analysis by immunoblotting using the indicated antibodies. Lysates were subsequently incubated with GFP-nanobody coupled beads (B) or Separase antibody and IgG-control coupled sepharose beads (C). Beads were eluted by boiling in SDS sample buffer, subjected to immunoblot analysis using the indicated antibodies (antibodies used against tags are indicated in brackets).

used as an additional control). WCE- and IP- samples were analyzed by immunoblot. Successful and simultaneous exit from mitosis into a G1-like state can be judged, for example, by a decrease in the mitosis specific phosphorylation of histone H3 at Ser10 and dephosphorylation of Cdc27. Additionally, the progression into a G1-like state can be evaluated by a decrease in Cyclin B1 abundance due to APC/C^{Cdc20} mediated degradation and by enrichment of auto-cleaved Separase over time (Juan et al., 1998; Kraft et al., 2003; Papi et al., 2005; Zou et al., 2002) (Fig. 12A).

The amount of Sororin interacting with full length Separase shifts approximately 40 min after ZM addition to a more pronounced interaction with cleaved Separase, probably due to a higher abundance of auto-cleaved Separase during mitotic exit. The same interaction pattern regarding Separase-Sororin can be observed by the reciprocal approach using Separase antibody coupled beads (Fig. 12C). These results once again support a Separase-Sororin interaction in mitosis. However, a “second wave” of complex formation, as it has been reported for Separase-Cyclin B1, in late mitosis/early G1 cannot be observed (Fig. 12C).

To exclude a possible essential involvement of phosphorylation by AurB kinase in this interaction pattern, the same experiment was repeated, but instead of adding ZM to release mitotic cells into anaphase, taxol was removed by excessive washing steps. Samples were taken for five hours, every 30 min. The results mirrored those described above. The same applies to nocodazole treated cells, after washout to exclude the involvement of pulling forces by the spindle apparatus regarding the Separase-Sororin interaction (data not shown).

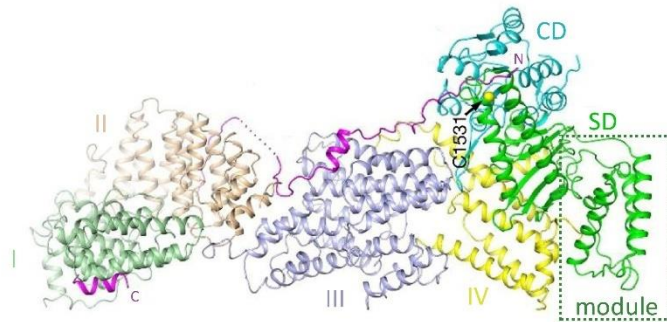
2.2 Mapping Separase-Sororin interaction sites on either protein

2.2.1 Sororin interacts with all domains of Separase

Separase's main inhibitor Securin is a mostly unfolded protein containing very few elements of secondary structure elements (Bachmann et al., 2016; Csizmok et al., 2008; Sánchez-Puig et al., 2005). The N-terminal half of Securin is completely disordered and as demonstrated by yeast-two-hybrid-assays, interacts with the C-terminus of Separase. Securin's C-terminal half on the other hand contains a few segments that adopt a secondary structure and are able to interact with the N-terminus of Separase (Bachmann et al., 2016; Csizmok et al., 2008; Jäger

et al., 2004; Sánchez-Puig et al., 2005; Viadiu et al., 2005). Recently the crystal structure of full length Separase, in complex with Securin, was resolved for the corresponding protein complexes of yeast (Luo and Tong, 2017). The corresponding structure of the Separase-Securin complex of *C. elegans* was also elucidated using Cryo-EM (Boland et al., 2017). However, no crystal structure for Sororin is available. We used circular dichroism-spectroscopy to make a first general analysis of Sororin's structural characteristics. By doing so, we identified very little degree of secondary structure. Therefore, we assume that Sororin, much like Securin, is a protein of mostly disordered composition with probably few helical areas (data not shown; Greenfield, 2006).

A



B

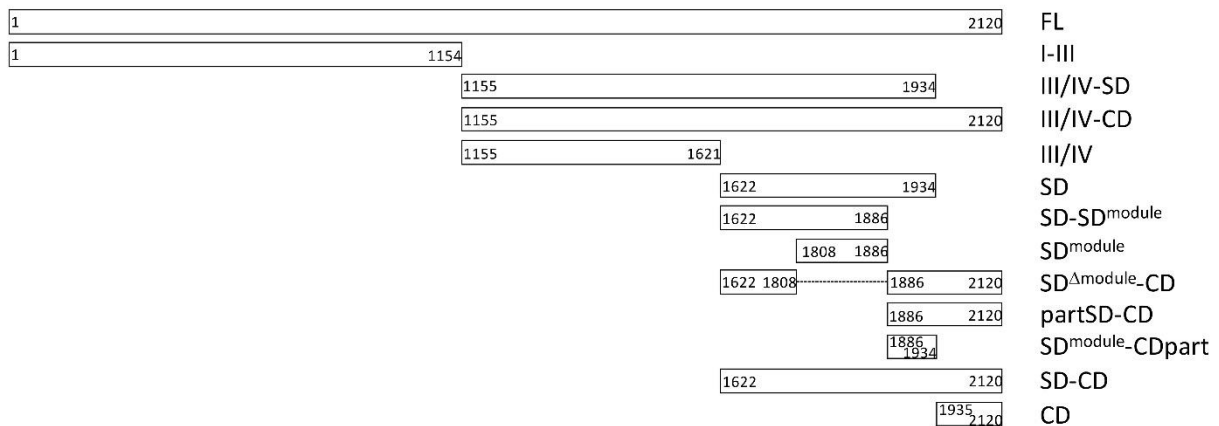


Figure 13 | Separase fragments - overview. (A) Separase domains were designed based on the crystal structure and sequence alignments of Separase from *S. cerevisiae* and *C. elegans*. (Modified from Luo and Tong, 2017, used with permission by Springer nature). Securin is illustrated in pink (N: N-terminus, C: C-terminus). See Text for details. (B) Overview of human Separase fragments based on the domain designation from (A). Corresponding aa-sections are indicated. A dotted line indicates a deleted section, this section was substituted by a GlyGlySer-linker. See text for further details.

Thus, we proposed an interaction pattern of the Sororin-Separase complex similar to the Securin-Separase complex. To test this hypothesis, we initially designed a variety of Separase-fragments. In order to generate soluble protein-segments we co-aligned the sequences of human FL Separase with the sequences of yeast and *C. elegans* Separase, for which a respective crystal or Cryo-EM structure is available, respectively (Boland et al., 2017; Luo and Tong, 2017). Separase fragments were designed in between of secondary structure elements containing at least one potential Securin-interaction site to possibly enhance solubility *in vivo* (Boland et al., 2017; Luo and Tong, 2017). The resulting fragments of human Separase were designated as follows, based on Luo and Tong, 2017: I-III (spanning the entire and mostly poorly conserved N-terminal region of Separase), a C-terminal extension from domain II within the N-terminus reaching up to domain IV, the SD- and CD-domain, respectively (Fig. 13; see also chapter 1.5, Fig. 5). The C-terminus was resolved in more detail starting with the SD-domain, parts thereof with extensions to the CD-domain. The so-called SD^{module} describes the small globular domain extending from the far end of the protease as depicted by the crystal structure (Luo and Tong, 2017, Fig. 13A). All Separase-fragments were N-terminally Myc-tagged, transiently expressed in HEK293T cells and turned out to be soluble in human cell culture based on the signal intensity prior and after high speed-centrifugation of cell lysates (data not shown). Subsequently all Separase-fragments were transiently co-expressed with Sororin-eGFP in HEK293T cells. Potential protein-complexes were isolated by reciprocal IP of the respective Separase-fragments using its Myc-tag (Fig. 14) or Sororin-IP using its GFP-tag (data not shown), followed by western blot analysis. Sororin co-purified with all generated Separase-fragments, except the SD^{module}, in human cell culture (Fig. 14). However, interaction of Sororin seems to be less apparent with fragments of the N-terminal half of Separase (repeated experiments always show interaction slightly above background (data not shown), while it appeared especially strong with the conserved C-terminal half of Separase (Fig. 14). It should be critically mentioned here that the interaction is always strongest when high transient protein expression levels are reached. However, the described results could be confirmed several times (Fig. 14; data not shown). This indicates that Sororin entertains extensive contacts with Separase over its entire length, and hence, that Sororin indeed interacts with Separase similar to Securin.

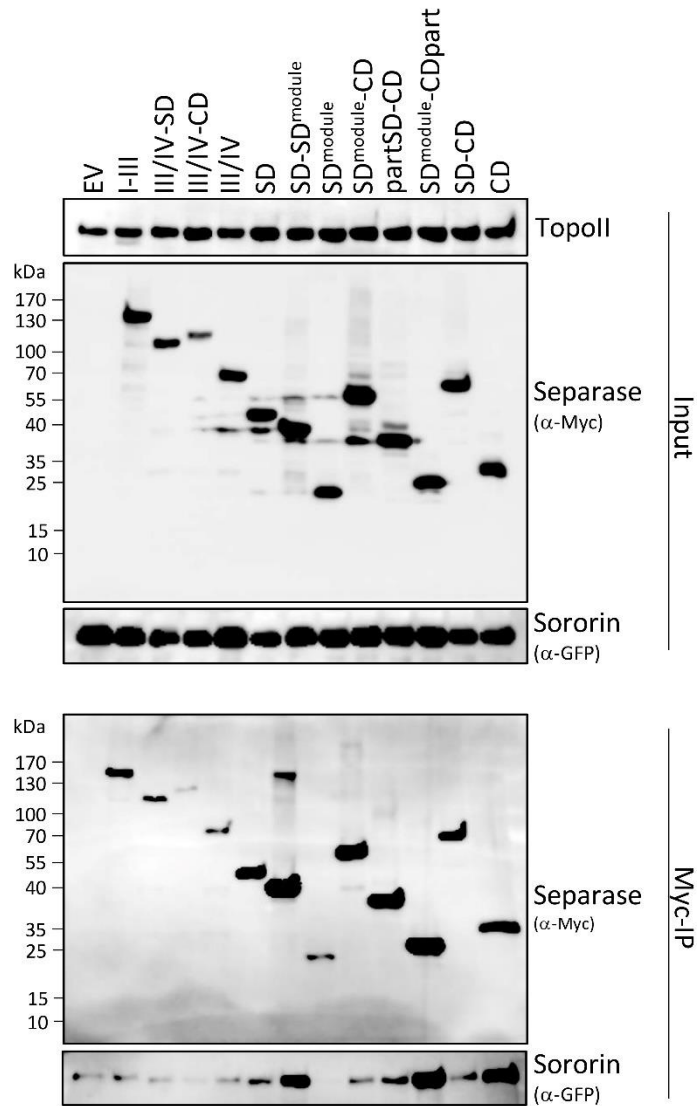


Figure 14| Sororin interacts predominantly with the conserved C-terminus of Separase. HEK293T cells were transiently transfected with plasmids encoding N-terminally Myc-tagged Separase fragments. Fragments were designed based on sequence alignments and structural information from both *S. cerevisiae* and *C. elegans* Separase structures. Plasmid DNA encoding Sororin-eGFP was transiently co-transfected. 36h post transfection cells were synchronized in mitosis by taxol treatment for 14 h. Subsequently cells were lysed, Input samples from cleared lysates were prepared by boiling with SDS sample buffer. Cell lysates were subjected to IP using Myc-antibody coupled agarose. Beads were eluted by boiling in SDS sample buffer. All samples were analysed by Immunoblot analysis using indicated antibodies (antibodies used against tags are indicated in brackets; kDa kilodalton).

2.2.2 Sororin's N-terminus interacts with Separase

In comparison to the mapping of the Sororin-Separase interaction with respect to required domains of Separase, we wanted to identify interaction “domains” within Sororin that interact with Separase. Since no crystal structure for Sororin is available (see above), we divided Sororin in four equal parts. In doing so, we avoided the destruction or separation of conserved motifs, such as the N-terminal KEN-Box or conserved stretches in the proteins C-terminal half that are important for cohesion, cohesion binding and chromatin association (Pfleger and Kirschner, 2000; Wu et al., 2011). The resulting fragments, based on the FL protein were named A (aa 1-87), B (aa 88-150), C (aa 151-208) and D (aa 209-252) (Fig. 15A), all fragments were C-terminally GFP-tagged. After expression of corresponding expression plasmids in HEK293T cells, taxol was added to arrest cells in prometaphase. Cells were again divided equally and ZM was added for 55 min to override the taxol induced mitotic arrest. Cells of both time points (“0” in prometaphase and “55” in late mitosis) were lysed and isolation of the respective fragments by GFP-IP was performed. Subsequent western blot analysis indicates that fragments A and D are able to weakly interact with Cohesin, i.e., Scc1. Interestingly only fragment A interacts with Separase; fragments B, C and D however do not (Fig. 15B). Also, as already demonstrated for the full length Sororin, the association of Sororin with Separase slightly increases in late mitosis, when most Separase has undergone auto-cleavage (Fig. 15A, B). A further experiment, in which the N-terminus (ΔA) or the C-terminus (ΔD) of otherwise full length Sororin were deleted, confirms this finding. FL-Sororin interacts with both Separase and Cohesin. Sororin missing its N-terminus (ΔA) interacts significantly weaker with Separase but Cohesin-interaction can still be observed. Importantly Sororin ^{ΔA} still slightly interacts with Separase, indicating other parts of Sororin to contribute to this interaction. In contrast, Sororin lacking its C-terminus (ΔD) still interacts with Separase efficiently, but Cohesin interaction is impaired (Fig. 15C).

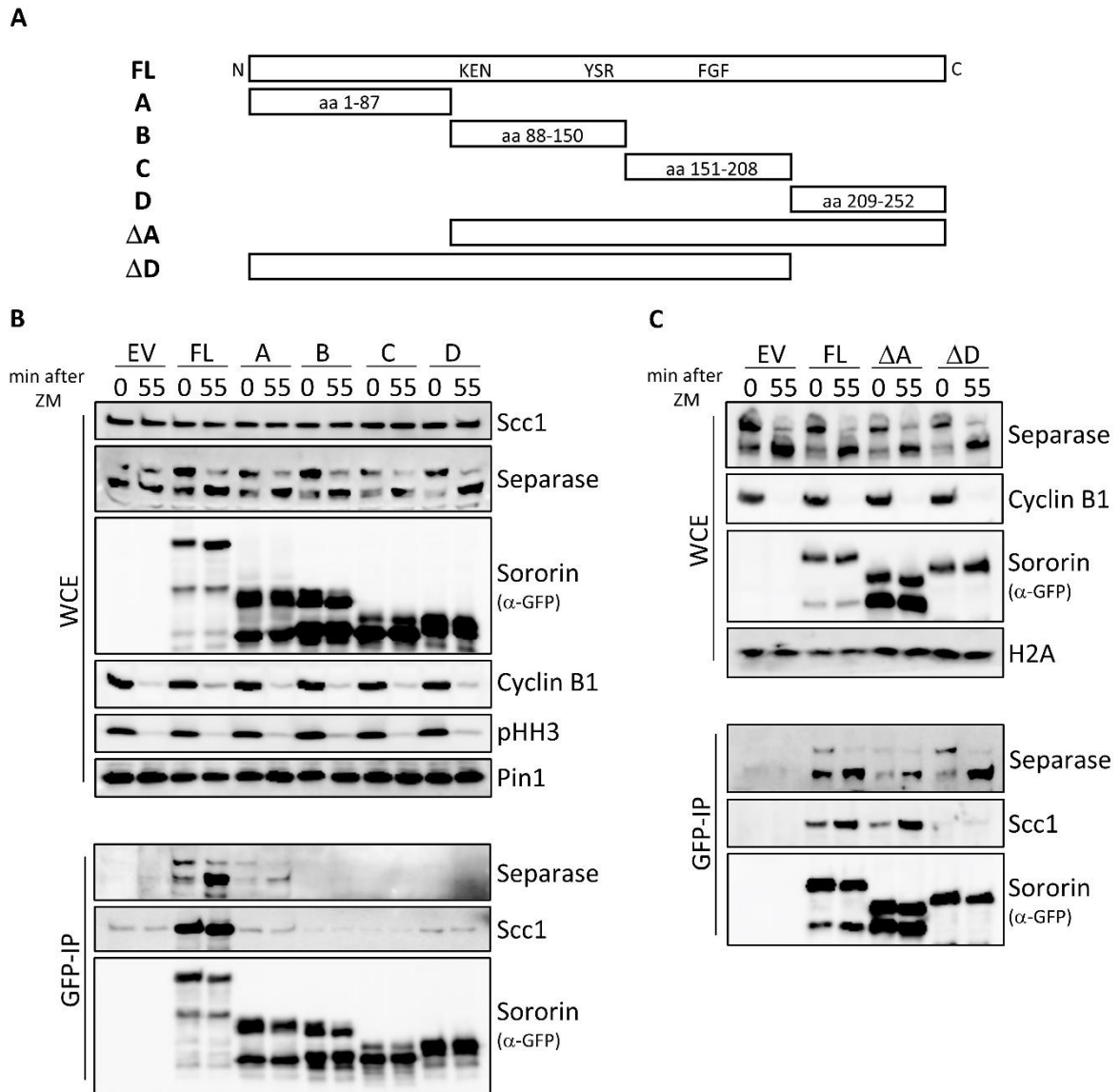


Figure 15| Separase interacts with the N-terminus of Sororin. (A) Sororin fragment overview. The length and arrangement of fragments A, B, C and D is indicated within each fragment. Fragments were designed based on motifs necessary for Sororin’s function, whose highlighted in the FL segment. See text for details. (B) HeLa K cells were transiently transfected with plasmids encoding C-terminally eGFP tagged Sororin fragments compared to the FL and EV. Cells were arrested in mitosis approximately 36h after transfection by taxol treatment. Additional 14h later cells were either harvested by mitotic shake-off (“0”) or further treated after shake-off with ZM for 55 min (“55”). WCE’s were boiled with SDS sample buffer and analysed by immunoblotting using the indicated antibodies. Subsequently, cleared cell lysates were prepared and incubated with GFP nanobody coupled beads. Precipitated proteins were eluted by boiling the beads in SDS sample buffer. Samples were analysed by immunoblotting using the indicated antibodies, Pin1 was used as a loading control (antibodies used against tags are indicated in brackets). (C) HeLa K cells were transiently transfected with plasmids encoding Sororin-GFP with either a deletion of fragment A (ΔA) or fragment D (ΔD), compared to EV and Sororin FL. Cells were treated and analysed according to the description in (B), H2A was used as a loading control.

2.3 Functional characterization of the Separase-Sororin complex

2.3.1 Sororin re-inhibits active Separase *in vitro*

Next, we asked whether Sororin might not only be an interactor of Separase but possibly also an inhibitor of the protease. To test this hypothesis, His₆-SUMO3-tagged Sororin^{WT} was expressed in *E. coli* from a corresponding expression plasmid. His₆-SUMO3-GFP, which is similar in size and charge, was separately expressed as a control. Furthermore, active Separase was produced separately.

To this end the Separase-Securin complex was affinity purified from transiently transfected, prometaphase arrested HEK293T cells via a GFP-TEV-tag on Separase's N-terminus. To remove associated inhibitory Securin and activate the protease, loaded anti-GFP nanobody beads were incubated in an anaphase-arrested *Xenopus* egg extract with active APC/C^{Cdc20}. Following ubiquitin-dependent degradation of Securin, Separase was recovered by washing the beads and finally eluted by TEV-proteas treatment (Gorr et al., 2005; Hellmuth et al., 2014; Stemmann et al., 2001). For active Separase (ac.) Separase^{P1127A} was used. The Separase proline¹¹²⁷ to alanine¹¹²⁷ mutation (human Separase) is not only resistant to high CDK1-Cyclin B1 levels in *Xenopus* egg extracts, but it is also resistant to cis/trans isomerization and, hence, trapped in the more long-lived, i.e. hyperactive, conformer (see introduction; Gorr et al., 2005, Hellmuth et al., 2015). Separase^{C2029S} served as a protease-dead (PD) negative control (Stemmann et al., 2001).

Securin-free active Separase and recombinant His₆-SUMO3-Sororin^{WT} or His₆-SUMO3-eGFP, respectively, were pre-incubated. Finally, Separase's proteolytic activity was assessed. To this end *in vitro* expressed and ³⁵S-labeled Cohesin-subunit Scc1 was added as the proteolytic substrate. Following incubation, samples were analyzed by SDS-PAGE (sodium dodecyl sulfate and polyacrylamide gel electrophoresis), Coomassie Brilliant Blue (CBB) staining and autoradiography. As expected, incubation of His₆-SUMO3-eGFP had no effect on Separase's proteolytic activity and Scc1 was cleaved (Fig. 16). Surprisingly, pre-incubation of Separase with His₆-SUMO3-hSororin^{WT} abrogated Separase's proteolytic activity towards the Cohesin subunit (Fig. 16), indicating that Sororin not only is a previously unidentified interaction partner of Separase, but also an inhibitor.

Results

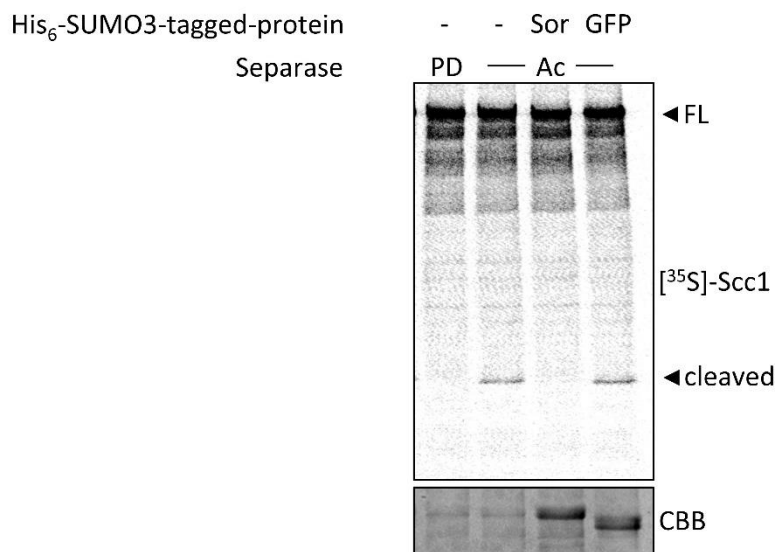


Figure 16 | Sororin reinhibits active Separase *in vitro*. Recombinant His₆-SUMO3-Sororin (Sor) or His₆-SUMO3-GFP (GFP) were pre-incubated with active Separase (Ac). Protease dead Separase (PD) was used as a control. Radioactively labelled *in vitro* expressed ³⁵S-Scc1 was added. Samples were boiled with SDS sample buffer, subjected to SDS-PAGE and Coomassie Brilliant Blue (CBB) staining. The corresponding gel was dried and Scc1 cleavage fragments (arrowhead) were analysed by autoradiography.

2.3.2 Separase re-inhibition is mediated by the N-terminus of Sororin

As demonstrated previously (see Chapter 2.2.2), Sororin's N-terminus (Fragment A) interacts with Separase *in vivo*. In this context we checked next, whether Fragment A of Sororin is responsible for re-inhibition of active Separase *in vitro*. Therefore, all four Sororin fragments were expressed in *E. coli* with a N-terminal His₆-SUMO3 tag. Recombinant proteins were subsequently purified and assessed either alone or in combination for inhibitory capacity. Securin-free active Separase and recombinant His₆-SUMO3-tagged Sororin fragments, combinations of two fragments or His₆-SUMO3-eGFP, respectively, were pre-incubated. Separase's proteolytic activity was assessed by autoradiographic analysis of the finally added ³⁵S-labeled Cohesin-subunit Scc1. In accordance with previous results, only Fragment A (and combinations that contained it) is able to re-inhibit active Separase *in vitro*. This confirms Sororin's N-terminus to be the important part with regard to interaction with human Separase (Fig. 17).

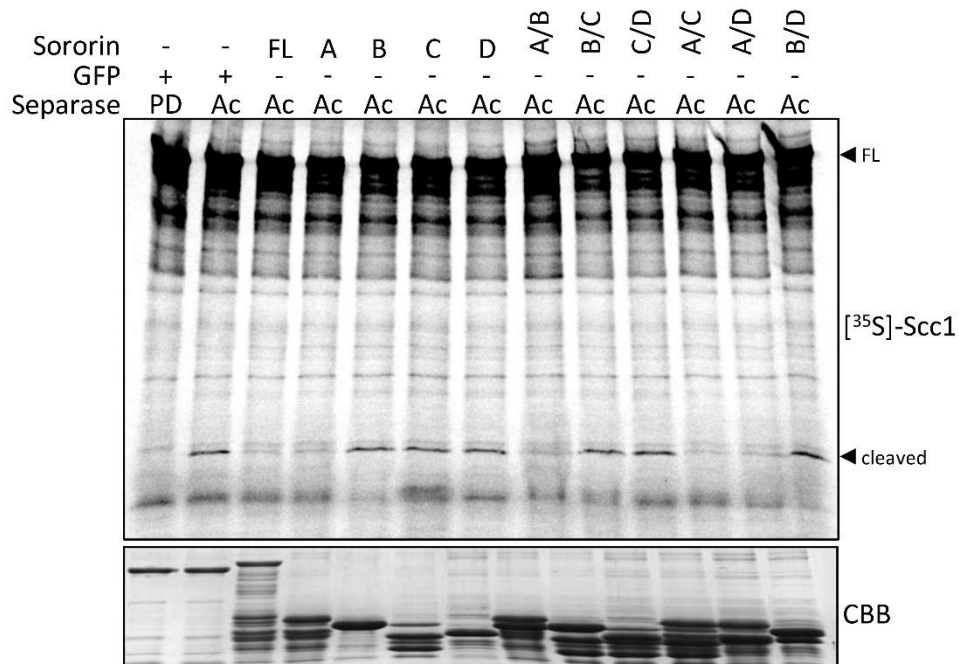


Figure 17] Sororin's N-terminus reinhibits active Separase *in vitro*. Recombinant His₆-SUMO3-Sororin, His₆-SUMO3 tagged Sororin fragments (A, B, C, D, individually or in combination as indicated) or His₆-SUMO3-GFP (GFP) were pre-incubated with active Separase (Ac). Protease dead Separase (PD) was used as a control. Radioactively labelled *in vitro* expressed ³⁵S-Scc1 was added. Samples were boiled with SDS sample buffer, subjected to SDS-PAGE and Coomassie Brilliant Blue (CBB) staining. The corresponding gel was dried and Scc1 cleavage fragments (arrowhead) were analysed by autoradiography.

2.3.3 Sororin is not a universal inhibitor of Separase

Next to the cohesion subunit Scc1/Rad21 and its meiotic counterpart Rec8, other substrates of human/vertebrate Separase have been identified as well. For example, active Separase cleaves itself at three different cleavage sites (Zou et al., 2002). Another example are the anti-apoptotic factors Mcl1 and Bcl-xL (Chen et al., 2007), that are phosphorylated by the kinase Nek2A in mitosis, which makes both – Mcl1 and Bcl-xL – susceptible for Separase cleavage. Once cleaved these anti-apoptotic factors are turned into pro-apoptotic factors triggering cell death in cells that lost the integrity of the SAC (Hellmuth and Stemmann, 2020). Since a variety of proteins are Separase substrates, as outlined above, we tested next, whether Sororin is able to inhibit Separase in general, or if this phenotype might be Cohesin-specific. Therefore, several Separase substrates were expressed *in vitro* and ³⁵S-labeled. Namely Scc1, a small fragment of Scc1 sandwiched between two fluorescent tags, containing a Separase cleavage

site, which is reportedly cleaved *in vitro* (i.e., Scc1-Sensor: aa 142-476; Shindo et al., 2012) and the meiotic Scc1 counterpart Rec8. Additionally, a small part of Separase (domain III-IV, aa 1155-1621) containing the auto-cleavage site of Separase, Securin with its pseudosubstrate site mutated to a Separase-cleavable motif and Mcl1 missing its transmembrane domain (Δ TM, aa 1-327) (Hellmuth and Stemmann, 2020). Since Rec8-cleavage by Separase *in vitro* is boosted upon phosphorylation by Plk1 (Kudo et al., 2009), *in vitro* expressed Rec8 was further treated with purified Plk1 (data not shown). The kinase was subsequently inhibited by addition of BI-2536 (Steggmaier et al., 2007). Again Securin-free active Separase and recombinant His₆-SUMO3-Sororin^{WT} or His₆-SUMO3-eGFP, respectively, were pre-incubated. Separase's proteolytic activity was assessed by autoradiographic analysis of the finally added ³⁵S-labeled substrates. (Fig. 18). Surprisingly, only the Separase mediated cleavage of Cohesion subunits was efficiently inhibited upon addition of recombinant Sororin to active Separase *in vitro*. This is also true for the Scc1 sensor. Interestingly also the Separase-domain containing the auto-cleavage site, is efficiently cleaved upon addition of active Separase, cleavage is again chiefly prevented upon addition of recombinant Sororin. However, Mcl1 Δ TM and the Securin-variant, whose pseudo-cleavage consensus site ExxP was mutated to ExxR (Luo and Tong, 2018; Fig. 18A) are efficiently cleaved, even in the presence of Sororin. The same experiment was repeated with Fragment A of Sororin, leading to the same results (Fig. 18B). All non-Cohesin Separase substrates are efficiently cleaved in the presence of Sororin FL and fragment A, respectively, the Cohesin subunits – or parts thereof – and Separase, however are not (Fig. 18B). This also applies to the protease itself, indicating a Cohesin-specific function for the Sororin mediated Separase inhibition, rather than Sororin being a general inhibitor of Separase.

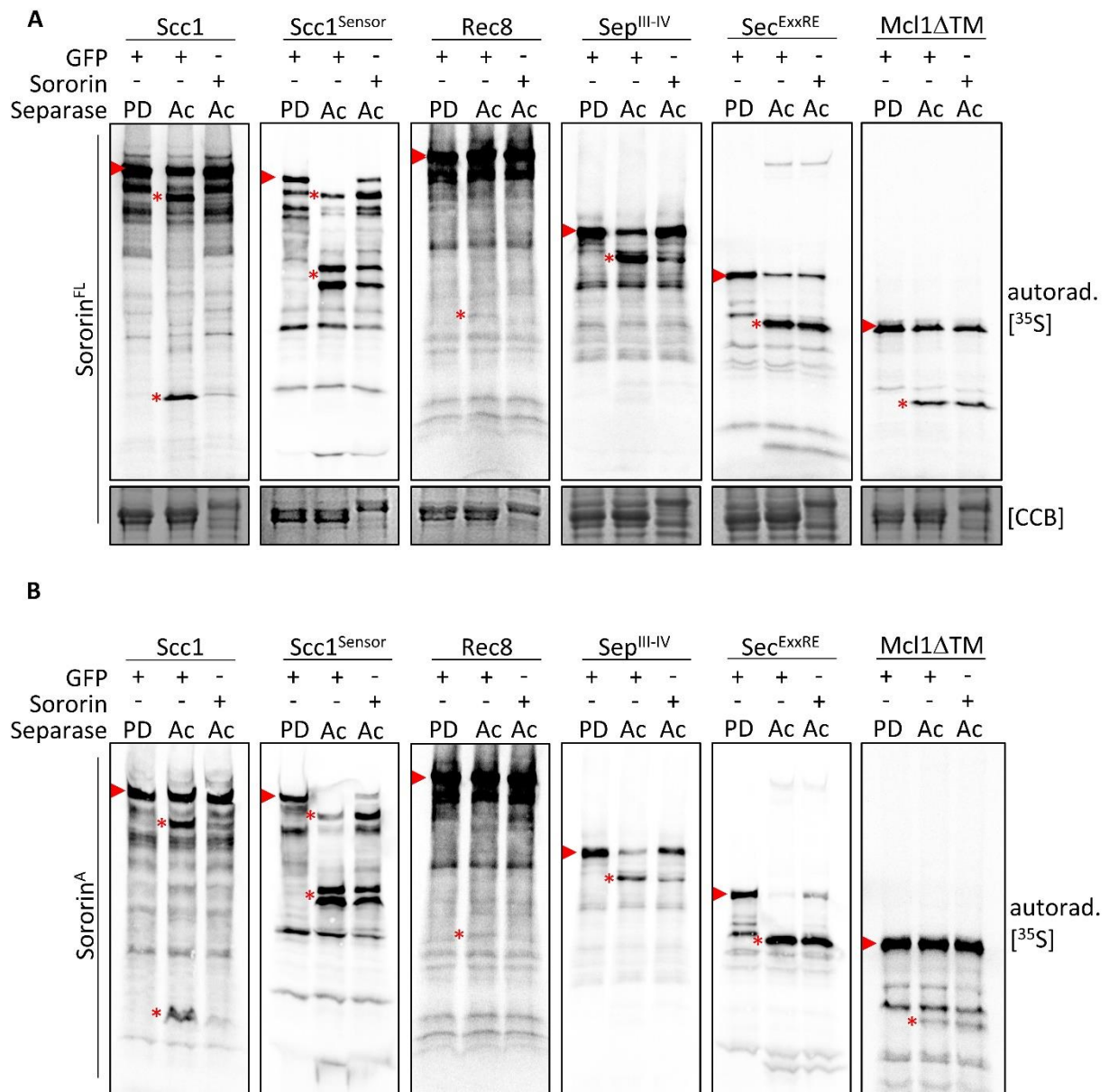


Figure 18 | Sororin's inhibitory effect is limited to Kleisin and Separase auto-cleavage. (A) Recombinant His₆-SUMO3-Sororin^{FL} or (B) His₆-SUMO3-Sororin^A (Sor) or His₆-SUMO3-GFP (GFP) were pre-incubated with active Separase (Ac). Protease dead Separase (PD) was used as a control. Radioactively labelled in vitro expressed ³⁵S-labeled proteins were added. Rec8 was additionally phosphorylated by Plk1 before incubation with active Separase. The Kinase however was subsequently inhibited by its specific inhibitor BI. Samples were boiled with SDS sample buffer, subjected to SDS-PAGE and Coomassie Brilliant Blue (CBB) staining. The corresponding gels were dried and FL proteins (arrowhead) and cleavage fragments (star), respectively, were analysed by autoradiography.

2.4 Sororin's ability to inhibit Separase is dependent on phosphorylation

2.4.1 Preventing Sororin's phosphorylation *in vivo* has no effect on the Sororin-Separase interaction

It is well demonstrated that Sororin is phosphorylated in mitosis. Phosphorylation prevents Sororin's interaction with Pds5, thereby enabling the association of Wapl with Pds5 and subsequent Cohesin ring opening. In contrast, dephosphorylation of Sororin by Sgo1-PP2A at centromeres leads to stable interaction with Cohesin and hence protection of sister chromatid cohesion (Liu et al., 2013; Nishiyama et al., 2013; reviewed in Murayama and Uhlmann, 2015). The coding sequence of mouse Sororin has 37 S/T-residues, 17 of those are confirmed phosphorylation sites, 15 of those are phosphorylated specifically in mitosis and 11 are conserved in the coding sequence of the human protein. All of them have been verified to be phosphorylated by mitotic kinases, such as Cdk1, AurB and Plk1 (Borton et al., 2016; Dreier et al., 2011; Nishiyama et al., 2013; Zhang et al., 2012).

Previous studies showed that mutation of all nine potential CDK1-phosphorylation sites in Sororin (Ser21, Thr48, Ser75, Ser79, Thr111, Thr115, Thr159, Ser181, Ser209) to phosphorylation resistant alanine (Sororin^{9A}) delays Sororin and hence, Cohesin release from chromatin, which also causes lagging chromosomes in anaphase (Nishiyama et al., 2013). Furthermore, the requirement of Sgo1-PP2A for protection of centromeric cohesion is dispensable if Sororin can no longer be phosphorylated by CDK1 (Dreier et al., 2011; Liu et al., 2013). Additionally, preventing phosphorylation of Sororin by AurB, has a similar, but less pronounced effect. Phosphorylation by AurB reduces Sororin's ability to associate with Pds5 (Nishiyama et al., 2013), but completely eliminating all AurB phosphorylation sites (Thr6, Ser29, Ser33, Ser79, Ser83, Ser148, Ser164; Sororin^{7A}) does not cause Sororin to be overly associated with chromatin. In summary this argues for a multi-layered and phosphorylation-dependent regulation of Sororin, in order to achieve Sororin's release from chromatin, which, however, is largely independent of Plk1 (Borton et al., 2016; Nishiyama et al., 2013). We generated respective phosphorylation resistant Sororin mutants by site-specific mutagenesis. Both, Sororin^{9A} and Sororin^{7A} were transiently expressed in HEK293T cells and subsequently isolated via an N-terminal GFP-tag from mitotically arrested cells. Consistently Sororin^{9A} showed stronger Cohesin interaction compared to Sororin^{WT}, as judged by precipitated amounts of Smc3 and Pds5 for Sororin^{9A}. Sororin^{7A} also interacts with Cohesin, but to a smaller

extend, which contradicts the existing literature (Dreier et al., 2011). Interestingly only interaction with Pds5 seems to be strongly impaired in association with Sororin^{7A}, association with Scc1 however is not (Fig. 19). This is in accordance with previous observations, that the Sororin-Cohesin (i.e., Scc1) interaction is not solely dependent on the bridging protein Pds5 but also occurs with Scc1 itself (unpublished observation, data not shown).

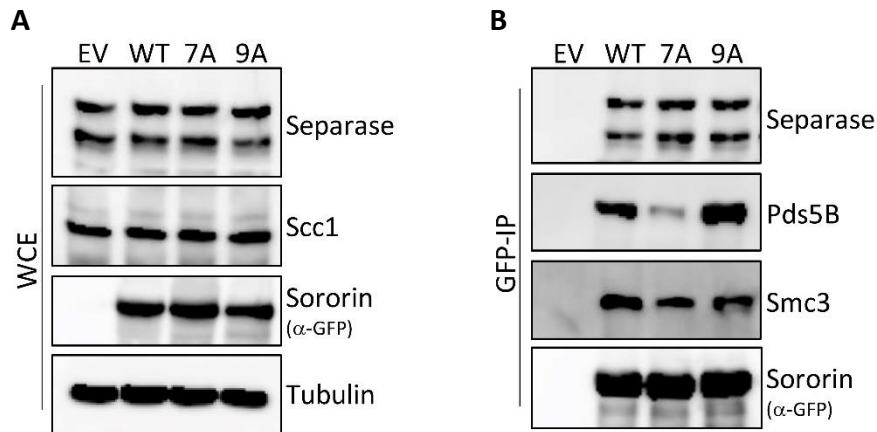


Figure 19 | Sororin variants that can no longer be phosphorylated by AurB or CDK1 still interact with Separase. HeLa K cells were transiently transfected with plasmids encoding C-terminally eGFP tagged Sororin variants as indicated compared to the EV. Cells were arrested in mitosis by taxol treatment approximately 36h after transfection. Additional 14h later cells were harvested by mitotic shake-off. After cell lysis the majority of the respective WCEs were treated with Benzonase and incubated with GFP nanobody coupled beads (GFP-IP). Precipitated proteins were eluted by boiling the beads in SDS sample buffer (B). Small WCE-samples, prior to incubation with GFP nanobody coupled beads, were boiled with SDS sample buffer for “Input”-samples (A). Samples were analysed by immunoblotting using the indicated antibodies (antibodies used against tags are indicated in brackets).

As outlined above, the functionality of Sororin is strongly dependent on (mitotic) phosphorylation, i.e., the ability to tightly interact with Pds5 in a dephosphorylated state in order to protect centromeric cohesion. Therefore, we expected to see Sororin to interact less well with Separase (Fig. 19). We additionally mutated all mitosis specific phosphorylation sites conserved among vertebrates to phosphorylation resistant alanine residues (Ser33, Ser79, Ser83, Thr111, Thr115; Ser 124, Ser125, - Ser126, Ser139, Thr159, Ser164) resulting in the Sororin variant Sororin^{11A}, to exclude phosphorylation by Plk1, CDK1 and AurB (Nishiyama et al., 2013). Here too there is no discernible effect (Fig. 20). In the reverse assumption a “phosphorylation-mimicking” mutant of Sororin, with the respective residues (plus Ser181;

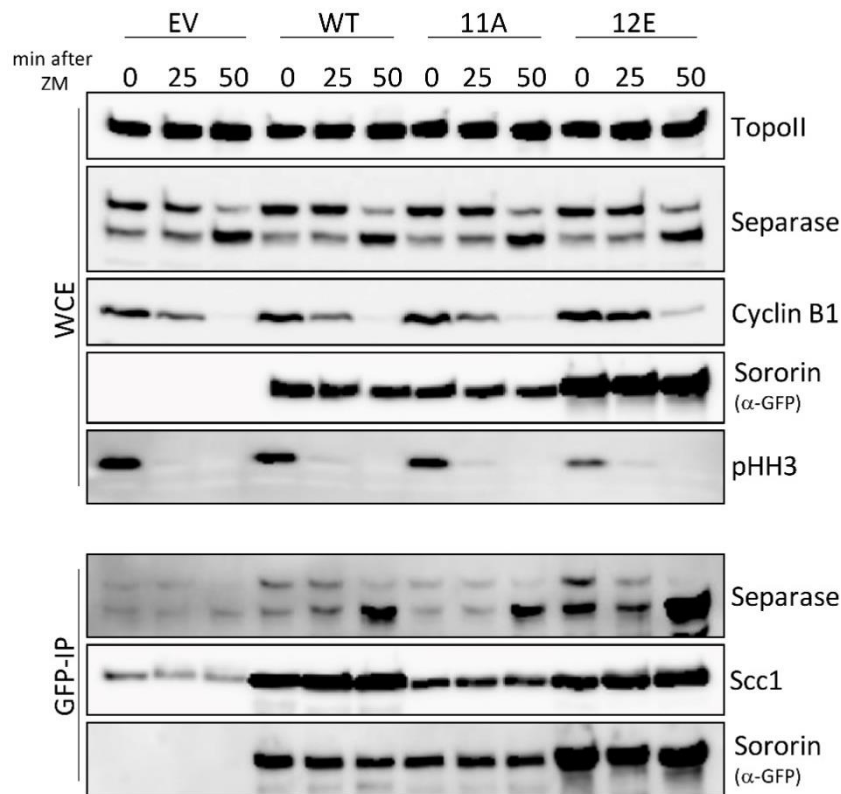


Figure 20| Abolishing or mimicking phosphorylation of Sororin has no effect on its capability to interact with Separase. HeLa K cells were transiently transfected with plasmids encoding C-terminally eGFP tagged Sororin variants as indicated compared to the EV. Cells were arrested in mitosis approximately 36h after transfection by taxol treatment. Additional 14h later cells were either harvested by mitotic shake-off (“0”) and partially further treated after shake-off with ZM for 25 min and 50 min (“25” and “50”). WCE’s were boiled with SDS sample buffer and analysed by immunoblotting using the indicated antibodies. Subsequently, cell lysates were treated with Benzonase and incubated with GFP nanobody coupled beads. Precipitated proteins were eluted by boiling the beads in SDS sample buffer. Samples were analysed by immunoblotting using the indicated antibodies (antibodies used against tags are indicated in brackets).

Nishiyama et al., 2013) mutated to glutamic acid (Sororin^{12E}), should show stronger interaction with Separase. Again, this is not apparent *in vivo* (Fig. 20).

Solely based on co-purification experiments from cells, phosphorylations seems to have no effect on the Separase-Sororin interaction, albeit it does affect Sororin-Cohesin interaction.

Therefore, we postulate that one of the 20 remaining S/T-residues, which have not yet been shown to be phosphorylated, may still undergo phosphorylation and influence the formation of the Separase-Sororin complex.

2.4.2 Phosphorylation by mitotic kinases render Sororin unable to inhibit Separase *in vitro*

To further analyze the effect of mitotic phosphorylation on Sororin's capability to efficiently interact with Separase, recombinant FL His₆-SUMO3-Sororin was *in vitro* phosphorylated by recombinant AurB, CDK1-Cyclin B1 or Plk1. Successful phosphorylation and, hence, kinase activities were confirmed by both visible mobility shifts and incorporation of radioactive phosphate (Fig. 21). The respective kinases were inhibited by their specific inhibitors (AurB: ZM, Plk1: BI, CDK1: Roscovitine) and Securin-free active or PD Separase was added. Separase's proteolytic activity was assessed by autoradiographic analysis of the finally added *in vitro* expressed and ³⁵S-labeled Scc1. Remarkably, phosphorylation by AurB and CDK1 rendered Sororin unable to re-inhibit active Separase, whereas phosphorylation by Plk1 had no effect on Sororin's inhibitory function (Fig. 21).

To exclude any effect on Separase activity by residual active kinases, the same experiment was repeated. After phosphorylation His₆-SUMO3-Sororin (or -GFP) was re-isolated via its affinity tag and the respective mitotic kinases were removed by extensive washing steps. The loss of Sororin's capability to inhibit Separase *in vitro*, mediated by phosphorylation of AurB and CDK1, but not Plk1 was again evident (data not shown). These results strongly indicate that the inhibitory effect of Sororin on Separase is extinguished by phosphorylation of Sororin by the kinases AurB and CDK1. This *in vitro* result is in seeming contradiction to the pull-down experiment of Soroin^{12E}.

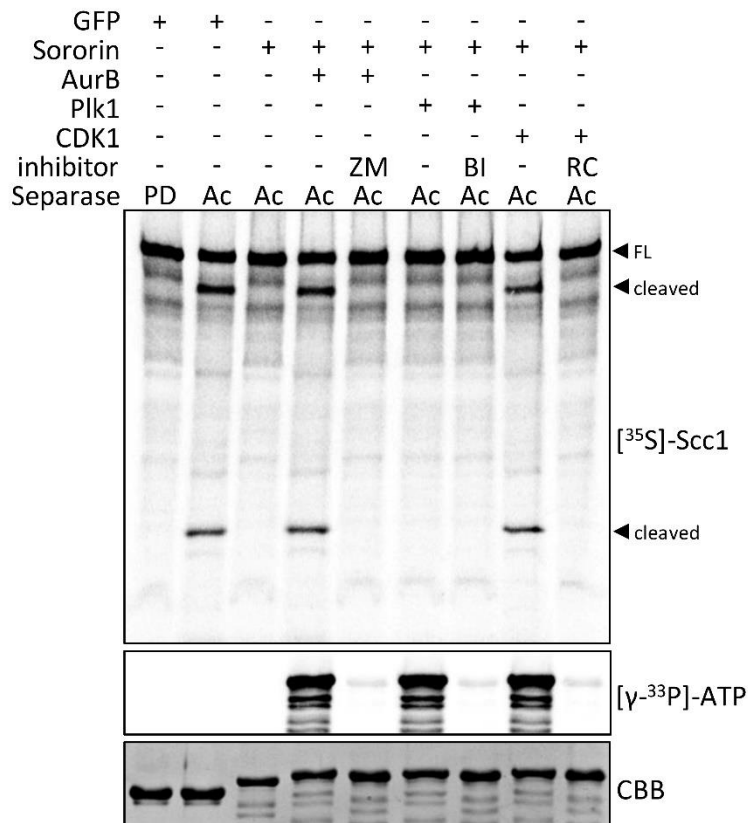


Figure 21 | Sororin inhibits Scc1 cleavage by Separase in a phosphorylation dependent manner. Recombinant His₆-SUMO3-Sororin^{FL} was phosphorylated by AurB, CDK1 and Plk1, respectively. Kinases were inhibited if indicated (ZM: ZM447439/AurB, BI: BI-2536/Plk1, RC: Roscovitine/CDK1). Phosphorylated His₆-SUMO3-Sororin^{FL} or His₆-SUMO3-GFP (GFP) were pre-incubated with active Separase (Ac). Protease dead Separase (PD) was used as a control. Radioactively labelled *in vitro* expressed and ³⁵S-labeled Scc1 was added. Samples were boiled with SDS sample buffer after incubation, subjected to SDS-PAGE and Coomassie Brilliant Blue (CBB) staining. The corresponding gel was dried and FL proteins and cleavage fragments (indicated by arrowheads), respectively, were analysed by autoradiography. Additionally, Sororin was phosphorylated as described using radioactively labelled ATP to demonstrate phosphorylation and kinase inhibition, respectively (middle panel, [γ -³³P]-ATP).

2.4.3 Phosphorylation of Sororin’s N-terminus has no impact on Sororin-Separase complex formation

In chapter 2.2.2 (see above) we show that the N-terminus of Sororin (i.e., fragment A) is responsible for the interaction with Separase. Thus, we speculated that AurB and Cdk1 control Sororin’s inhibitory activity by phosphorylation of the N-terminus. Accordingly, we tested the

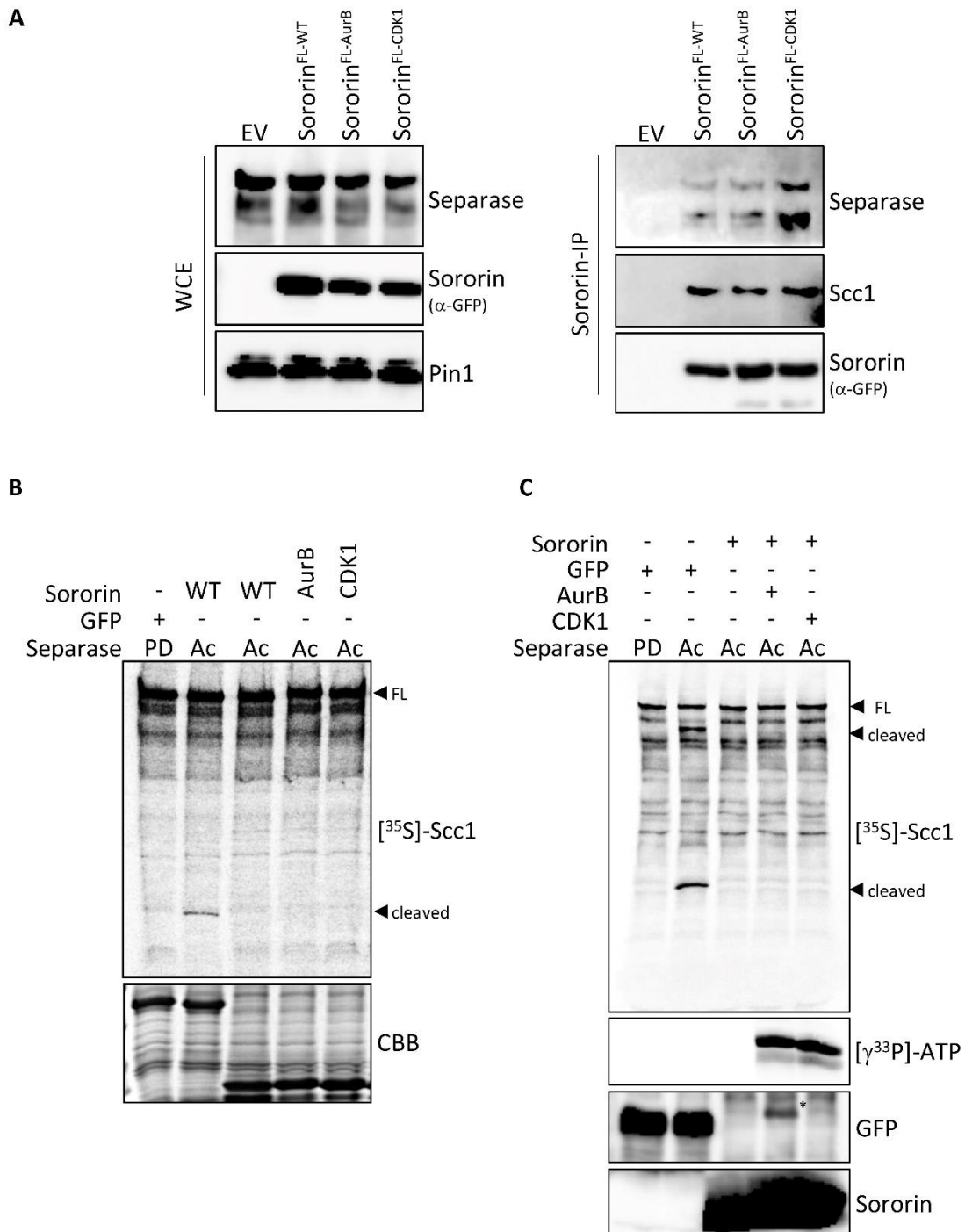


Figure 22 | Sororin variants mimicking phosphorylation by AurB or CDK1 still interact with Separase. See next page for legend.

Figure 22 | Sororin variants mimicking phosphorylation by AurB or CDK1 still interact with Separase. (A) HeLa K cells were transiently transfected with plasmids encoding C-terminally eGFP tagged Sororin FL-variants as indicated compared to the EV. Cells were arrested in mitosis approximately 36h after transfection by taxol treatment. Additional 14h later cells were either harvested by mitotic shake-off. WCE's were boiled with SDS sample buffer and analysed by immunoblotting using the indicated antibodies. Subsequently, cell lysates were treated with Benzonase and incubated with GFP nanobody coupled beads. Precipitated proteins were eluted by boiling the beads in SDS sample buffer. Samples were analysed by immunoblotting using the indicated antibodies (antibodies used against tags are indicated in brackets). (B) Recombinant His₆-SUMO3-Sororin phosphomimicking fragment variants as indicated or His₆-SUMO3-GFP (GFP) were pre-incubated with active Separase (Ac). Protease dead Separase (PD) was used as a control. Radioactively labelled *in vitro* expressed ³⁵S-Scc1 was added. Samples were boiled with SDS sample buffer, subjected to SDS-PAGE and Coomassie Brilliant Blue (CBB) staining. The corresponding gel was dried and Scc1 cleavage fragments (arrowhead) were analysed by autoradiography. (C) Recombinant His₆-SUMO3-Sororin phosphomimicking fragment variants as indicated were *in vitro* phosphorylated by their corresponding kinase. His₆-SUMO3-GFP (GFP) was used as a control. The corresponding Separase cleavage-assay was performed as described. An unspecific background band is marked with an Asterix (*). Successful phosphorylation was examined by a separate corresponding assay using radioactively labelled [³³P]-ATP.

effect of AurB and Cdk1 mediated phosphorylation on fragment A of Sororin. Mass spectrometry identified six phosphorylation sites within the first 87 aa of Sororin's N-terminus (Nishiyama et al., 2013). Using *E. coli*, we generated recombinant protein mutants that mimic phosphorylation for either AurB (Thr6, Ser29, Ser33, Ser79, Ser83; Sororin^{FL-AurB}) or CDK1 (Ser21, Thr48, Ser75, Ser79; Sororin^{FL-CDK1})-phosphorylation sites, respectively. Mimicking of the phosphorylated state of a protein is achieved by substitution of the serine/threonine phosphorylation site by an acidic negatively charged aspartate residue. The mutations were introduced into Sororin^{FL} and expressed in *E. coli*, however, they were not soluble (data not shown). Therefore, they were again expressed in human cell culture but again no apparent effect on the Sororin-Separase interaction *in vivo* was discernable (Fig. 22A). Additionally, His₆-SUMO3-hSororin^{FL}, with the respective introduced mutations was not soluble in *E.coli* (data not shown). Therefore, we expressed only the N-terminal fragment in bacterial cell culture. The purified proteins were again pre-incubated with active Separase and Separase's proteolytic activity was assessed by autoradiographic analysis of the finally added ³⁵S-labeled Scc1. Active Separase is efficiently re-inhibited by Sororin's N-terminus. The analyzed mutants, mimicking phosphorylation at indicated sites, however re-inhibited active Separase in a highly comparable manner.

As already mentioned, phosphorylation mimicry involves replacing the serine/threonine phosphorylation site with an acidic aspartate residue to replicate the phosphorylated state of a protein. This mimicry of phosphorylation by a single residue substitution might not be functional (Pearlman et al., 2011). Therefore, the N-terminal fragment of Sororin was first

phosphorylated by AurB and CDK1, respectively. Then phosphorylated Sororin was incubated as described before and Separase-activity was again analyzed by ³⁵S-labeled Scc1 (Fig. 22B). Phosphorylation occurred as judged by autoradiography with radioactively labeled ³³P-ATP. However, even though phosphorylated, the N-terminus of Sororin still efficiently inhibits active Separase *in vitro* (Fig. 22C).

Taken together Sororin's ability to inhibit Separase is highly dependent on phosphorylation of Sororin. However, even though Sororin interacts with Separase predominantly via its N-terminus, phosphorylation of the N-terminus has no effect on Separase's proteolytic activity in context of a Sororin-Separase complex. This observation indicates that phosphorylation of other and/or additional residues in the middle or C-terminal part of Sororin are responsible for preventing Sororin's ability to inhibit active Separase. It will be interesting to analyze this further.

3 Discussion

Stable cohesion of sister chromatids is established in a co-replicative manner, dependent on acetylation of Smc3 by Esco1 and Esco2 (Rolef Ben-Shahar et al., 2008; Unal et al., 2008; Zhang et al. 2008). Acetylation of Lys105/106 of Smc3 facilitates recruitment of the Wapl-competitor Sororin to Cohesin, thereby displacing Wapl from Pds5 and establishing stable cohesion (Ladurner et al., 2016; Lafont et al., 2010; Nishiyama et al., 2010). During mitosis Cohesin is removed in a stepwise manner. In the first step, also called the prophase pathway, Cohesin along chromosome arms is removed in a phosphorylation dependent manner (reviewed in Morales and Losada, 2018; Waizenegger et al., 2000). Sororin is phosphorylated by mitotic kinases (AurB and CDK1), which results in the dissociation of Sororin from Pds5 and allows reassociation of Wapl to Pds5 and, hence, ring-opening (Dreier et al., 2011; Gandhi et al., 2006; Nishiyama et al., 2010; Nishiyama et al., 2013). Centromeric Cohesin is protected against the prophase pathway until metaphase to maintain sister chromatid cohesion. Therefore Sgo1-PP2A is recruited to centromeres, which keeps Sororin in a dephosphorylated state by the action of PP2A (Liu et al., 2013; Tang et al., 2006). At the metaphase to anaphase transition Separase is activated due to destruction of Securin by the APC/C^{Cdc20}, which results in proteolytic cleavage of Scc1 and finally triggers sister chromatid separation (Hauf et al., 2001; Uhlmann et al., 1999).

In this study we identified Sororin as a new interactor of human Separase. We clearly show that Separase interacts with Sororin (Fig. 7, Fig. 10). Importantly, we also show that Sororin is able to inhibit Separase *in vitro*, as measured by impaired cleavage of Scc1 (Fig. 16). This interaction and inhibitory function of Sororin on Separase is modulated via phosphorylation of Sororin by the mitotic kinases AurB and CDK1. Phosphorylation by said kinases results in Sororin losing its ability to inhibit Separase. Phosphorylation by another important mitotic kinase Plk1, however has no such effect (Fig.21). Additionally, we show that the N-terminus of Sororin is required for Separase interaction (Fig. 17). Overall, we provide evidence for adding a new component to the portfolio of Separase's interactors and inhibitors.

3.1 The Separase-Sororin interaction is likely not conserved in *Xenopus* and *Drosophila*

Intrigued by this newly identified interaction of the two essential master regulators of the mammalian cell cycle, we tested whether said interaction is conserved among species. Much like Separase, the overall function of Sororin is conserved, the sequence however, is not, even among vertebrates. In yeast for example a homologous sequence of Sororin cannot be found, instead it was suggested that this protein is functionally replaced by the fungal Smc3 acetyltransferase Eco1 (Borges et al., 2013; Lafont et al., 2010; Zhang and Pati, 2012). However, for both – Separase and Sororin – a few conserved sequence elements are reported, which are important for the proteins function among different species (Luo and Tong, 2018; Nishiyama et al., 2010; Wu et al., 2011; Zhang and Pati, 2012). We tested the existence of a conserved Separase-Sororin complex among taxa, first by using cultured *Xenopus laevis* S3 cells. To this end, *Xenopus* cDNA was isolated, which encodes a closely related protein functionally related to mammalian Sororin with respect to Cohesin interaction (Nishiyama et al., 2010). Using *Xenopus* cell culture, the Sororin-Separase interaction could not be demonstrated in *Xenopus* S3 cells, suggesting complex formation is most likely not conserved in amphibia (Fig. S3). Furthermore, we tested whether the Sororin-Separase interaction is detectable in *Drosophila melanogaster*. Both proteins have unique characteristics: That is, in contrast to mammalian Separase, the functional equivalent in *Drosophila* is a dimeric protein-complex consisting of the two proteins Three rows (THR) and SSE. The latter appears to correspond to the more conserved C-terminal domain of Separase, although with a highly divergent protease domain compared to Separase's from other species (Jäger et al., 2001). In contrast, THR has no known sequence-homologs and likely correlates to the TPR-repeats of other Separase's, which is missing in the N-terminal region of *Drosophila* Separase/SSE. The *Drosophila* Separase hetero-dimeric complex is inhibited by the essential protein Pimples (PIM) (Jäger et al., 2001; Jäger et al., 2004). The *Drosophila* protein Dalmatian (Dmt) was characterized as a Sororin ortholog exerting Sororin-like Cohesin establishment functions (Nishiyama et al., 2010). It was recently demonstrated, that Dmt is actually a hybrid protein harboring a conserved C-terminal Sororin-domain and a N-terminal domain with Sgo1-like Cohesin protective functions (Nishiyama et al., 2010; Yamada et al., 2017). Depleting either protein (Sororin or Sgo1, respectively), using siRNAs in human cells, leads to premature sister chromatid separation (McGuinness et al., 2005; Rankin et al., 2005). Each depletion can be

rescued to a considerable degree by Dmt expression (Yamada et al., 2017; data not shown). We were not able to isolate a *Drosophila* Separase-Sororin/Dmt complex from cultured *Drosophila* S2 cells (Fig S3). Taken together these experiments in *Xenopus* and *Drosophila* cells indicate that the Separase-Sororin complex is not conserved among evolutionary distant taxa (Wheeler and Brändli, 2009). However, the Sororin-Separase complex is conserved in mice, as demonstrated by IP western blot analysis (data not shown), arguing for conservation of complex formation in mammals.

3.2 Separase interacts with its inhibitors in a mutually exclusive manner

Importantly, we show herein that Sororin is able to inhibit active Separase *in vitro*, thereby adding a fourth inhibitor to the list of Separase inhibiting proteins (Fig. 16). It has been extensively demonstrated that Separase's interaction with its well characterized main inhibitors Securin and CDK1-Cyclin B1 is mutually exclusive (Gorr et al., 2005; Hellmuth et al., 2015b). This mutual exclusiveness in Separase binding extends to the recently identified Separase inhibitor Sgo2-Mad2 (Hellmuth et al., 2020). The multitude of Separase inhibitors are thought to add additional levels of regulation in order to govern anaphase. Separase deregulation would otherwise result in incomplete or premature Cohesin removal, anaphase bridges and ultimately disease (Hellmuth and Stemmann, 2020; Shindo et al., 2021). Using TAP-analysis we can show that Sororin-associated Separase cannot interact with the other three established inhibitors at the same time (Fig. 10). Surprisingly, however, we are able to demonstrate a multimeric complex consisting of Separase, Sororin and Scc1 (i.e., Cohesin) (Fig. 10).

It was previously demonstrated that Scc1 cleavage is DNA-dependent, which in turn means that cytoplasmic Cohesin is resistant to active Separase during anaphase (Sun et al., 2009; Kucej and Zou, 2010). Intact Cohesin, removed in early mitosis by the prophase pathway, can therefore be recycled in the next cell cycle because it is not cleaved by Separase (Kucej and Zou, 2010; Sun et al., 2006; Waizenegger et al., 2000). Cohesin that was removed from chromosome arms is no longer in complex with Sororin due to phosphorylation of the latter by mitotic kinases (Nishiyama et al., 2013). Additionally, reassociation of Sororin with Cohesin is prevented by action of the deacetylase HDAC8 (Hos1 in yeast), which deacetylates Smc3 upon Cohesin's dissociation from chromosomes. This ensures the availability of unacetylated

Smc3 for *de novo* acetylation in the next cell cycle, which is necessary for efficient cohesion (Beckouët et al., 2010; Borges et al., 2010; Li et al., 2017). Interestingly, the replisome is thought to be required to recruit dynamic Sororin to chromatin. However, because the replisome is not present during G2 it cannot be responsible for initial and then continued binding of Sororin (Ladurner et al., 2016; Lengronne et al., 2006; Moldovan et al., 2006). Therefore, the authors further speculate that an additional unknown factor, besides acetylated Smc3, allows Sororin to bind to Cohesin in G2 (Ladurner et al., 2016). Once Smc3 is acetylated by Esco1, whose recruitment is mediated by Pds5 (Minamino et al., 2015; Vaur et al., 2012), Sororin is able to bind to Cohesin, bridged by Pds5. Interaction with Pds5 is thereby thought to be facilitated by Sororin's FGF-motif. However, a second motif conserved among vertebrates was identified: the YSR-motif (Nishiyama et al., 2010; Ouyang et al., 2016). Mutating either motif can abolish Sororin's interaction with Pds5 (Nishiyama et al., 2010; Ouyang et al., 2016; Wu et al., 2010; reviewed in Zhang et al., 2021). Trying to reproduce these results we were only able to verify the YSR-motif of Sororin to be important for Pds5 and hence, Cohesin-interaction (Fig. S6). Those motif-mutations however, had no effect on Separase-Sororin complex formation (Fig. S6). Interestingly, using fragments of Scc1, we also observed by *in vitro* and *in vivo* analysis that Sororin is able to strongly interact with the N- (aa 1-294) and C-terminus (aa 573-753) of Scc1, but rather weakly with the middle part (aa 295-572). These interactions are independent of its ability to form a complex with Pds5 (Fig. S6). Therefore, we propose that Scc1 itself might be this abovementioned, additional factor, which is responsible for Sororin's continued recruitment to Cohesin. Furthermore, it is conceivable that complex-formation of Separase, Sororin and Cohesin (i.e., Scc1) either shields Scc1 from Separase or specifically recruits Separase to the Cohesin subunit. It is tempting to speculate that Sororin serves the dual purpose of recruiting Separase to Cohesin, while simultaneously protecting Cohesin/Scc1/Rec8 from premature cleavage. If true, this would raise the question of how Sororin's protective activity is switched off (see 3.7)

3.3 Sororin interacts with Cohesin – independently of Pds5

This highly hypothetical model is supported by the observation that Sororin is not a general inhibitor, but predominantly protects Cohesin (i.e., Scc1; Rec8) and Separase itself (Fig. 18). The Scc1-Sensor also used in this study, is derived from a rather large part of Scc1 (aa 142-

476), containing the Separase cleavage site and also the N-terminal part of Scc1, that is able to interact with Sororin independently of Pds5 (Shindo et al., 2012; Fig. S6). Recent observations also implicate that shorter Sensor-peptides, still containing the Separase cleavage site, are less optimal substrates for Separase mediated cleavage. Therefore Shindo et al., 2021 speculate that the original sensor (Shindo et al., 2012) - in addition to the cleavage site - contains another domain that facilitates or boosts cleavage. Consistently, mutating Separase cleavage sites within Scc1 had no effect on the Separase-Sororin interaction (data not shown). Taken together this suggests that substrate-cleavage is somehow enhanced within cells (Lin et al., 2016; Rosen et al., 2019; Sun et al., 2009). Consistently, it was recently demonstrated that Scc1 contains a docking interaction site (exosite), termed the LPE-motif in addition to its Separase cleavage site, which is located within the N-terminal region of Scc1 analyzed in this study (Fig. S3). Interestingly, this exosite is also found within Securin (Rosen et al., 2019) and even more astounding, also in the Sororin peptide-sequence. However, mutating the corresponding motif of Sororin, no significant effect in terms of Sororin-Separase-interaction, Sororin-Scc1-interaction, or Scc1-protection from Separase by Sororin could be observed.

3.4 Mapping Sororin interaction sites on Separase

To further study the Sororin-Separase interaction the identification of a separation of function Sororin- or Separase-variant is essential, because Sororin not only inhibits Separase (this study), but also protects centromeric Cohesin from the prophase pathway. For functional characterization of the importance of the Separase-Sororin interaction it is therefore crucial to isolate Sororin variants that can still function in protection from Wapl but not inhibit Separase any longer and vice versa.

Therefore, we first aimed to identify a Separase-variant deficient in Sororin-interaction and used the basic assumption, that Sororin-Separase complex formation might be exclusive to one of the two *cis/trans* isoforms of Separase. It has been previously reported that Separase is mostly present in *trans*-conformation, thereby interacting with Securin. Upon removal of Securin, phosphorylation and Pin1-mediated isomerization during mitosis, the Separase equilibrium shifts to the *cis*-conformation, which is mostly associated with CDK1-Cyclin B1 and resistant to Securin-interaction (Hellmuth et al., 2015b). Time resolved Sororin- and Separase-

IPs, respectively, followed by immunoblot analysis demonstrate Separase-Sororin complex formation in early mitosis, where the *trans*-conformer is dominant. During mitotic exit Sororin interaction with Separase, now in *cis*-conformation, can still be observed (Fig. 12). It should be emphasized that the interaction with *cis*-Separase seems to become even stronger, which is evident from the increasing interaction of Sororin with auto-cleaved Separase (Fig. 12). Separase variants that are either non-cleavable or engineered to be fully cleaved by co-expressed TEV-protease, show no preference for Sororin-interaction (data not shown). Therefore, we assume that the observed strong interaction with auto-cleaved Separase during mitotic exit is probably explained by the high abundance of cleaved Separase in late mitosis, rather than increased preference for auto-cleaved Separase. In summary, Sororin-interaction with Separase seems to be independent of the protease's isomerization and auto-cleavage.

In human cells the Separase-Securin complex further associates with PP2A, which keeps Securin in a dephosphorylated state, thereby preventing premature APC/C-mediated destruction and, hence, Separase-activation (Hellmuth et al., 2014). An attractive initial model for modulating Sororin's function within the Separase-Sororin complex and for complex formation in the first place was the well characterized interaction of Separase and PP2A (Gil-Bernabé et al., 2006; Hellmuth et al. 2014; Holland et al., 2007). However, mutating a conserved MxxlxxE-motif, responsible for PP2A interaction within Separase (Hellmuth et al., 2014; Hertz et al., 2016), had no effect on Separase-Sororin complex formation or the phosphorylation-status of Sororin, respectively (data not shown).

Identifying a Sororin-binding deficient Separase-variant by educated guessing turned out be quite challenging. Therefore, we sought to use a broader approach by identifying a minimal segment of Separase, that retains Sororin-binding. To this end, we generated a variety of Separase-fragments based on recently published crystal and Cryo-EM structures of yeast and *C. elegans* Separase in complex with Securin, respectively (Boland et al., 2017; Luo and Tong, 2017). Co-translational association of Securin with nascent Separase is important for proper folding of the protease and, hence, solubility and function (Hellmuth et al., 2015a, Hornig et al., 2002). Therefore, Separase fragments were designed to end in between of secondary structure elements containing at least one potential Securin-interaction site to possibly enhance their solubility *in vivo* (Fig. 13, Fig. 14). All tested fragments of Separase turned out

to be soluble upon expression in human cell culture (Fig. 14). C-terminal fragments containing a small globular domain (aa1808-1886), termed the Separase module, are additionally soluble when expressed in *E. coli*. This argues that this domain achieves a natively folded state even in the absence of Securin (data not shown). Furthermore, we are able to demonstrate Sororin-interaction with all generated domains, except for the Separase module (Fig. 14). However, this might help to shed further light on Sororin's mode of inhibition: the Separase module is arranged next to domain IV according to Separase's crystal structure (Fig. 13), which is adjacent to the previously identified WR-motif of Separase; the latter is involved in substrate recognition (Winter et al., 2015; Luo and Tong, 2018). Mutating the WR-motif abolished Scc1-cleavage by Separase, even though the catalytic dyad remains intact (unpublished results). It was recently demonstrated, that Securin inhibits Separase by acting as a competitive inhibitor utilizing a non-cleavable pseudosubstrate sequence which blocks Separase's active site: mutating the Pro of a conserved $D/EIExxP$ (x: any residue) consensus motif to Arg, turns Securin into a substrate of Separase (Luo and Tong, 2018). The same applies to the mode of Separase-inhibition by Sgo2-Mad2. Here, too, Sgo2 acts as a pseudo substrate in order to inhibit Separase (Hellmuth et al., 2020). However, changing residues at a +3 position relative to a Glu did not result in Sororin being cleaved by Separase (data not shown). Therefore, Sororin most likely does not inhibit Separase by using a pseudo substrate motif (Fig. 14). Despite this important difference between Sororin and Securin, both inhibitors share the characteristic of being natively unfolded. This assumption is supported by data obtained using circular dichroism-spectroscopy, which showed that Sororin contains very little secondary structure elements (data not shown). This indicates that Sororin, as well as Securin, is a mostly disordered protein, which also interacts preferably with Separase's C-terminal SD- and CD-domain. However, we do not have definitive proof for that assumption, which makes further analysis necessary. Taken together, we assume that the mostly disordered protein Sororin, like Securin, interacts with Separase over the entire length (Boland et al., 2017; Csizmok et al., 2008; Holland et al., 2007; Jäger et al., 2004; Luo and Tong, 2018; Nasmyth et al., 2023; Viadiu et al., 2005), but preferentially with the conserved C-terminal part of the enzyme.

3.5 Mapping Separase-interaction sites on Sororin

In the reverse approach, we wanted to identify a region or possibly a specific motif within Sororin that is responsible for Separase-binding. As already mentioned before, much like Separase, the function of the Sororin protein is conserved, the sequence however is not, as demonstrated by alignment of orthologs (Wu et al., 2011). However, a few conserved domains, within the Sororin protein, were reported, such as an arginine (R)-rich region in the otherwise highly divergent N-terminus. Additionally, a conserved KEN-box, which is responsible for Sororin's instability throughout the cell cycle by APC/C^{Cdh1} dependent degradation (Rankin et al., 2005; Wu et al., 2011). The FGF- and YSR-motifs, respectively, located in Sororin's middle, are also relatively well conserved among species. The same applies to Sororin's C-terminus, which is also called the "Sororin-domain" (Nishiyama et al., 2010; Wu et al., 2011). This Sororin-domain is critical for Sororin's function, as deleting parts thereof causes impaired Cohesin-interaction, which in turn also causes impaired chromatin-interaction and as a consequence premature sister chromatid separation (Nishiyama et al., 2010; Wu et al., 2011). Therefore, Sororin was divided into four similar sized fragments, while avoiding the destruction of conserved motifs and domains (Fig. 15).

By using *in vivo* and *in vitro* approaches we are able to clearly show that the first 87 aa of Sororin (Fragment A) is sufficient and most likely necessary for Separase interaction and inhibition (Fig. 17). Importantly, deleting the N-terminus (ΔA) of Sororin had no effect on Cohesin binding (Fig. 15) and cohesion (data not shown), arguing for the desired separation of function Sororin-variant. By utilizing this Sororin-variant (ΔA), it may be feasible to analyze the interaction between Separase and Sororin, as it allows for a specific loss of Separase-interaction while preserving Cohesin-interaction *in vivo*.

Interestingly, it has previously been demonstrated that deleting a large portion of Sororin's N-terminus has no effect on Cohesin-interaction or sister chromatid separation (Wu et al., 2011). However, I noticed that N-terminally truncated Sororin-variants were preliminary (but not exclusively) localized in the cytoplasm in asynchronous living cells, as analyzed by immunofluorescence microscopy (Fig. S4 and S5). In summary this indicates that the N-terminal part of Sororin is a newly discovered NLS. However, this was not further analyzed in

this work, since no obvious phenotype regarding Sororin-Separase interaction could be observed using N-terminally truncated Sororin-variants.

3.6 Sororin's function is dependent on phosphorylation

Sororin's conserved function in mediating sister chromatid cohesion is negatively regulated by phosphorylation by mitotic kinases, predominantly AurB and CDK1 (Borton et al., 2015; Dreier et al., 2011; Nishiyama et al., 2013; Zhang et al., 2012). Once phosphorylated the interaction with Cohesin is lost by disrupting the Sororin-Pds5 interaction, suggesting phosphorylation causes Sororin to be released from chromatin (Dreier et al., 2011; Liu et al., 2013). By using phosphorylation resistant Sororin-mutants, cohesion between chromosome arms is increased, demonstrating the purpose of phosphorylation by AurB and CDK1 is to remove Sororin from Cohesin. This in turn disrupts stable cohesion and ultimately allows removal of Cohesin from chromosome arms by the prophase pathway. At centromeres phosphorylation is counteracted by Sgo1-PP2A in order to protect centromeric cohesion until anaphase-onset (Dreier et al., 2011; Liu et al., 2013; Nishiyama et al., 2013). By expressing a Sororin variant with all Ser/Thr residues changed to phosphorylation resistant Ala (Sororin^{11A}), previous studies demonstrated increased persistence of Sororin on chromosome arms (Nishiyama et al., 2013). In contrast, a phosphomimicking variant (Sororin^{12E}) showed less stable interaction with chromatin (Nishiyama et al., 2013). Using corresponding phosphorylation resistant or phosphomimicking mutants in human cell culture however did not have the hoped-for effect. No significant effect on Separase-Sororin complex formation could be observed (Fig. 20). The same applies to variants that are specifically resistant to phosphorylation by AurB or CDK1 (Sororin^{9A}, Sororin^{7A}, Fig. 19), Separase-Sororin interaction remained the same in comparison to Sororin^{WT}. We were therefore not able to demonstrate phosphorylation dependent interaction defects *in vivo* (Fig. 19, Fig. 20). Here, a cell line in which the N-terminal 88 aa part of both Sororin encoding alleles is deleted by homologous knock-in using CRISPR/Cas9 would be helpful. This cell-line should be able to mediate cohesion, but Separase-interaction should be impaired.

Additionally, one could utilize a targeted protein degradation system, such as the AID/Tir1-system to specifically remove AID-tagged Sororin during mitosis. To achieve specific protein degradation in mitotic cells using this AID-system, a stable cell line expressing the SCF-complex

component Tir1 would be necessary. Adding the plant hormone Auxin at a specific time, such as during early mitosis, rapid degradation of a co-expressed, AID-tagged protein by the proteasome – for example Sororin – would be triggered (Nishimura et al., 2009). In metaphase, Sororin could be safely switched off since the prophase pathway is presumably no longer active and separase is not yet active. Thus, the physiological relevance of the Separase-Sororin interaction could be studied *in vivo* using both temporal- a target-specific degradation.

By further utilizing *in vitro* phosphorylation of recombinant Sororin by AurB, CDK1 and Plk1, we clearly demonstrate that Sororin's ability to be an inhibitor of Separase *in vitro* is dependent on phosphorylation by AurB and CDK1, but not Plk1 (Fig.21). Considering that the N-terminus of Sororin is responsible for Separase interaction, this observation can be partially explained: By using mass spectrometry, four Plk1 phosphorylation sites were identified in Sororin's peptide sequence. None of those Plk1-phosphorylation sites are located within the first 100 aa of Sororin (Dreier et al., 2011; Nishiyama et al., 2013). This might explain why Plk1-phosphorylation of Sororin has no effect on Sororin's ability to inhibit Separase.

Since fragment A of Sororin is responsible for Separase interaction and inhibition, respectively we created corresponding phosphomimicking mutants of fragment A. Considering our previous results, we expected these phosphomimicking mutants to lose their ability in inhibiting Separase *in vitro*. Surprisingly, that was not the case (Fig. 22). To exclude insufficient phosphomimicking by acidic residues did not effectively work in this case, fragment A of Sororin^{WT} was treated *in vitro* with AurB or CDK1. In stark contrast to phosphorylation of Sororin^{FL}, phosphorylation of Sororin's N-terminus did not hinder Sororin's inhibitory function on Separase activity *in vitro* (Fig. 22).

Taken all results of this work into consideration, a basic and speculative model of Sororin's mode of interaction can be proposed. Sororin possibly interacts with Separase similar to Securin, namely over the entire length of the protease. However, we frequently observed stronger interaction with the C-terminal part of Separase. This might be due to missing N-terminal Separase domains in the experimental setup, which could be critical for strong Sororin interaction. Another possible explanation would be that the interaction of Sororin with the C-terminus of Separase is quite stable, while interaction with the N-terminus of Separase is rather transient, possibly due to a conformational change of Sororin (Fig. 23). This

hypothetical conformational change might be induced by phosphorylation, which is supported by the observation that Sororin's ability to inhibit Separase *in vitro* can be reversed by phosphorylation. Additionally, Sororin's N-terminus alone is able to inhibit Separase *in vitro*, phosphorylation of this N-terminus however has no effect and is not able to reverse Sororin's inhibitory function. As demonstrated previously, Securin uses a conserved LPE-motif to bind to a so far unknown exosite within Separase in addition to blocking the active center of Separase by acting as a pseudosubstrate (Liu and Tong, 2018; Rosen et al., 2019). Scc1 exhibits a similar motif, which is also responsible for interaction with Separase (Hara et al., 2014; Rosen et al., 2019). Interaction of Separase with the conserved LPE-motif of Scc1 further modulates substrate affinity and cleavage efficiency. Securin binding to the same exosite of Separase, likely prevents Scc1-interaction

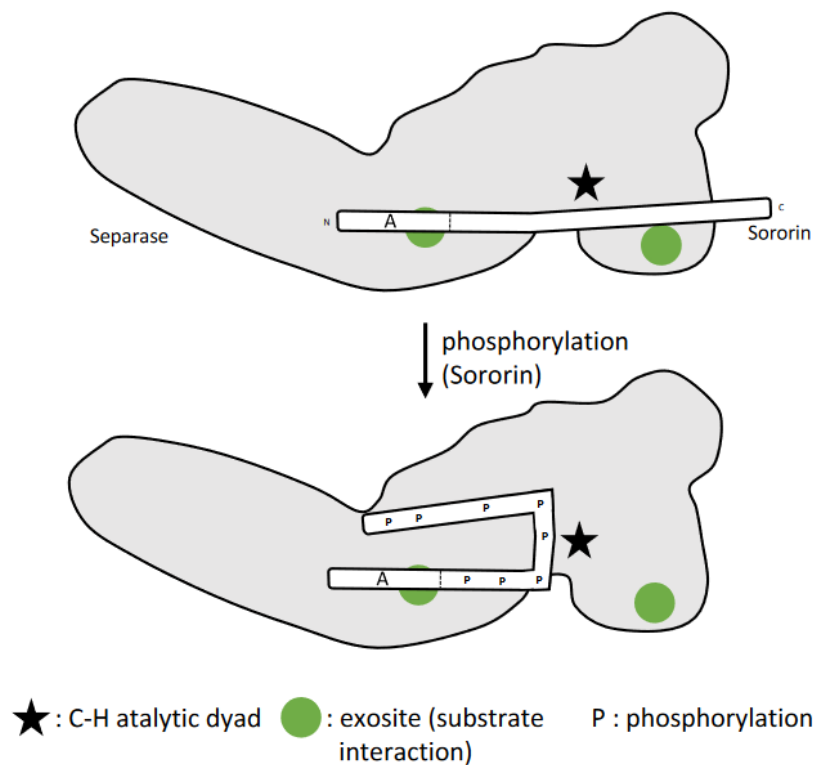


Figure 23| Putative model for Separase-Sororin complex formation and regulation. Sororin interacts with Separase predominantly via its N-terminus (fragment A) binding to the conserved C-terminal region of the protease. This interaction occurs possibly by using a so far unknown exosite within Separase. Inhibition of Separase by Sororin can be reversed by phosphorylation induced conformational change. See Text for details, P: phosphorylated residues.

(Rosen et al., 2019). Sororin harbors an LPE-motif (aa 41-43) in the N-terminus and a similar MPE-motif (aa 222-224) in the C-terminus. Both are not well conserved and mutating both motifs to Ala has no effect on Separase-Interaction (data not shown). Since Separase inhibition is not mediated by Sororin acting like a pseudosubstrate and is also not inhibited via an LPE-motif, there must be another, as yet unknown mechanism. Further research is necessary in order to clarify how Sororin inhibits Separase and what the function of this interaction is.

3.7 CDK1-Cyclin B1 interacts with Sororin by utilizing a CLD

Finally, we are able to clearly demonstrate another rather unexpected interaction in this work. We noticed an interaction between Sororin and CDK1-Cyclin B1 and also CDK1-Cyclin B2 (Fig. 10 and data not shown). Hereafter Sororin-Cyclin B1/2 is used to describe both the Sororin-CDK1-Cyclin B1 and Sororin-CDK1-Cyclin B2 complex. However, this interaction is mutually exclusive with Separase as demonstrated by TAP (Fig. 10), arguing for the simultaneous co-existence of a Separase-Sororin(-Scc1) complex, a Separase-Cyclin B1 complex and a Sororin-Cyclin B1/2 complex in mitotic human cells. Sororin-Cyclin B1/2 interaction is strongest in early mitosis and almost lost in telophase (data not shown). This argues for a specific function of this complex during mitosis. CDK1 kinase activity, however, is not inhibited by Sororin (data not shown). An obvious model would be that CDK1-Cyclin B1/2 interaction with Sororin regulates phosphorylation, which is essential for Sororin's function as an antagonist of Wapl during mitosis and might impact Sororin's ability to act as a Separase inhibitor. Typically, Cyclins bind to a so-called CIM (cyclin interaction motif), consisting of a putative RxL-Motif, of a CDK-substrate. Cyclin-association to a substrate then leads to recruitment of the corresponding CDK. This allows efficient phosphorylation of the respective substrates (Adams et al., 1996; Dreier et al., 2011; Schulman et al., 1998). Indeed, Sororin has two putative RxL-motifs (aa114-116 and aa134-138), possibly responsible for CDK1 interaction (Dreier et al., 2011). Mutating the latter putative CIM (R134A, L136A) however has little effect on Sororin, since Sororin is still able to interact with chromatin and rescues the mitotic arrest induced by an endogenous knockdown (Dreier et al., 2011). Additionally, Sororin is still efficiently phosphorylated, suggesting phosphorylation of Sororin by CDK1 independently of the second CIM-motif (Dreier et al., 2011). Since mutation of this motif (R134A and L136A, Dreier et al., 2011) had no obvious effect on Sororin, we investigated the more N-terminally located

putative CIM motif (aa114-116) in this study by analogous mutation (R114A, L116A: Sororin^{CIM}). Sororin^{CIM} appears to rescue a mitotic arrest only partially by knockdown of endogenous sororin (data not shown) and interacts weakly with Cohesin (Fig. S7C). Sororin^{CIM} is efficiently phosphorylated *in vivo* (Fig. S7C) and *in vitro* by isolated CDK1-CyclinB1 (data not shown). However, mutation of this putative CIM-motif has no effect on Sororin-Separase complex formation, and we are still able to observe Cyclin B1-Sororin interaction (Fig. S7C). Interestingly, we found a putative CLD (Cdc6-like domain), similar to the same motif found in Separase, within the coding sequence of Sororin (Fig. S7B). The yeast protein Cdc6 - a component of the pre-replicative Complex (pre-RC) - associates with Cdc28-Clb2 (the yeast homolog of CDK1-Cyclin B1) (Mimura et al., 2004). Mutating a similar sequence (41% similarity between Separase and Cdc6) within the Separase protein prevents CDK1-interaction with Separase (Boos et al., 2008). Deleting this putative CLD of Sororin (aa 211-221), we were able to abrogate CDK1-Cyclin B1/2-Sororin interaction significantly. Additionally, a mobility shift caused by phosphorylation, can no longer be observed (Fig. S7C). Surprisingly, we can also show a clear reduction in Separase-Sororin complex formation upon deleting this putative CLD. Scc1 interaction however is not impaired (Fig. S7C). Why the CLD in Sororin is also impacting Separase-interaction remains unresolved. Interestingly, other than Separase-Sororin interaction, Cyclin B1-Sororin complex formation is conserved among Taxa. We were able to demonstrate Cyclin B1-Sororin interaction in *Xenopus* xS3 cultured cells. Also, Cyclin B1-Dmt interaction can be demonstrated by transient transfection of GFP-Dmt encoding plasmid-DNA in human cell culture and subsequent co-IP (data not shown), arguing for a conserved protein interaction and possibly an important but so far unknown process. Consistently, Sororin was recently identified as a promoter of cell proliferation in bladder cancer by regulating Cyclins and CDK's (Fu et al., 2020).

3.8 Separase-Sororin complex formation – a possible role in female meiosis?

One possible function, which would connect all the presented results, might lay in meiosis. How Separase is kept inactive in oocytes during early meiosis II remains an unresolved issue. Securin – Separase's main inhibitor – inhibits Separase in early meiosis I, and RNAi mediated depletion of Securin in metaphase I-arrested oocytes results in premature SCS. However, Securin is degraded at the end of meiosis I and remains undetectable in meiosis II (Nabti et al.,

2008). Therefore, Securin is most likely not the only protein, keeping Separase in check during meiosis II. CDK1-Cyclin B1 also seems to be dispensable for proper sister chromatid separation in this context (Nabti et al., 2008), indicating a potentially unknown factor of Separase-regulation during early female meiosis. Interestingly, Sororin is expressed in oocytes, however, it seems to be insignificant for non-proteolytic Cohesin removal in oocytes (Gómez et al., 2016; McNicoll et al., 2013; Silva et al., 2020).

Efficient progression through meiosis is dependent on the Cohesin subunit Rec8. Phosphorylation of Rec8 and, hence, cleavage by Separase is responsible for the removal of arm Cohesin in meiosis I and finally sister chromatid separation in meiosis II (Kudo et al., 2009; Riedel et al., 2006). An additional layer of Separase regulation by Sororin might be redundant in early mitosis at a time when Separase is inhibited predominantly by association with Securin, CDK1-Cyclin B1 or Sgo2-Mad2 (see above). However, Separase-Sororin interaction might be relevant during early meiosis II. Consistently, endogenous Sororin can be detected on spread chromosomes from meiosis I and meiosis II mouse oocytes and appears to be particularly enriched at centromeres (Katja Wassmann, personal communication). Additionally, morpholino mediated knockdown of Sororin in mouse oocytes arrested in meiosis I results in scattered chromosomes (Katja Wassmann, personal communication). A possible role for the Separase-Sororin complex is further supported by the notion that Sororin not only interacts with Scc1- but also with Rec8-containing Cohesin rings (Wolf et al., 2018) and also protects them against active Separase (Fig. 18).

To investigate a possible Separase-Sororin interaction in mouse oocytes, an AID-tagged Sororin variant could also be used, as previously described. Sororin, harbouring an AID-tag, also can be degraded in a temporally precise and induced manner by its tag in mouse oocytes to investigate the role of sororin on separase-mediated Cohesin cleavage in meiosis II. Furthermore, the previously described ΔA variant, which has a possible separation of function, could also be used here.

4 Materials and Methods

Unless otherwise stated, analytically pure chemicals and reagents were obtained from Applied Biosystems, AppliChem, Biomol, Bio-Rad, Difco, Fluka, GE Healthcare, Invitrogen/Life Technologies, Merck, Millipore, New England Biolabs, Promega, Roth, Roche, Serva, Sigma, Thermo Fisher Scientific.

Deionized and sterile water was used for all methods. If necessary, sterile solutions and sterile materials were used.

4.1 Materials

4.1.1 Hard- and Software

Chemiluminescence signals of western blots as well as Coomassie Brilliant Blue stained gels were analyzed using a "LAS-4000" or "LAS-3000" system and corresponding image reader software (FUJIFILM Europe GmbH), respectively. Signals from radioactively labeled proteins were digitized using the "FLA-7000" system and corresponding image reader software (FUJIFILM Europe GmbH). The image data thus obtained was processed using "Adobe Photoshop CS4", "Adobe Illustrator CC" (Adobe Systems Inc., USA) and "Microsoft PowerPoint 2007" (Microsoft Corp., Luxembourg).

The centrifuges used were provided by Beckmann Coulter and Eppendorf. Incubators for culturing cells were bought from Heracell and New Brunswick. Precision pipettes were obtained from Eppendorf and Gilson.

Statistical analyses and presentations were performed using "Microsoft Excel 2007" (Microsoft Corp., Luxembourg). For bioinformatic analyses of DNA and protein sequences the "DNA Lasergene 8" program package (DNASTAR, Inc., Madison, WI, USA) was used.

Database and literature searches were performed online using services provided by the "National Center for Biotechnology Information" (<http://www.ncbi.nlm.nih.gov/>).

4.1.2 Antibodies

All primary antibodies used for Western blot analysis were stored in PBS/1 % (w/v) BSA and 0,02 % (v/v) NaN₃. Secondary antibodies were used in 5 % (w/v) skimmed milk/1x PBS.

Antibodies for IFM were used in 3 % (w/v) BSA/1x PBS.

Primary antibodies

target protein	species and clonality	dilution/concentration	reference
Cdc27	goat, polyclonal	Western blot: 1:1000	Hellmuth et al., 2014
Cyclin A2	rabbit, monoclonal	Western blot: 1:1000	abcam, ab181591
Cyclin B1	mouse, monoclonal	Western blot: 1:1000	Milipore, 05-373
Flag	mouse, monoclonal	Western blot: 1:1000	Sigma, F3165, clone M2
GFP	mouse, monoclonal	Western blot: 1:10.000 (4 µg/ml)	Hybridoma supernatant, kindly provided by Simona Sacconi, purified by Markus Hermann
H2A			
Myc	mouse, polyclonal	Western blot: 1:10.000 (0.2 µg/ml)	Hybridoma supernatant, Developmental Studies Hybridoma Bank, clone 9E10, purified by Markus Hermann
Scc1	mouse, monoclonal	Western blot: 1:1000	Milipore, 05-908
Separase-N	rabbit, polyclonal	Western blot: 1:1500	Stemmann et al., 2001
Securin	mouse, monoclonal	Western blot: 1:1000	MBL, K0090-3, clone DCS-280
Smc3	rabbit, polyclonal	Western blot: 1:1000	Bethyl / A300-060A
Sororin (#1)	rabbit, polyclonal	Western blot: 1:1000	this study
Sororin (#2)	rabbit, polyclonal	used for IP	this study
Pds5	rabbit, polyclonal	Western blot: 1:1000	Kindly provided by Susannah Rankin
pHH3	rabbit, polyclonal	Western blot: 1:1000	Merck, 06-570
Pin1	rabbit, polyclonal	Western blot: 1:10.000 (2.76 µg/ml)	Hellmuth et al., 2015
Topoisomerase II α	mouse, monoclonal	Western blot: 1:1000	Enzo, clone 1C5, ADI-KAM-CC210-E

name	use	dilution	reference
Tubulin	mouse, monoclonal	Western blot: 1:200	Hybridoma supernatant, Developmental Studies Hybridoma Bank, clone 12G10, purified by Markus Hermann

Secondary antibodies

name	use	dilution	reference
HRP-conjugated goat anti-mouse IgG	Western blot	1:20.000	Sigma, A9917
HRP-conjugated goat anti-rabbit IgG	Western blot	1:20.000	Sigma, A0545
HRP-conjugated mouse anti-rabbit IgG (heavy chain specific)	Western blot	1:20.000	Abcam, ab99702
HRP-conjugated mouse anti-rabbit IgG (light chain specific)	Western blot	1:20.000	Abcam, ab99697

For precipitation of GFP-tagged proteins, the cell lysates were incubated with NHS-activated sepharose (GE Healthcare) covalently coupled to GFP single-chain camel nanobodies (Rothbauer et al., 2008; provided by Markus Hermann, University of Bayreuth). Flag-tagged proteins were isolated using Anti-Flag M2 Affinity Gel (Sigma, A2220), Myc-tagged were incubated with Anti-Myc beads (Sigma, A7470)

4.1.3 Plasmids

All plasmids listed here have a multiple cloning site extended to include the sequences for the restriction enzyme sites *FseI* and *Ascl*. Furthermore, all listed pCS2-plasmids have an ampicillin (Amp) resistance cassette, all pET28M-plasmids have a kanamycin resistance cassette. If not otherwise stated, all genes are the human homologs (dm: *Drosophila*, x: *Xenopus*, m: mouse).

name	insert	tag(s)	backbone	reference
pSX100	Securin	-	pCS2	Hui Zou
pMW448	xSeparase	N-GFP	pCS2	Martin Wühr
pLG1966	Scc1	eGFP-C	pCS2	Laura Schöckel
pIW3100	Separase	N-Myc ₆	pCS2	Irina Weber
pFL3463	Separase P1127A	N-eGFP-TEV ₄	pCS2	Franziska Langhammer
pPW3481	Sororin	N-His ₆ -SUMO3	pET28M	Peter Wolf
pPW3500	mRec8	eGFP-C	pCS2	Peter Wolf
pPW3502	Separase P1127A PD	N-eGFP-TEV ₄ -	pCS2	Peter Wolf
pBN3622	Sororin fragment A (aa 1-87)	N-His ₆ -SUMO3	pET28M	this study
pBN3623	Sororin fragment B (aa 88-150)	N-His ₆ -SUMO3	pET28M	this study
pBN3624	Sororin fragment C (aa 151-208)	N-His ₆ -SUMO3	pET28M	this study
pBN3625	Sororin fragment D (aa 209-252)	N-His ₆ -SUMO3	pET28M	this study
pBN3681	Separase domain SD (aa 1622-1934)	N-Myc ₆	pCS2	this study
pBN3682	Separase domain CD (aa 1935-2120)	N-Myc ₆	pCS2	this study
pBN3684	Separase domain SD-CD (aa 1622-2120)	N-Myc ₆	pCS2	this study
pBN3691	Securin P119R	-	pCS2	this study
pBN3726	xSororin	N-eGFP	pCS2	this study
pBN3746	dmDalmatian	N-Myc ₆ -TEV ₂	pCS2	this study
pBN3747	dmSSE	N-eGFP	pCS2	this study
pBN3748	dmTHR	-	pCS2	this study
pBN3845	Sororin	eGFP-C	pCS2	this study
pWM3750	Mcl1 Δ TM (aa 1-327)	TEV-Flag ₃ -C	pCS2	Maria Weber
pBN3793	Separase domain III/IV-SD (aa 1155-1934)	N-Myc ₆	pCS2	this study
pBN3794	Separase domain I-III (aa 1-1371)	N-Myc ₆	pCS2	this study
pBN3797	Separase domain III/IV (aa 1155-1621)	N-Myc ₆	pCS2	this study

name	insert	tag(s)	backbone	reference
pBN3798	Separase domain III/IV-CD (aa 1155-2120)	N-Myc ₆	pCS2	this study
pBN3799	Separase SD ^{Δmodule} -CD (aa 1622-1808 + 1886-2120)	N-Myc ₆	pCS2	this study
pBN3800	Separase domain partSD-CD (aa 1886-2120)	N-Myc ₆	pCS2	this study
pBN3801	Separase SD ^{Δmodule} -CDpart (aa 1886-1934)	N-Myc ₆	pCS2	this study
pBN3802	Separase domain SD-SD ^{module} (aa 1622-1886)	N-Myc ₆	pCS2	this study
pBN3803	Separase SD ^{module} (aa 1808-1886)	N-Myc ₆	pCS2	this study
pBN3952	Sororin 11A	eGFP-C	pCS2	this study
pBN3953	Sororin 12E	eGFP-C	pCS2	this study
pBN3954	Sororin FL-AurB (phosphomimicking)	eGFP-C	pCS2	this study
pBN3955	Sororin FL-Cdk1 (phosphomimicking)	eGFP-C	pCS2	this study
pBN3957	Sororin CIMmut (R114A, L116A)	eGFP-C	pCS2	this study
pBN3958	Sororin ΔCLD (Δaa 211-222)	eGFP-C	pCS2	this study
pBN3984	Sororin fragment A (aa 1-87)	eGFP-C	pCS2	this study
pBN3985	Sororin fragment B (aa 88-150)	eGFP-C	pCS2	this study
pBN3986	Sororin fragment C (aa 151-208)	eGFP-C	pCS2	this study
pBN3987	Sororin fragment D (aa 209-252)	eGFP-C	pCS2	this study
pJH4006	Sororin	TEV2-eGFP-C	pCS2	Jutta Hübner
pBN4095	Sororin FGF > AGA	eGFP-C	pCS2	this study
pBN4096	Sororin YSR > ASE	eGFP-C	pCS2	this study
pBN4157	Sororin A-B (aa 1-150)	eGFP-C	pCS2	this study
pBN4158	Sororin A-B Δ1R (aa 8-150)	eGFP-C	pCS2	this study

name	insert	tag(s)	backbone	reference
pBN4159	Sororin A-B Δ2R (aa 32-150)	eGFP-C	pCS2	this study
pBN4160	Sororin A-B Δ3R (aa 82-150)	eGFP-C	pCS2	this study
pBN4161	Sororin ΔA (aa 88-252)	eGFP-C	pCS2	this study
pBN4165	Sororin ΔD (aa 1-209)	eGFP-C	pCS2	this study
pBN4196	Scc1 FL	N-Flag ₃	pCS2	this study
pBN4197	Scc1 N (aa 1-294)	N-Flag ₃	pCS2	this study
pBN4198	Scc1 mid (aa 295-572)	N-Flag ₃	pCS2	this study
pBN4199	Scc1 C (aa 573-753)	N-Flag ₃	pCS2	this study
pBN4206	Sororin 7A	eGFP-C	pCS2	this study
pBN4207	Sororin 9A	eGFP-C	pCS2	this study

4.1.4 Buffers and solutions

Coomassie staining solution	25 % (v/v) isopropanol 10 % (v/v) acetic acid 0.05 % (w/v) Coomassie Blue R250
Coupling buffer	200 mM NaHCO ₃ 500 mM NaCl pH 8.3
Destaining solution (Coomassie)	10% (v/v) acetic acid
Elution buffer (IMAC)	1x PBS 400 mM NaCl (total) 250 mM imidazole 10 mM DTT
Elution buffer (antibodies)	100 mM glycine 100 mM NaCl pH 2.5

Materials and Methods

Fixation solution	40 % (v/v) methanol 10 % (v/v) acetic acid
Freezing medium	90% (v/v) fetal bovine serum 10% (v/v) DMSO
Glycerol buffer	1x PBS 50 % (v/v) glycerol
2x HBS (500 ml)	8 g NaCl 0.37 g KCl 106.5 mg Na ₂ HPO ₄ 1 g glucose 5 g HEPES pH 7.05 (sterile filtered)
Imject buffer (Thermo Fisher)	83 mM Na ₃ PO ₄ 900 mM NaCl 100 mM sorbitol pH 7.2
Laemmli running buffer (1x)	25 mM Tris 192 mM glycine 0.1 % SDS (w/v)
LB-medium	1 % (w/v) tryptone 0.5 % (w/v) yeast extract 1 % (w/v) NaCl
LB-agar (plates)	LB-medium with 1.5 % (w/v) agar
LP2	20 mM Tris-HCl, pH 7.6 100 mM NaCl 10 mM NaF 20 mM β-glycerophosphate 5 mM MgCl ₂ 0.1% (v/v) Triton X-100 5 % (v/v) glycerol
LP2*	as LP2 but with 1 tablet/50ml 1x complete protease inhibitor cocktail (Roche Diagnostics)

Materials and Methods

Lysis buffer (IMAC)	1x PBS 400 mM NaCl (total) 5 mM imidazole 10 mM DTT
Neutralization buffer	1x PBS 50 mM Tris/HCl pH 9
NHS buffer A	500 mM ethanolamine 500 mM NaCl pH 8.3
NHS buffer B	100 mM NaAc 500 mM NaCl pH 4
PBS (10x)	1.37 M NaCl 27 mM KCl 80 mM Na ₂ HPO ₄ 14 mM KH ₂ PO ₄ pH 7.4
TBE (1x)	90 mM Tris 90 mM boric acid 2 mM EDTA pH 8.0
TPE (1x)	90 mM Tris 90 mM phosphoric acid 2.5 mM EDTA pH 8.0
Transfer buffer (1x)	25 mM Tris 192 mM glycine 15 % methanol (v/v)
Sororin storage buffer	20 mM Tris 100 mM NaCl pH 6.9

SDS sample buffer (4x)	40% glycerol (v/v) 250 mM Tris-HCl, pH 6.8 8 % SDS (w/v) 2 M β -mercaptoethanol 0.04 % bromphenol blue (w/v)
SDS sample buffer* (4x)	as SDS sample buffer (4x), without β -mercaptoethanol
wash buffer (1x)	1x TBS 0.05 % Tween-20 (v/v)
wash buffer (IMAC)	1x PBS 400 mM NaCl (total) 25 mM imidazole 10 mM DTT
wash buffer (antibodies)	5 mM Tris/HCl 150 mM NaCl pH 6.8

4.2 Microbiological techniques

4.2.1 *E. coli* strains and media

Chemically competent (Stratagene/Agilent Technologies, Santa Clara, CA, USA) *E. coli* XL1-Blue cells were used to amplify plasmid DNA. For protein expression chemically competent *E. coli* Rosetta 2 (DE3) and Arctic Express (DE3) (Agilent Technologies) cells were used.

Genotype:

XL1-Blue: endA1 gyrA96(nal^R) thi-1 recA1 relA1 lac glnV44 F'[:Tn10 proAB⁺ lacI^q

Δ (lacZ)M15] hsdR17(r⁻ m⁺)

Rosetta 2 (DE3): F⁻ ompT gal dcm lon[?] hsdS_B(r_B⁻m_B⁻) λ (DE3 [lacI lacUV5-T7p07 ind1 sam7 nin5]) [malB⁺]_{K-12}(λ ^S) pRARE2 (Cm^R)

Arctic Express (DE3): *E. coli* B F⁻ ompT hsdS(r⁻ m⁻) dcm⁺ Tet^r gal λ(DE3) endA Hte [cpn10 BB cpn60 Gent^r]

LB (lysogeny broth) medium was used for the cultivation of *E. coli*. LB liquid medium and LB agar were autoclaved (20 min, 121°C, 2 bar) and stored at 4°C before use.

4.2.2 Cultivation of *E. coli*

Cultivation of *E. coli* in LB liquid medium was performed by shaking at 150 rpm and 37°C. Cells plated on LB agar plates were also incubated at 37°C. For selection of transformed bacteria suitable antibiotics were used in consideration of utilized plasmids and strains [Ampicillin (final concentration: 100 µg/ml), Kanamycin (final concentration: 30 µg/ml), Chloramphenicol (final concentration: 34 µg/ml), Gentamycin (final concentration: 7 µg/ml)]. Cultures plated on agar plates were stored at 4°C.

4.2.3 Preparation of chemically competent *E. coli* cells

In order to prepare chemically competent bacteria 300 ml of LB-medium was inoculated with 2-4 ml of an overnight (o/n) culture of the respective bacteria with an OD₆₀₀ of 0.1 and cultured at 37°C and 150 rpm to an OD₆₀₀ of 0.5. The culture was cooled on ice for 15 min and harvested by centrifugation (15 min, 4°C, 3000 g). All following steps were performed at 4°C and using sterile equipment and buffers. The bacterial pellet was resuspended in 90 ml Tbf1 buffer and incubated on ice for 15 min. After an additional centrifugation (15 min, 4°C, 1500 g) the pelleted bacteria were resuspended in 15 ml Tbf2 buffer and incubated on ice. Finally, aliquots (50 µl) of this bacterial suspension were prepared, snap-frozen and stored at -80°C.

4.2.4 Transformation of chemically competent *E. coli*

An aliquot (50 µl) of chemically competent *E. coli* cells was thawed on ice and 10 µl ligation preparations or 1 µl purified plasmid DNA was added. After incubation of 20 min on ice, the cells were heat shocked for 90 seconds at 42°C. After a short cooling of the cells on ice, 500 µl LB medium was added. The cells were incubated for 30-45 min at 37°C with shaking (200 rpm).

200 µl of this total batch were plated onto dried LB-Amp plates. Incubation was performed at 37°C overnight. For a retransformation of purified plasmid DNA, the transformation mixture was added to 50 ml LB-medium supplemented with the respective antibiotics and incubated overnight at 37°C while shaking (200 rpm).

4.3 Molecular biological techniques

4.3.1 Isolation of plasmid DNA from *E. coli*

Depending on the needed amount and purity of plasmid DNA, different commercially available kit-based plasmid isolation methods were used (mini preparation: up to 25 µg total yield of plasmid DNA; midi preparation: up to 350 µg total yield of plasmid DNA)

Mini-Preparation of plasmid DNA from *E. coli* XL1-Blue

1.5 ml of an over-night bacterial culture (37°C, 200 rpm) was transferred to a 1.5 ml reaction tube and centrifuged (1 min, RT, 4,500 g). The supernatant was discarded, and the cell pellet was processed with the "GeneJET Plasmid Miniprep Kit" (Thermo Fisher Scientific, St. Leon-Rot) according to the manufacturer's instructions.

Midi preparation of plasmid DNA from *E. coli* XL1-Blue

50 ml of an overnight bacterial culture (37°C, 200 rpm) were transferred to a 50 ml Greiner reaction tube and centrifuged (10-15 min, 4°C, 2,900 g). The supernatant was discarded, the cell pellet was processed with the "Plasmid Plus Midi Kit" (QIAGEN, Hilden) according to the manufacturer's instructions.

4.3.2 DNA hydrolysis by restriction endonucleases

Preparative restriction hydrolysis

2-4 µg of the DNA to be examined were mixed with 1 U of suitable site-specific restriction enzymes (5-20 U/µl, NEB, Frankfurt am Main) and 5 µl of the recommended 10x buffer in a 50 µl total volume. Samples were incubated for 1-3 hours at 37-65°C according to the manufacturer's instructions. If necessary, the restriction enzymes were heat inactivated for 10 min according to the manufacturer's instructions. In case of a required buffer exchange for

two different and incompatible restriction enzymes, the DNA was purified using the "GeneJET PCR Purification" kit (Thermo Fisher Scientific, St. Leon- Rot) according to the manufacturer's instructions. The DNA was eluted in 30 µl EB buffer. The analysis was performed by agarose gel electrophoresis.

Analytical restriction hydrolysis

250 ng of the plasmid purified by mini-preparation was incubated with 0.5 U of suitable restriction enzymes (5-20 U/µl, NEB, Frankfurt am Main) and 1 µl of the recommended 10x buffer in a 10 µl total volume. Samples were incubated for one hour at 37-65°C according to the manufacturer's instructions, the DNA fragments were analyzed by agarose gel electrophoresis (see 4.3.4).

4.3.3 Dephosphorylation of DNA-fragments

To prevent the religation of linearized vectors, the 5'-phosphates were removed by mixing 2-4 µg hydrolyzed DNA with 5 U antarctic phosphatase (5 U/µl; NEB, Frankfurt am Main) and 4 µl associated 10x buffer in a 40 µl total volume. Samples were incubated for 1-2 hours at 37°C, followed by removal of the enzyme and a buffer exchange using the "GeneJET PCR Purification" kit (Thermo Fisher Scientific, St. Leon-Rot) according to the manufacturer's instructions. DNA was finally eluted in 30 µl EB buffer.

4.3.4 Separation and analysis of DNA fragments by agarose gel electrophoresis

For purification and analysis, DNA fragments were separated using 0.8-2 % (w/v) agarose gels. 1x TPE or TBE buffer was used as the basis for the gel preparation and as a running buffer. Ethidium bromide was used in the agarose gels at a final concentration of 0.5 µg/ml. The samples to be separated were mixed with DNA loading buffer (to 1x; NEB, Frankfurt am Main). Separation of the desired fragments was performed by applying a voltage of 120 V for 45-60 min. The visualization of DNA was enabled by the intercalation of ethidium bromide into DNA and was performed by a UV transilluminator (Syngene, Frederick, USA) at a wavelength of 324 nm. The molecular weight standards "LMW" and "SPP1" (Department of Genetics, University of Bayreuth) was used to estimate the size of the DNA fragments detectable in the gel. The

desired DNA band, if necessary, was excised on a UV table (UVT-14L; Herolab, Wiesloch) using a scalpel.

4.3.5 Gel extraction of DNA fragments

For gel extraction of DNA fragments after excision (see 3.3.4) the GeneJET Gel Extraction Kit (Thermo Fisher Scientific, St. Leon-Rot) was used according to the manufacturer's instructions. DNA was dissolved in 30 µl elution buffer.

4.3.6 Polymerase chain reaction (PCR)

For the amplification of DNA fragments, a TC-512 thermal cycler (Techne, Staffordshire, UK) was used. Typical reactions were conducted in a total volume of 50 µl.

Composition

DNA template	10-200 ng
Oligonucleotides (100 pmol/µl)	0.3 µl each (forward/reverse)
Deoxyribonucleotide mix (10 nM)	1 µl
Phusion DNA polymerase (2 U/µl)	0.5 µl
5x HF-/GC buffer	10 µl
	add 50 µl with ddH ₂ O

(Oligonucleotides were obtained from Sigma-Aldrich, deoxyribonucleotides, Phusion DNA polymerase and corresponding buffers were purchased from Thermo Fisher Scientific, St. Leon-Rot)

DNA polymerase was always added last to prevent possible degradation of the oligonucleotides by the 3' → 5' exonuclease activity of the polymerase. HF buffer was used for the amplification of plasmid DNA fragments, GC buffer for the amplification of cDNA fragments.

General programs:

<u>Regular amplification</u>			<u>To add restriction sites</u>	
initial denaturation	98°C – 30''		initial denaturation	98°C – 30''
denaturation	98°C – 10''	30x	denaturation	98°C – 10''
annealing	45-72°C – 30''		annealing	45-72°C – 30''
extension	72°C – 30''/kb		extension	72°C – 30''/kb
final extension	72°C – 4'		denaturation	98°C – 10''
final hold	4°C - ∞		annealing	45-72°C – 30''
			extension	72°C – 30''/kb
			final extension	72°C – 4'
			final hold	4°C - ∞

The initial denaturation was performed at 98°C, followed by 30 amplification cycles on average. The annealing temperature was individually adapted to the oligonucleotide pair used (David-Bowstein T_m). Depending on the length of the desired amplification product, an appropriate extension time was selected (15-30''/kb). The final elongation was performed for 4 min. Afterwards the reaction was stopped by cooling to 4°C.

A PCR reaction was performed in two steps to add specific sites for restriction endonucleases. First the appropriate annealing temperature was selected for the amplification of the starting sequence (average: 15 cycles), then for the amplification of the entire recombinant sequence with additional restriction sites (average: 15 cycles). Times and temperatures for denaturation and extension were selected as described.

4.3.7 Ligation of DNA fragments

For ligation, the insert was used in a molar excess of 1:4 (vector:insert) over the linearized and dephosphorylated vector. The amount of insert was calculated according to the formula:

$$mas_{insert} [ng] = 4 \times mass_{vector} [ng] \times length_{insert} [bp] / length_{vector} [bp]$$

The ligation reaction was performed in the presence of 2 U T4 ligase and the corresponding buffer (to 1x; NEB, Frankfurt am Main) for 1 h at 37°C or overnight at 4°C in a total volume of 40 µl. This was followed by removal of the enzyme and a buffer exchange using the "GeneJET

PCR Purification" kit (Thermo Fisher Scientific, St. Leon-Rot) according to the manufacturer's instructions. DNA was finally eluted in 30 μ l EB buffer.

4.3.8 DNA sequencing

The sequencing services of plasmid DNA were conducted by SeqLab (Sequence Laboratories, Göttingen) and Eurofins Genomics (Ebersberg). Sequencing samples consisted of 1200 ng plasmid DNA and 20 pmol of the respective sequencing primer in a total volume of 15 μ l.

4.3.9 Determination of mRNA, DNA and protein concentrations in solutions

The determination of the purity and concentration of DNA and mRNA in solutions was performed by spectrophotometric measurement (ND-1000, PeqLab, Erlangen) at a wavelength of 260 nm. An OD_{260} nm= 1 corresponds to a concentration of 50 μ g/ml double-stranded DNA and 4 μ g/ml RNA.

Protein concentrations in solutions were also determined by spectrophotometric measurements (ND-1000, PeqLab, Erlangen). An OD_{280} nm= 1 corresponds to a protein concentration of 1 mg/ml.

4.4 Protein biochemical methods

4.4.1 SDS-Polyacrylamide gel electrophoresis (SDS-PAGE)

The separation of proteins according to their molecular mass under denaturing conditions was performed by SDS-polyacrylamide gel electrophoresis (SDS-PAGE). Gradient gels (resolving gel: 8-17 % acrylamide, stacking gel: 7 % acrylamide) were used and poured with the "SG100" system (Hoefer Inc.). Before loading, samples were mixed with SDS sample buffer to a 1x final concentration and incubated for 10 min at 99°C. Electrophoresis was performed in a "Mighty Small II for 8x7 cm gels" chamber (Hoefer Inc.) in the presence of 1x Laemmli running buffer and a constant voltage of 130 V (30 mA/gel) for 90-120 min. For estimating the molecular weight, the PageRuler Prestained Protein Ladder (Thermo Scientific) was used.

4.4.2 Immunoblotting (Western blot)

For the electrophoretic transfer of proteins separated by SDS-PAGE a polyvinylidene fluoride membrane (PVDF, pore size 0.2 μm ; Serva) was used. The membrane was first activated in 100 % methanol and then equilibrated in transfer buffer for about 2 min. Suitable extra thick blot papers (filter paper, BioRAD) and the SDS gels were also equilibrated in transfer buffer. Protein transfer was performed in a semi-dry turboblotting apparatus (BioRAD) at 60 mA per membrane for 90 min (1 mA/cm²). After transfer, the membrane was incubated in blocking buffer for 60 min to block unspecific binding sites and was subsequently washed three times for 10 min with wash buffer. The incubation of the primary antibody (stored in 1x PBS, 1 % (w/v) BSA; 0.02 % (v/v) NaN₃) was carried out either for two hours at room temperature or at 4°C overnight on a shaker. Unbound antibodies were removed by washing three times for 5 min. Incubation with corresponding HRP-conjugated secondary antibodies was performed in blocking buffer for one hour at room temperature. After six additional washing steps for 10 min each, the chemiluminescence produced by the reaction of HRP and luminol was detected either with home-made fresh developer solution (per membrane 2 ml solution 1, 800 μl solution 2 and 2.4 μl solution 3; add 5 ml with ddH₂O) or with the two-component system "Lumigen ECL Ultra (TMA-6)" (Lumigen, Michigan, USA) according to the manufacturer's instructions. The digitization of the detected protein bands was performed with the CCD camera of the "LAS-4000" system (FUJIFILM Europe GmbH, Düsseldorf, Germany).

4.4.3 Coomassie staining

For Coomassie staining, SDS-PAGE gels were first incubated in Coomassie staining solution for 1-2 h or overnight on a shaker at RT. Before documentation using the CCD camera of the LAS-3000" system (FUJIFILM Europe GmbH, Düsseldorf, Germany) gels were repeatedly washed with destaining solution.

4.4.4 Protein expression in *E. coli*

E. coli "Rosetta 2 + DE3"-cells were transformed with plasmids encoding His₆-SUMO3-tagged proteins (see. 4.2.4). Bacteria were incubated in 20 ml LB-medium (o/n, 37°C, 150 rpm). Subsequently a 1 l LB-culture was inoculated to a final OD₆₀₀: 0.05 and incubated (37°C, 150 rpm) until OD₆₀₀: 0.8 was reached. Protein expression was induced by adding Isopropyl β -d-1-

thiogalactopyranoside (IPTG) to a final concentration of 0.25 mM. After induction cells were further incubated (3 h, 37°C, 150 rpm). Finally, cells were harvested by centrifugation (10 min, 4°C, 5500 g), the cell pellet was subsequently washed with 1x PBS and again centrifuged (10 min, 4°C, 4000 rpm (Heraeus Varifuge 3.0R)). The resulting cell pellet was either directly processed or snap frozen and stored at -80°C.

4.4.5 Ni²⁺-NTA affinity purification of His₆-SUMO3-tagged proteins

All purification steps were performed on ice, if not otherwise stated. Bacteria obtained from 1 l of expression culture were suspended in 15 ml ice cold lysis buffer for immobilized metal affinity chromatography (IMAC), per 1 g of cell pellet. Cells were either mechanically lysed by the Sonoplus ultrasonic homogeniser “Sonoplus HD 2070” using a Sonotrode MS 73 (Bandelin, Germany) with operating parameters: 5 x 10 % cycles with 60 % power or by cycling the cell suspension for 10 min in a high-pressure homogenizer (EmulsiFlex-C5; Avestin, Germany). Cell debris and bacterial inclusion bodies were removed by centrifugation (10 min, 4°C, 14.000 g) after successful cell disruption. The resulting supernatant was further subjected to IMAC and therefore incubated with 1 ml of equilibrated Ni²⁺-NTA resin (Machery-Nagel), for 1h at 4°C and gentle rotation. The beads were subsequently washed twice with IMAC wash buffer; bound protein was eluted with 500 µl IMAC elution buffer. The resulting peak fractions containing the most amount of protein were dialyzed two times against 1 l dialysis or storage buffer using a dialysis membrane with a molecular weight cut-off (MWCO) of 3.5 kDa (SnakeSkin Dialysis Tubing; 3.5 K MWCO; Thermo Fisher).

If the His₆-SUMO3-tag was to be removed, SenP2 protease was added to the eluate before dialysis. Subsequently, a second round of Ni²⁺-NTA purification removed both the separated His₆-SUMO3-tag and His-tagged SenP2 protease. For this purpose, 400 µl of equilibrated Ni²⁺-NTA resin was incubated with the dialysate (1 h, 4°C, gentle rotation). The flow-through corresponding to the purified protein was measured again, aliquoted, snap-frozen, and stored at -80°C.

4.4.6 Non-covalent coupling of antibodies to sepharose beads

For non-covalent coupling either protein G or protein A sepharose beads (GE healthcare) were used depending on the desired antibody. Corresponding beads were first washed twice with 1 ml of 1x PBS, 1 % (w/v) BSA. All centrifugation steps utilizing beads were performed at 200 *g* and 4°C. In general, 4 µg purified antibody per 10 µl bead suspension was used. In addition, 100 µl of PBS 1% (w/v) BSA was added to each coupling reaction (90 min, RT, gentle rotation). Following coupling beads were washed twice with 1 ml of PBS 1% (w/v) BSA, pelleted and resuspended in an appropriate volume of cell lysis buffer (LP2*). Using a cut-off tip, the bead suspension was further divided among several tubes if necessary.

Covalently coupled beads for Flag- and Myc-IP respectively were purchased by Sigma, GFP-nanobody coupled beads were kindly provided by Markus Hermann.

4.4.7 Immunoprecipitation (IP)

For IP Taxol arrested cells were usually either harvested by flushing from the corresponding cell culture dish with medium or 1x PBS (HEK293T cells) or by “mitotic shake-off” (HeLa K cells). For the latter the corresponding culture dish was tapped against a hard surface several times to detach round and therefore mitotic cells. Subsequently harvested cells were pelleted (3 min, RT, 300 *g*), resuspended in an appropriate volume of LP2* lysis buffer and lysed using a dounce homogenizer with a tight pestle (Wheaton) and 12 strokes on ice. For DNA digestion lysates were additionally treated with Benzonase (1:1000; Santa Cruz) for 1h at 4°C. For Taxol-ZM-override (for time resolved analysis) cells were harvested by mitotic shake-off, divided equally and treated with 5 µM ZM447439 (Tocris Biosciences, United Kingdom) for the indicated time points (see Results). Each cell culture sample (see below) was quickly washed, the pellet was snap frozen and stored at -80°C. Before analysis frozen cell pellets were thawed on ice. Further treatment was performed as described.

For IP of endogenous or tagged proteins between 500 µl and 1 ml of cell lysates and 10 µl of beads were used. All centrifugation steps utilizing beads were performed at 200 *g* and 4°C. Corresponding beads were washed twice using LP2* and subsequently incubated with the cell lysates for 3 h or o/n at 4°C. After IP the lysates were discarded, and beads were washed six times with 1 ml of LP2*. Finally, the beads were mixed with 1x SDS-sample buffer and boiled (5 min, 98°C). Beads were boiled in the presence of β-mercaptoethanol in case of covalently

coupled antibodies to corresponding beads and without β -mercaptoethanol in case of non-covalently coupled antibodies to beads. In case of the latter β -mercaptoethanol was added to eluates to a final concentration of 1 M after the removal of the beads. Beads and eluates were separated utilizing Mobicol microcolumns and microfilter with a pore size of 0,35 μm (MoBiTec). Usually, 15 μl of eluates were analysed by SDS-PAGE and Western blot.

4.4.8 Tandem affinity purification (TAP)

To elucidate whether Sororin and Separas interact in a mutually exclusive manner, TAP was performed. To this end HEK293T cells were transiently transfected with plasmid DNA encoding GFP-tagged Sororin or EV. Cells were first blocked at the G1/S boundaries as described in chapter 4.5.6, after release cells were further treated with taxol to arrest cells in early mitosis. Cells were further released into mitosis by addition of ZM or directly harvested and lysed (in 30 ml LP2*) as described (see chapters 4.4.7, 4.5.6 and 4.5.7). For the first purification step 500 μl GFP nanobody coupled beads were used. After incubation o/n at 4°C the beads were washed 5 times with 5 ml LP2* and once with 5 ml LP2. Bound proteins were eluted by addition of 150 μl TEV-protease (5000 units/ml, provided by Markus Hermann, University of Bayreuth). Beads and eluates were separated utilizing Mobicol microcolumns and microfilter with a pore size of 0,35 μm (MoBiTec). Samples of each eluate were boiled with SDS sample buffer for analysis by SDS-PAGE and immunoblot. Remaining eluates were diluted with 1 ml LP2*, equally divided and further incubated with Separase-antibody or unspecific IgG coupled beads (see chapter 4.4.6) for 4 h at 4°C. This second step of TAP was eluted as described (see chapter 4.4.7).

4.4.8 Preparation of protein-coupled NHS-activated sepharose

For coupling of purified proteins to NHS (N-hydroxysuccinimide)-activated sepharose beads were transferred into a column (Poly-Prep, BioRad), 1ml of beads were used. Beads were first activated using 6 ml of 1 mM ice cold HCl. Subsequently, the antigen solution, which was previously purified and dialyzed against coupling buffer, was pumped in a circuit over the column using a P1 pump (GE Healthcare) at a flow rate of 1 ml min⁻¹ for 30 min. Subsequently, the antigen solution, which was previously purified and dialyzed against coupling buffer, was pumped in a circuit over the column using a P1 pump (GE Healthcare) at a flow rate of 1 ml

min⁻¹ for 30 min, after which the column was washed with 1.5 ml coupling buffer. Unoccupied binding sites were covered by washing with 6 ml NHS buffer A and subsequently washed with 6 ml NHS buffer B. This was repeated three times as described. The final washing step was performed using 1x PBS, 50 % (v/v) glycerol. The column was either used directly or stored in a 50 ml tube containing 20 % EtOH at -20°C.

4.4.9 Testelution of antigen coupled NHS-activated sepharose

To ensure that none of the coupled proteins detach during elution due to the low pH value of the elution buffer (pH 2.5) used for antibody elution, a test elution was carried out beforehand at 4 °C. This was done by first washing the antigen coupled column (see 4.4.8) with ten column volume (CV, volume inside of a packed column not occupied by buffer) 1x PBS to remove the storage buffer. All steps were performed using a P1 pump (GE Healthcare) with a flow rate of 1ml min⁻¹. This was followed by wash steps with 5 CV 1x PBS and 5 CV antibody wash buffer. Elution was performed ten times with one CV antibody elution buffer. Eluates were immediately neutralized using 700 µl neutralisation buffer. The column was then washed with neutralization buffer until pH 7 was reached, as measured by pH test strips, and finally washed again with 10 ml 1x PBS.

4.4.9 Affinity chromatography for antibody purification

For immunization in order to obtain specific antibodies recognizing human Sororin, His6-SUMO3-hSororin dialysed against Imject buffer (selfmade, Thermo Fisher) was used (see also Chapter 4.4.5). Immunization of two rabbits was performed by Charles River Laboratories (France). Test sera from each rabbit were collected on day (D)0 and D38, the final bleed was collected on D52. Sera were filtered (20 µm) and tested for antigen-recognition by SDS-PAGE and immunoblot of HEK293T WCE's and 1 µg purified Antigen (see 4.4.4). Sera were diluted 1:500 using 1x PBS (supplement Figure 2).

After successful test elution (see 4.4.8), affinity purification of the rabbit sera was performed. The sera were circulatingly applied to the antigen coupled columns using a P1 pump (GE Healthcare) at 4 °C. Washing and elution steps were equivalent to the test elution steps (see Chapter 4.4.9). The column was stored in storage buffer at 4 °C after neutralization and thorough rinsing with 1x PBS. Samples were taken from the wash fractions and eluates for

SDS-PAGE. Eluates were combined (“high” and “low” according to the amount of measured protein) and dialyzed in a membrane for proteins larger than 10 kDa (SnakeSkin Dialysis Tubing, 10 K MWCO, Thermo Fisher) at 4 °C in glycerol buffer in two steps (once with 1 l for 1 h and in fresh buffer o/n) and then stored at -20 °C until use.

4.4.10 Purification of active human Separase

For purification of active human Separase HEK293T cells were transiently transfected (see 4.5.5) with plasmid DNA encoding untagged Securin^{WT} and GFP-TEV-tagged hyperactive Separase harbouring a mutation at Pro1127 to Ala (Hellmuth et al., 2015) or PD-Separase (Cys2029 to Ser) (Stemmann et al., 2001), respectively. The IP was performed as described (see Chapter 4.4.7) using GFP-nanobody coupled beads for 3 h at 4°C and gentle rotation. After incubation the beads were washed once with LP2* and once with CSF-XB buffer (Murray, 1991). The beads with bound Separase-Securin complexes were further incubated with 10-20 CV of *Xenopus laevis* egg extracts/CSF-extracts (CSF-extracts were prepared as described (Murray, 1991)) for 30 min at 18°C. Extracts were supplemented with 500 nM recombinant $\Delta 90$ -Cyclin B1. and released into anaphase by adding calcium to mimic fertilization. $\Delta 90$ Cyclin B1 is due to its missing destruction box non-degradable, which prevents mitotic exit, therefore APC/C^{Cdc20}-activity remains high and Securin can be efficiently degraded (Stemmann et al., 2001). After incubation in CSF-extract, the beads-extract suspension was subsequently diluted with CSF-XB. Afterwards the beads were re-isolated (4 min, 4°C, 300 g), once washed with 10 CV CSF-XB, and once with 10 CV LP2 (importantly without protease inhibitors). Separase was then eluted by addition of TEV-protease for 20 min at RT, the eluate was further isolated via Mobicol microcolumns and microfilters with a pore size of 0,35 μm (MoBiTec). The final eluate was aliquoted á 20 μl , snap-frozen and stored at -80°C until use.

4.4.11 Coupled *in vitro* transcription and translation (IVTT)

For *in vitro* transcription/translation reactions (IVTTs), proteins were produced by a coupled transcription/translation system directly from expression plasmids. The pCS2-plasmids used here express the recombinant genes under the control of a SP6-promoter. For protein expression, the SP6-RNA-polymerase and the translational components of a reticulocyte lysate (TNT[®] SP6 Coupled Reticulocyte Lysate System, Promega) was used according to the

manufacturer's instructions in a total volume of 5-50 μl and 1 μg of plasmid DNA. For the radioactive labelling of the expressed protein ^{35}S -Methionine (Hartmann Analytic) was added. The reaction was performed for 90 min at 30 °C and stopped by snap-freezing. IVTTs were stored at -80°C until use.

4.4.12 *in vitro* kinase assay

For *in vitro* phosphorylation 1 μg of respective recombinant proteins were incubated in a total volume of 15 μl with 1x kinase buffer, 50 μM ATP and 1 μCi [γ - ^{33}P]-ATP. For respective "cold" reactions the radioactively labelled [γ - ^{33}P]-ATP was substituted with the same amount of ATP. When indicated 100 μM Roscovitine (CDK1-inhibitor), 5 μM ZM447439 (AurB-inhibitor), 100 nM BI2536 (Plk1-inhibitor) or the corresponding volume of the solvent DMSO was added. The reaction was incubated for 10-15 min at 30°C and afterwards stopped by either boiling with SDS-sample buffer (10 min, 98°C) or further processed (see Chapter 4.4.1).

For immediate analysis boiled samples were subjected to SDS-PAGE and the gel was subsequently fixed using fixation solution for 30 min. After fixation the gel was washed several times with ddH₂O for 10 min, afterwards the gel was carefully placed on a wet Whatman paper and dried using a vacuum drier ("Model 483", BioRad), for 90 min at 80°C. The dried gel was covered with an imaging plate (BAS-MS, FUJIFILM Europe), 12-48 h after exposure the imaging plate was analysed using a phosphoimager and corresponding software (FLA-7000; FUJIFILM Europe). For analysis of total amounts of protein, the gels were subjected to Coomassie staining and analysis as described (see chapter 4.4.3). After imaging the Coomassie stained gel was washed with ddH₂O, dried and analysed as described (see above).

4.4.13 *in vitro* cleavage assay

In order to analyse Separase-activity towards various substrates (see results), 2 μl of respective IVTTs (see chapter 4.4.11) were incubated with 2 μl of active Separase (see chapter 4.4.10) für 10 min at 30°C. For Sororin-inhibition assays 2 μl of active (or PD) Separase were previously incubated with 1 μg of recombinant protein for 5 min at 30°C, 2 μl of substrate proteins (IVTTs) were further added. After incubation for 10 min at 30°C the reaction was stopped by boiling with SDS sample buffer (10 min, 98°C). In case of analysis of

phosphorylation, recombinant proteins were first treated with respective kinases as described (see chapter 4.4.12). Addition of Separase and substrate proteins was performed as described.

4.5 Cell biological methods

4.5.1 Cell lines

HEK293T: human embryonic kidney cells, transformed with the SV40 large T-antigen

HeLa K: human cervix epithelial adenocarcinoma cells, subclone K

xS3: spontaneously immortalized cell line from *Xenopus laevis*, Nieuwkoop Faber (NF) stage 18 (blastula) (Nieuwkoop and Faber, 1968)

S2: Schneider 2 cells, semi-adherent, derived from a primary culture of late (20-24h old) *Drosophila melanogaster* embryos

4.5.2 Cultivation of mammalian cells

Mammalian monolayer cells were grown in cell culture dishes (Greiner Bio-One) in Dulbecco's modified Eagle Medium (DMEM, Biowest), supplemented with 10 % (v/v) heat-inactivated (30 min, 56°C) fetal calf serum (Biowest or Sigma). Optionally, a penicillin/streptomycin solution (1:100, Biowest) was added. Cells were kept at 37°C in a 5% CO₂ atmosphere and split in a ratio of 1:3 to 1:10 twice a week. To this end cells were carefully washed with 1x PBS. Cells were then incubated with pre-warmed trypsin/EDTA (Sigma) at 37 °C until they were easily detached from the cell culture dish. The addition of fresh pre-warmed medium stopped the reaction and was used to rinse the cells from the dish surface. The cell suspension was subsequently centrifuged (3 min, RT, 300 g). The cell pellet was resuspended and diluted using fresh pre-warmed medium and distributed on new cell culture dishes. Viable cell amounts were counted using a Vi-Cell counter (Beckman Coulter), if necessary.

4.5.3 Cultivation of *Xenopus* and *Drosophila* cells

Xenopus monolayer cells were grown in cell culture dishes (Greiner Bio-One) in Leibovitz Medium (Thermo Fisher), *Drosophila* cells were grown in cell culture dishes (Greiner Bio-One) in Schneider's *Drosophila* medium (Thermo Fisher), supplemented with 10 % (v/v) heat-inactivated (30 min, 56°C) fetal calf serum (Biowest or Sigma). Cells were kept at 28°C without CO₂ and split in a ratio of 1:3 to 1:10 twice a week. For splitting *Xenopus* cells, respective cells were carefully washed with 1x PBS. Cells were then incubated with trypsin/EDTA (Sigma) at RT until they were easily detached from the cell culture dish. The addition of fresh medium stopped the reaction and was used to rinse the cells from the dish surface. The cell suspension was subsequently centrifuged (3 min, RT, 300 g). The cell pellet was resuspended and diluted using fresh pre-warmed medium and distributed on new cell culture dishes. For splitting *Drosophila* cells, respective cells were detached from the dish surface by repeatedly rinsing with the current medium. The cell suspension was subsequently centrifuged (3 min, RT, 300 g), the cell pellet was resuspended and diluted using fresh pre-warmed medium and distributed on new cell culture dishes.

4.5.4 Storage of cells

Cells were harvested at 80% confluence for storage by trypsination as described (see chapter 4.5.2). The cell pellet was resuspended in freezing medium and aliquoted (1 ml) in round bottom cryo vials (Greiner Bio-One). Subsequently the cell suspension was slowly cooled to -80°C at a rate of 1°C/min in a cardboard box. For long term storage respective cryo vials were transferred to a liquid nitrogen tank.

In order to thaw a cryo stock, the respective vial was placed into a 37°C water bath (mammalian cells) or a RT water bath (*Xenopus* and *Drosophila* cells), centrifuged (3 min, RT, 300 g) and the supernatant was discarded to remove toxic DMSO. The cell pellet was resuspended in fresh pre-warmed medium and transferred to an appropriate cell culture dish containing fresh medium.

4.5.5 Transfection of cultured cells

HEK293T, *Xenopus* xS3 and *Drosophila* S2 cells were transfected at approximately 70-80% confluence using the calcium phosphate method (Graham & van der Eb, 1973). A few minutes

before transfection, chloroquine was added to the cells (25-50 μ M final concentration in the medium). The transfection mix was prepared according to the following overview:

diameter of dish	5.3 cm	10 cm	14.5 cm
volume of medium (in dish)	3.5 ml	9 ml	23 ml
amount of DNA	4 μ g	16 μ g	30 μ g
ddH₂O (add to)	300 μ l	800 μ l	2000 μ l
2 M CaCl₂	37.2 μ l	99.2 μ l	248 μ l
2x HBS	300 μ l	800 μ l	2000 μ l

DNA was first mixed with ddH₂O, afterwards 2 M CaCl₂ was added. 2x HBS was added slowly while low-speed vortexing. Within 10 min after HBS addition, the transfection mixture was carefully dripped onto the surface of the medium within ten min of preparation. 6-12 h after transfection, the medium was changed. Transfection of siRNA or a combination of siRNA and DNA was performed accordingly.

HeLa K cell's DNA were transfected at 60-70% confluency using the cationic polymer polyethylenimine (PEI, linear, MW 25,000, Polysciences). All reagents were brought to RT before preparing the transfection mixture. DNA was diluted in serum-free medium Gibco Opti-MEM (Reduced Serum Medium, Thermo Fisher) according to the following overview:

diameter of dish	2 cm	5.3 cm	10 cm	14.5 cm
medium	200 μ l	500 μ l	1 ml	2 ml
amount of DNA	3 μ g	5.5 μ g	8 μ g	12 μ g

The transfection mix was incubation at RT for 5 min, PEI was added at a ratio of 3:1 (PEI (μ g): DNA (μ g)) and incubated for 20 min at RT. The transfection mixture was afterwards dropped onto the surface of the medium. After 24-48 h (or if necessary), the medium was changed. Transfection of siRNA or a combination of siRNA and DNA was performed accordingly.

4.5.6 Synchronization of mammalian cells

In order to synchronize cells at the G1/S boundary thymidine was added to the culture medium to a final concentration of 2 mM (Sigma). After 16 h cells were released from the

thymidine-mediated arrest by washing once with 1x PBS and two more times with fresh pre-warmed medium for 20 min.

For a population of cells at the G2/M boundary, cells were harvested 8 h after release from a thymidine block.

To arrest cells in G2, cells were treated with RO3306 (Santa-Cruz) to a final concentration of 10 μ M 4 h after release from a thymidine block.

To arrest cells in prometaphase taxol (Calbiochem/Merck) was added to the culture medium to a final concentration of 0.2 μ g/ml for 14-16 h. For synchronization after a previous thymidine arrest, taxol was added 4 h after release.

4.5.7 Taxol-ZM-override

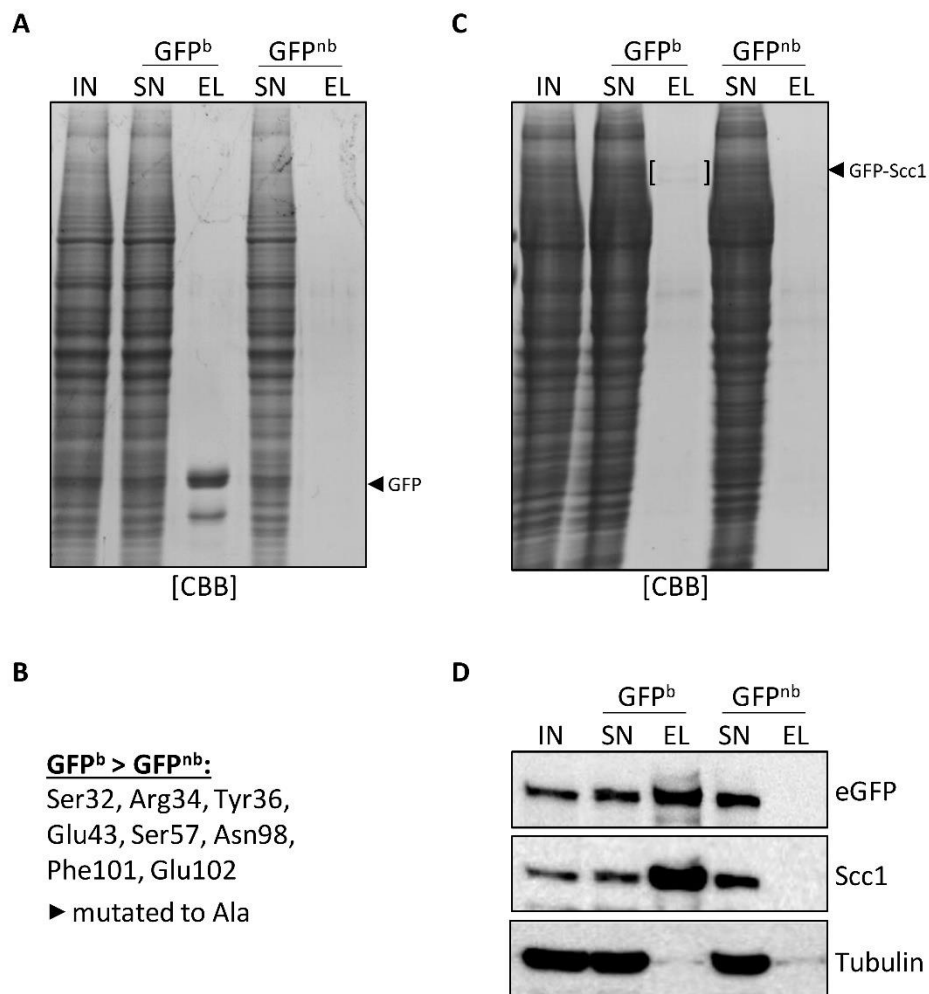
For time resolved experiments from prometaphase into a G1-like state using a taxol-ZM-override, cells were transfected with plasmid DNA 24 h before a thymidine block for 20 h. Cells were released from this first thymidine-block as described (see chapter 4.5.6) and a second thymidine block for 20 h was administered 8 h after cells were released from the first block. Taxol was added 4 h after release from the second thymidine block for 16 h. Afterwards cells were harvested: HEK293T cells were detached from the dish surface by repeatedly rinsing with the current medium. Mitotic HeLa K cells were detached by tapping the culture dish against a hard surface, loose cells were collected by collecting the current medium containing detached cells and additional rinsing the culture dish with fresh medium ("mitotic shake-off"). Harvested cells were centrifuged released into a pseudo-mitosis by evenly replating them into medium containing ZM447439 (Tocris, United Kingdom) to a final concentration of 5 μ M and subsequently harvested, washed and snap-frozen for further analysis by IP, SDS-PAGE and immunoblot. For flow cytometry experiments cells were fixed accordingly.

4.5.8 Quantitative analysis of cell cycle stages by flow cytometry

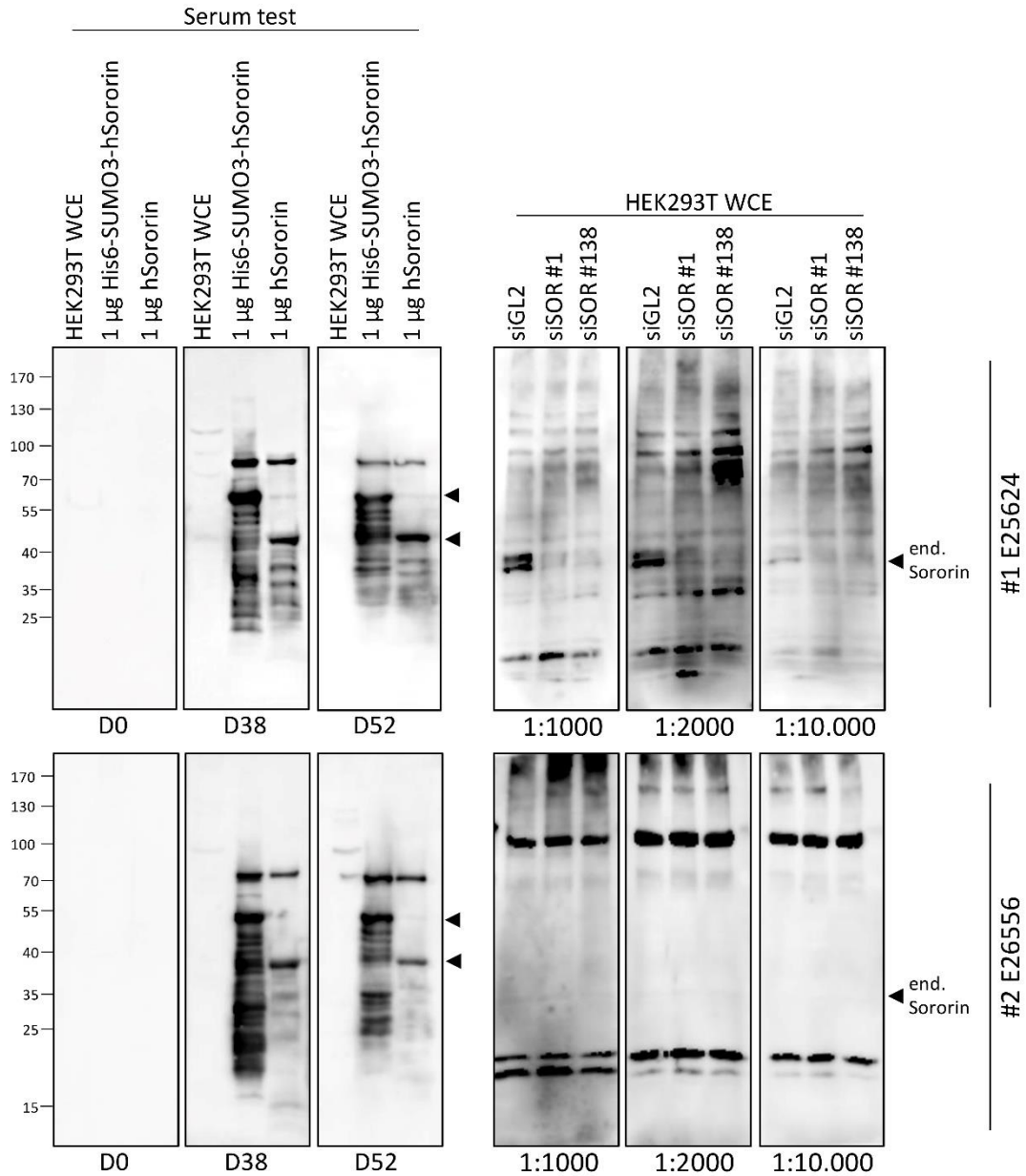
To define the cell cycle profile of a cell population, cells were harvested by trypsination from the corresponding cell culture dish and collected in a 15 ml tube. Subsequently cells were washed with 1x PBS (3 min, RT, 300 *g*), the pellet was resuspended in 200 μ l 1x PBS. For western blot analysis a sample of 20 μ l was boiled with SDS sample buffer (10 min, 98°C). Cells were fixed by dropwise addition of 7 ml ice cold 70% EtOH (-20°C) while vortexing and stored

for 1 h or o/n at -20°C. For analysis cells were washed twice with 10 ml PBS-B (5 min, RT, 300 *g*). DNA was stained by resuspending the cell pellet in 500 µl 69 µM propidium iodide (PI) solution (Sigma) in 38 mM tri-sodium citrate and supplemented with 100 µg/ml RNase A (Qiagen). After incubation of the cell suspension for 1 h at 37°C, cells were passed through nylon mesh (35 µm) integrated into the lid of a FACS tube (BD Biosciences). Cell cycle profiles were determined using a flow cytometer (Beckman Coulter Cytomics FC 500, Beckman Coulter) and corresponding CXP Analysis software (Beckman Coulter).

5 Supplement

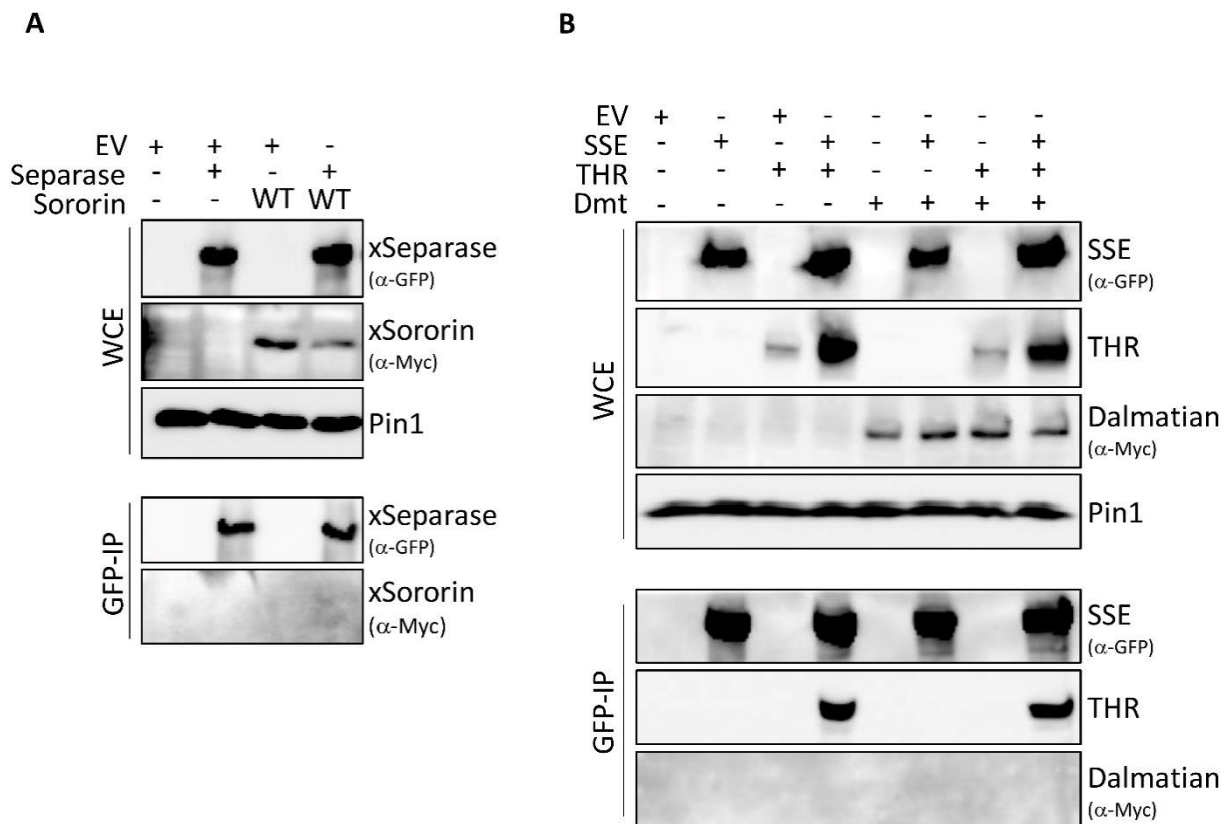


Supplement Figure 1 | Establishment of a non-binding GFP nanobody. HEK293T cells were transiently transfected with plasmids encoding either eGFP (A) or eGFP-Sccl (C, D). 48h after transfection cells were harvested and Input samples were collected. Cell lysates were subsequently incubated with bacterial expressed GFP binding or non-binding nanobodies covalently coupled to sepharose beads. After incubation a sample of the supernatant was collected, precipitated proteins were eluted by boiling of corresponding beads. Samples were analysed by SDS-PAGE and subsequent CBB-Staining (A, C) or immunoblot analysis using indicated antibodies in case of weakly purified eGFP-Sccl (D). (B) GFP non-binding nanobodies were prepared by mutating indicated residues (based on Kirchofer et al., 2010) to Ala. (b: binder, nb: non-binder, IN: input, SN: supernatant, EL: eluate, CBB: Coomassie brilliant blue)



Supplement Figure 2 | Establishment of two polyclonal rabbit antibodies raised against His6-SUMO3SororinFL.

Two rabbit sera (#1 E25624 top panel, #2 E26556 bottom panel) were tested for antigen recognition before inoculation (D0), after 38 days (D) and with the final bleed (D52) diluted 1:500 (left part). Non-manipulated WCEs from HEK293T cells were used for endogenous protein recognition, and 1 µg of each Sororin^{FL} with and without a His6-SUMO3-tag. Arrows indicate the respective recombinant proteins. Purified antibodies were tested using indicated dilutions (right). HEK293T cells were transfected with control siRNA targeting Luciferase as a control and two different siRNAs targeting Sororin (siSOR#1: Schmitz et al., 2007; siSOR#138: Wolf et al., 2018). Endogenous Sororin is marked with an arrowhead. E25624 was used for immunoblot analysis of endogenous and transiently expressed protein, however this antibody was not suitable for IP. E26556 was used for IP but not for immunoblot analysis. Neither antibody was able to successfully visualize Sororin in immunofluorescence microscopy (not shown)

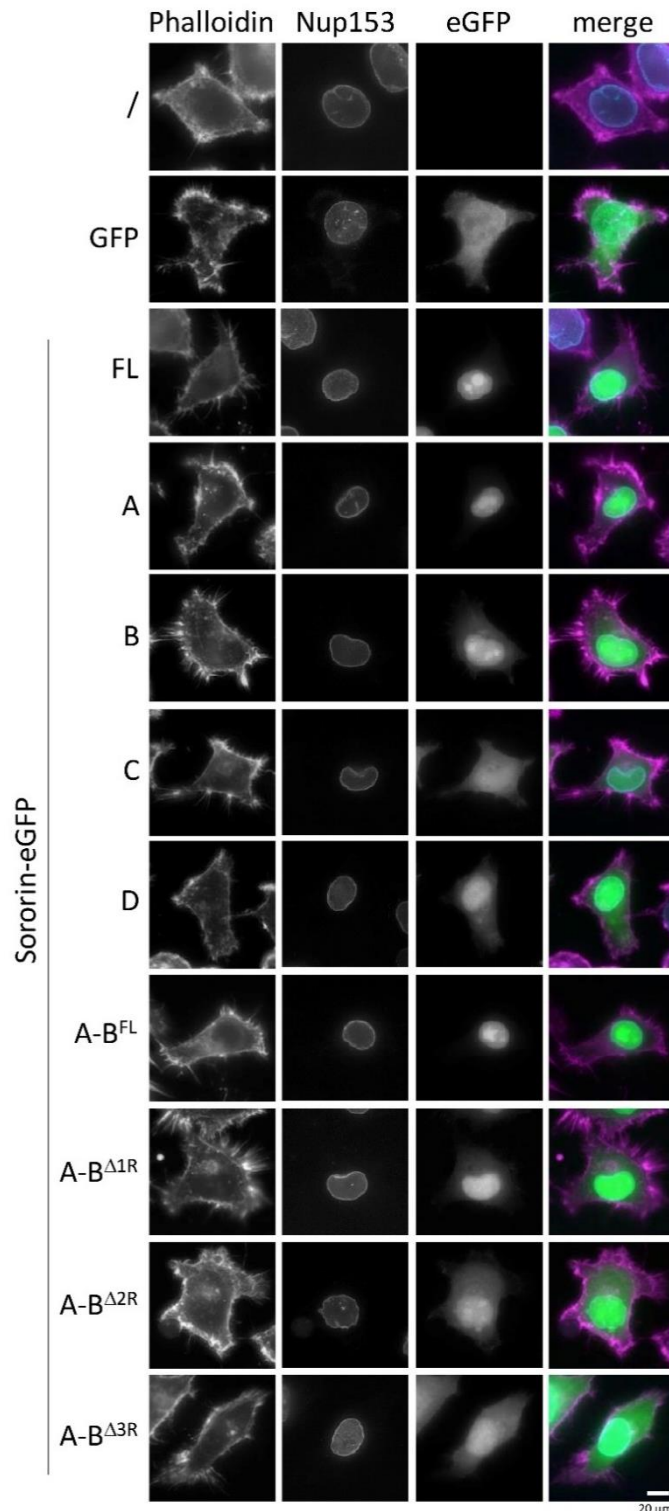


Supplement Figure 3 | Separase-Sororin complex formation is not conserved in *Xenopus* and *Drosophila*. (A) *Xenopus* S3 cells were transiently transfected with plasmids encoding either eGFP-xSeparase, xSororin-Myc or both combined, compared to EV transfected cells. Cells were arrested in mitosis approximately 36h after transfection by taxol treatment. Additional 14h later cells were either harvested. WCE's were boiled with SDS sample buffer and analysed by immunoblotting using the indicated antibodies. Subsequently, cell lysates were treated with Benzonase and incubated with GFP nanobody coupled beads. Precipitated proteins were eluted by boiling the beads in SDS sample buffer. Samples were analysed by immunoblotting using the indicated antibodies. (B) *Drosophila* S2 cells were transfected with plasmid DNA encoding GFP-tagged SSE, untagged THR or Myc-tagged Dmt and in combination as indicated compared to EV transfected cells. Cells were further analysed as described in (A). (x: *Xenopus*, EV: empty vector; antibodies used against tags are indicated in brackets).

A

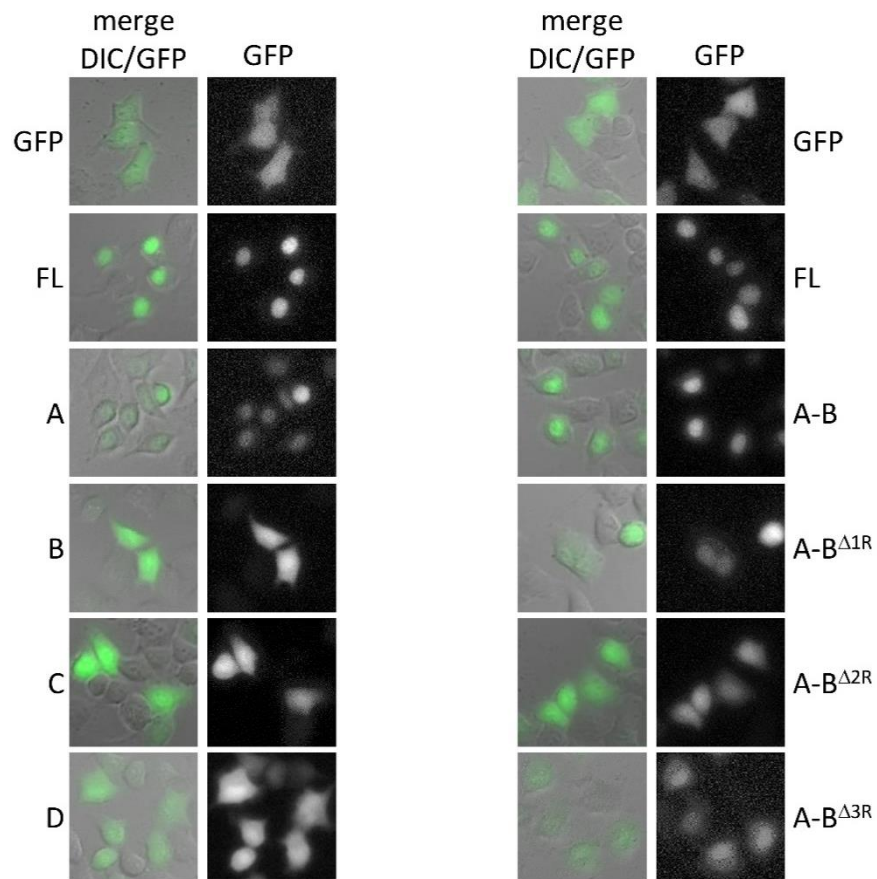


B



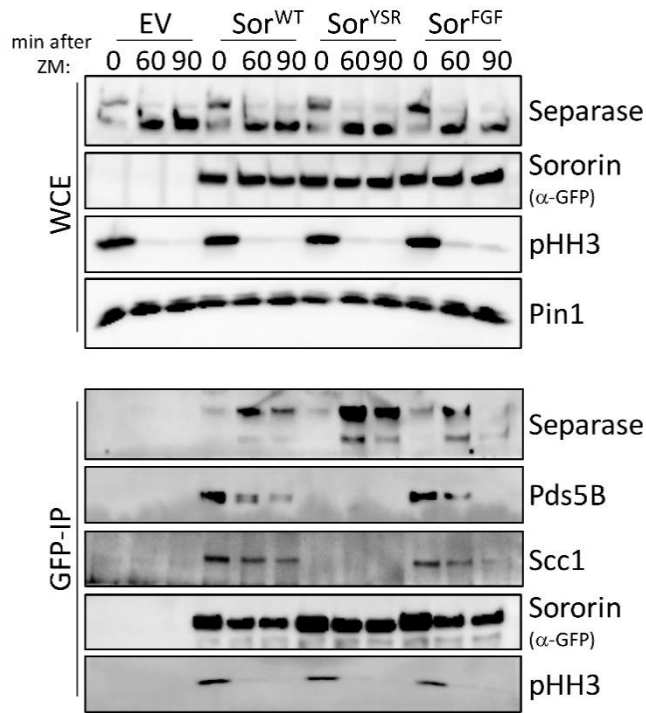
Supplement Figure 4 | Analyzing Sororin's N-terminus regarding a putative NLS. See next page for legend.

Supplement Figure 4 | Analyzing Sororin's N-terminus regarding a putative NLS. (A) Overview of the peptide sequence of Sororin Fragment A (Sor^A). R-rich regions, that were sequentially deleted are indicated by a dotted line. Since deletion up to $\Delta 3R$ would result in a very short peptide, Sororin was expressed in that context with fragment A and B (not pictured). (B) HEK29T cells were transiently transfected with plasmid DNA encoding eGFP-tagged Sororin fragments as indicated. After transfection (16h) cells were subjected to IFM and probed with indicated antibodies. Actin filaments were stained using Phalloidin. The scale bar represents 20 μm .

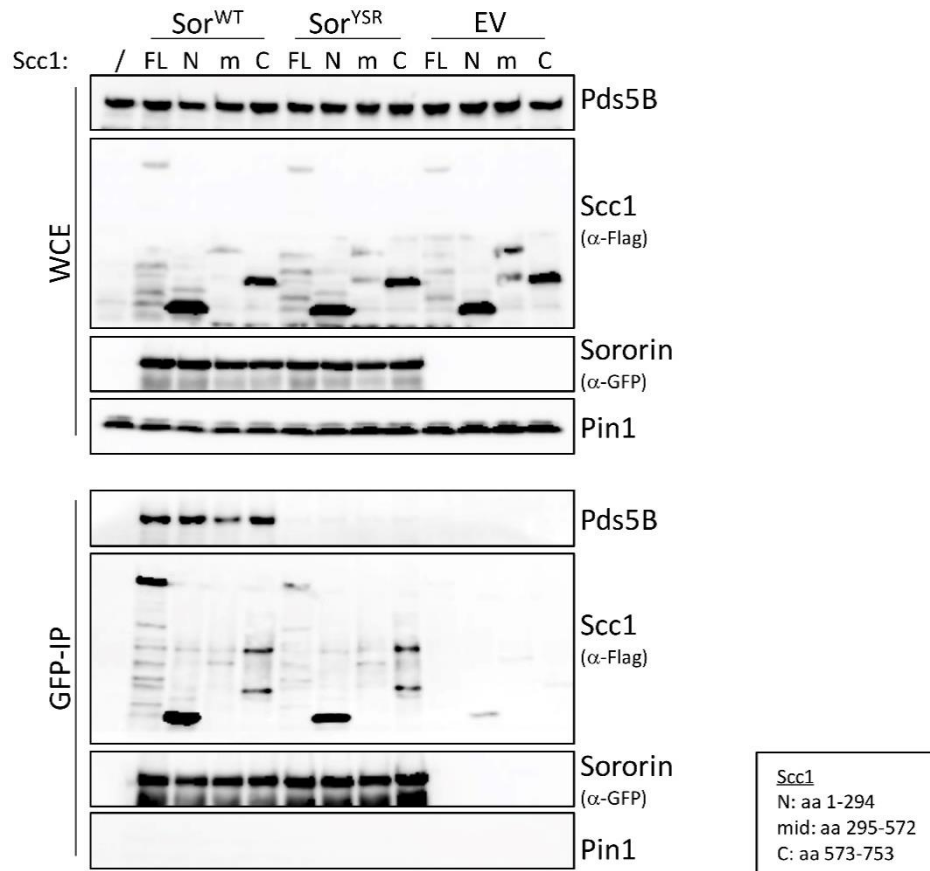


Supplement Figure 5 | Sororin's N-terminus acts as a putative NLS. HEK29T cells were transiently transfected with plasmid DNA encoding eGFP-tagged Sororin fragments as indicated. After transfection (16h) cells were subjected to analysis by live cell imaging. The scale bar represents 20 μ m.

A



B



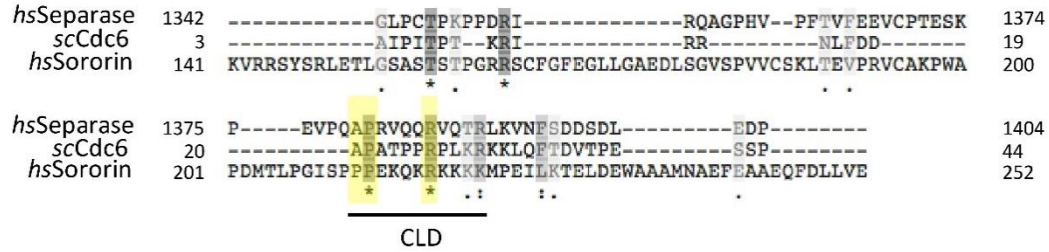
Supplement Figure 6 | Sororin interacts with Scc1 independently of Pds5. See next page for legend.

Supplement Figure 6 | Sororin interacts with Scc1 independently of Pds5. (A) HeLa K cells were transiently transfected with plasmids encoding C-terminally eGFP tagged Sororin variants as indicated compared to the EV. Cells were arrested in mitosis approximately 36h after transfection by taxol treatment. Additional 14h later cells were either harvested by mitotic shake-off (“0”) and partially further treated after shake-off with ZM for 60 min and 90 min (“60” and “90”). WCE’s were boiled with SDS sample buffer and analysed by immunoblotting using the indicated antibodies. Subsequently, cell lysates were treated with Benzonase and incubated with GFP nanobody coupled beads. Precipitated proteins were eluted by boiling the beads in SDS sample buffer. Samples were analysed by immunoblotting using the indicated antibodies (B) HeLa K cells were transiently transfected with plasmids encoding C-terminally eGFP tagged Sororin variants and Flag-tagged Scc1 fragments (/: empty vector, FL: full length, N-terminus (N): aa 1-294, middle part (mid): aa 295-572, C-terminus (C): aa 573-753) as indicated compared to the EV. Cells were arrested in mitosis approximately 36h after transfection by taxol treatment. Additional 14h later cells were either harvested and treated as described before (antibodies used against tags are indicated in brackets).

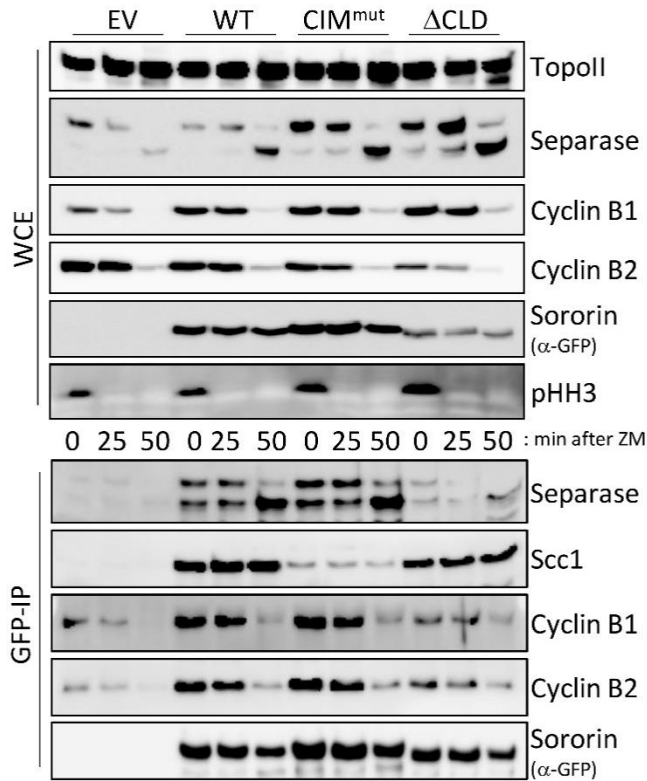
A



B



C



Supplement Figure 7 | Sororin interacts with Cyclin B1 via a putative CLD. See next page for legend.

Supplement Figure 7 | Sororin interacts with Cyclin B1 via a putative CLD. See next page for legend. (A) Sequence alignment of human Separase (aa 1342-1404) and yeast Cdc6 (aa 3-44). (B) Sequence alignment of human Separase (aa 1342-1404), yeast Cdc6 (aa 3-44) and human Sororin (aa 141-252). (A) & (B) Conserved residues are indicated by stars (*), conserved residues of a putative CLD are marked yellow, a putative CLD is underlined. (C) HeLa K cells were transiently transfected with plasmids encoding C-terminally eGFP tagged Sororin variants as indicated compared to the EV. Cells were arrested in mitosis approximately 36h after transfection by taxol treatment. Additional 14h later cells were either harvested by mitotic shake-off ("0") and partially further treated after shake-off with ZM for 25 min and 50 min ("25" and "50"). WCE's were boiled with SDS sample buffer and analysed by immunoblotting using the indicated antibodies. Subsequently, cell lysates were treated with Benzonase and incubated with GFP nanobody coupled beads. Precipitated proteins were eluted by boiling the beads in SDS sample buffer. Samples were analysed by immunoblotting using the indicated antibodies (mut: mutated, CIM: cyclin interacting motif, CLD: Cdc6-like domain; antibodies used against tags are indicated in brackets).

6 References

- Adams, P. D., Sellers, W. R., Sharma, S. K., Wu, A. D., Nalin, C. M., Kaelin, W. G. (1996).** Identification of a cyclin-cdk2 recognition motif present in substrates and p21-like cyclin-dependent kinase inhibitors. *Molecular and cellular biology* 16: 6623–6633.
- Agircan, F. G., Schiebel, E., Mardin, B. R. (2014).** Separate to operate: control of centrosome positioning and separation. *Philosophical transactions of the Royal Society of London. Series B, Biological sciences* 369. 1650: 20130461.
- Alexandru, G., Zachariae, W., Schleiffer, A., Nasmyth, K. (1999).** Sister chromatid separation and chromosome re-duplication are regulated by different mechanisms in response to spindle damage. *The EMBO journal* 18: 2707–2721.
- Anderson, D. E., Losada, A., Erickson, H. P., Hirano, T. (2002).** Condensin and cohesin display different arm conformations with characteristic hinge angles. *The Journal of cell biology* 156: 419–424.
- Aragón, L. (2018).** The Smc5/6 Complex: New and Old Functions of the Enigmatic Long-Distance Relative. *Annual review of genetics* 52: 89–107.
- Arumugam, P., Gruber, S., Tanaka, K., Haering, C. H., Mechtler, K., Nasmyth, K. (2003).** ATP hydrolysis is required for cohesin's association with chromosomes. *Current biology : CB* 13: 1941–1953.
- Bachmann, G., Richards, M. W., Winter, A., Beuron, F., Morris, E., Bayliss, R. (2016).** A closed conformation of the *Caenorhabditis elegans* separase-securin complex. *Open biology* 6: 160032.
- Beckouët, F., Hu, B., Roig, M. B., Sutani, T., Komata, M., Uluocak, P., Katis, V. L., Shirahige, K., Nasmyth, K. (2010).** An Smc3 acetylation cycle is essential for establishment of sister chromatid cohesion. *Molecular cell* 39: 689–699.
- Beckouët, F., Srinivasan, M., Roig, M. B., Chan, K.-L., Scheinost, J. C., Batty, P., Hu, B., Petela, N., Gligoris, T., Smith, A. C., Strmecki, L., Rowland, B. D., Nasmyth, K. (2016).** Releasing Activity Disengages Cohesin's Smc3/Sccl Interface in a Process Blocked by Acetylation. *Molecular cell* 61: 563–574.

- Bembenek, J. N., Richie, C. T., Squirrell, J. M., Campbell, J. M., Eliceiri, K. W., Poteryaev, D., Spang, A., Golden, A., White, J. G.** (2007). Cortical granule exocytosis in *C. elegans* is regulated by cell cycle components including separase. *Development (Cambridge, England)* 134: 3837–3848.
- Bembenek, J. N., White, J. G., Zheng, Y.** (2010). A role for separase in the regulation of RAB-11-positive vesicles at the cleavage furrow and midbody. *Current biology : CB* 20: 259–264.
- Boavida, A., Santos, D., Mahtab, M., Pisani, F. M.** (2021). Functional Coupling between DNA Replication and Sister Chromatid Cohesion Establishment. *International journal of molecular sciences* 22. 6: 2810.
- Boekhout, M., Wolthuis, R.** (2015). Nek2A destruction marks APC/C activation at the prophase-to-prometaphase transition by spindle-checkpoint-restricted Cdc20. *Journal of cell science* 128: 1639–1653.
- Boland, A., Martin, T. G., Zhang, Z., Yang, J., Bai, X.-C., Chang, L., Scheres, S. H. W., Barford, D.** (2017). Cryo-EM structure of a metazoan separase-securin complex at near-atomic resolution. *Nature structural & molecular biology* 24: 414–418.
- Borges, V., Lehane, C., Lopez-Serra, L., Flynn, H., Skehel, M., Rolef Ben-Shahar, T., Uhlmann, F.** (2010). Hos1 deacetylates Smc3 to close the cohesin acetylation cycle. *Molecular cell* 39: 677–688.
- Borton, M. T., Rashid, M. S., Dreier, M. R., Taylor, W. R.** (2016). Multiple Levels of Regulation of Sororin by Cdk1 and Aurora B. *Journal of cellular biochemistry* 117: 351–360.
- Buheitel, J., Stemmann, O.** (2013). Prophase pathway-dependent removal of cohesin from human chromosomes requires opening of the Smc3-Scc1 gate. *The EMBO journal* 32: 666–676.
- Bürmann, F., Lee, B.-G., Than, T., Sinn, L., O'Reilly, F. J., Yatskevich, S., Rappsilber, J., Hu, B., Nasmyth, K., Löwe, J.** (2019). A folded conformation of MukBEF and cohesin. *Nature structural & molecular biology* 26: 227–236.
- Bürmann, F., Shin, H.-C., Basquin, J., Soh, Y.-M., Giménez-Oya, V., Kim, Y.-G., Oh, B.-H., Gruber, S.** (2013). An asymmetric SMC-kleisin bridge in prokaryotic condensin. *Nature structural & molecular biology* 20: 371–379.

- Çamdere, G., Guacci, V., Stricklin, J., Koshland, D.** (2015). The ATPases of cohesin interface with regulators to modulate cohesin-mediated DNA tethering. *eLife* 4: e11315.
- Chai, J., Shiozaki, E., Srinivasula, S. M., Wu, Q., Datta, P., Alnemri, E. S., Shi, Y., Dataa, P.** (2001). Structural basis of caspase-7 inhibition by XIAP. *Cell* 104: 769–780.
- Chan, K.-L., Roig, M. B., Hu, B., Beckouët, F., Metson, J., Nasmyth, K.** (2012). Cohesin's DNA exit gate is distinct from its entrance gate and is regulated by acetylation. *Cell* 150: 961–974.
- Chapard, C., Jones, R., van Oepen, T., Scheinost, J. C., Nasmyth, K.** (2019). Sister DNA Entrapment between Juxtaposed Smc Heads and Kleisin of the Cohesin Complex. *Molecular cell* 75: 224-237.e5.
- Chatterjee, A., Zakian, S., Hu, X.-W., Singleton, M. R.** (2013). Structural insights into the regulation of cohesion establishment by Wpl1. *The EMBO journal* 32: 677–687.
- Chen, G., Deng, X.** (2018). Cell Synchronization by Double Thymidine Block. *Bio-protocol* 8. 17: e2994.
- Chen, M., Guerrero, A. D., Huang, L., Shabier, Z., Pan, M., Tan, T.-H., Wang, J.** (2007). Caspase-9-induced mitochondrial disruption through cleavage of anti-apoptotic BCL-2 family members. *The Journal of biological chemistry* 282: 33888–33895.
- Ciccia, A., Elledge, S. J.** (2010). The DNA damage response: making it safe to play with knives. *Molecular cell* 40: 179–204.
- Ciosk, R., Shirayama, M., Shevchenko, A., Tanaka, T., Toth, A., Nasmyth, K.** (2000). Cohesin's binding to chromosomes depends on a separate complex consisting of Scc2 and Scc4 proteins. *Molecular cell* 5: 243–254.
- Cipressa, F., Morciano, P., Bosso, G., Mannini, L., Galati, A., Raffa, G. D., Cacchione, S., Musio, A., Cenci, G.** (2016). A role for Separase in telomere protection. *Nature communications* 7: 10405.
- Collier, J. E., Lee, B.-G., Roig, M. B., Yatskevich, S., Petela, N. J., Metson, J., Voulgaris, M., Gonzalez Llamazares, A., Löwe, J., Nasmyth, K. A.** (2020). Transport of DNA within cohesin involves clamping on top of engaged heads by Scc2 and entrapment within the ring by Scc3. *eLife* 9: e59560.

Crasta, K., Huang, P., Morgan, G., Winey, M., Surana, U. (2006). Cdk1 regulates centrosome separation by restraining proteolysis of microtubule-associated proteins. *The EMBO journal* 25: 2551–2563.

Csizmok, V., Felli, I. C., Tompa, P., Banci, L., Bertini, I. (2008). Structural and dynamic characterization of intrinsically disordered human securin by NMR spectroscopy. *Journal of the American Chemical Society* 130: 16873–16879.

Davidson, I. F., Bauer, B., Goetz, D., Tang, W., Wutz, G., Peters, J.-M. (2019). DNA loop extrusion by human cohesin. *Science (New York, N.Y.)* 366: 1338–1345.

Diebold-Durand, M.-L., Lee, H., Ruiz Avila, L. B., Noh, H., Shin, H.-C., Im, H., Bock, F. P., Bürmann, F., Durand, A., Basfeld, A., Ham, S., Basquin, J., Oh, B.-H., Gruber, S. (2017). Structure of Full-Length SMC and Rearrangements Required for Chromosome Organization. *Molecular cell* 67: 334-347.e5.

DiNardo, S., Voelkel, K., Sternglanz, R. (1984). DNA topoisomerase II mutant of *Saccharomyces cerevisiae*: topoisomerase II is required for segregation of daughter molecules at the termination of DNA replication. *Proceedings of the National Academy of Sciences of the United States of America* 81: 2616–2620.

Dreier, M. R., Bekier, M. E., Taylor, W. R. (2011). Regulation of sororin by Cdk1-mediated phosphorylation. *Journal of cell science* 124: 2976–2987.

Eeftens, J. M., Katan, A. J., Kschonsak, M., Hassler, M., Wilde, L. de, Dief, E. M., Haering, C. H., Dekker, C. (2016). Condensin Smc2-Smc4 Dimers Are Flexible and Dynamic. *Cell reports* 14: 1813–1818.

Elbatsh, A. M. O., Haarhuis, J. H. I., Petela, N., Chopard, C., Fish, A., Celie, P. H., Stadnik, M., Ristic, D., Wyman, C., Medema, R. H., Nasmyth, K., Rowland, B. D. (2016). Cohesin Releases DNA through Asymmetric ATPase-Driven Ring Opening. *Molecular cell* 61: 575–588.

Fu, G., Xu, Z., Chen, X., Pan, H., Wang, Y., Jin, B. (2020). CDCA5 functions as a tumor promoter in bladder cancer by dysregulating mitochondria-mediated apoptosis, cell cycle regulation and PI3k/AKT/mTOR pathway activation. *Journal of Cancer* 11: 2408–2420.

Fukagawa, T., Earnshaw, W. C. (2014). The centromere: chromatin foundation for the kinetochore machinery. *Developmental cell* 30: 496–508.

Funabiki, H., Kumada, K., Yanagida, M. (1996). Fission yeast Cut1 and Cut2 are essential for sister chromatid separation, concentrate along the metaphase spindle and form large complexes. *The EMBO journal* 15: 6617–6628.

Gandhi, R., Gillespie, P. J., Hirano, T. (2006). Human Wapl is a cohesin-binding protein that promotes sister-chromatid resolution in mitotic prophase. *Current biology* : CB 16: 2406–2417.

Gautier, J., Minshull, J., Lohka, M., Glotzer, M., Hunt, T., Maller, J. L. (1990). Cyclin is a component of maturation-promoting factor from *Xenopus*. *Cell* 60: 487–494.

Georgatos, S. D., Pyrpasopoulou, A., Theodoropoulos, P. A. (1997). Nuclear envelope breakdown in mammalian cells involves stepwise lamina disassembly and microtubule-drive deformation of the nuclear membrane. *Journal of cell science* 110 (Pt 17): 2129–2140.

Gerlich, D., Koch, B., Dupeux, F., Peters, J.-M., Ellenberg, J. (2006). Live-cell imaging reveals a stable cohesin-chromatin interaction after but not before DNA replication. *Current biology* : CB 16: 1571–1578.

Gillespie, P. J., Hirano, T. (2004). Scc2 couples replication licensing to sister chromatid cohesion in *Xenopus* egg extracts. *Current biology* : CB 14: 1598–1603.

Gómez, R., Felipe-Medina, N., Ruiz-Torres, M., Berenguer, I., Viera, A., Pérez, S., Barbero, J. L., Llano, E., Fukuda, T., Alsheimer, M., Pendás, A. M., Losada, A., Suja, J. A. (2016). Sororin loads to the synaptonemal complex central region independently of meiotic cohesin complexes. *EMBO reports* 17: 695–707.

Graham, F. L., van der Eb, A. J. (1973). A new technique for the assay of infectivity of human adenovirus 5 DNA. *Virology* 52: 456–467.

Gruber, S., Arumugam, P., Katou, Y., Kuglitsch, D., Helmhart, W., Shirahige, K., Nasmyth, K. (2006). Evidence that loading of cohesin onto chromosomes involves opening of its SMC hinge. *Cell* 127: 523–537.

Gruber, S., Haering, C. H., Nasmyth, K. (2003). Chromosomal cohesin forms a ring. *Cell* 112: 765–777.

- Haering, C. H., Farcas, A.-M., Arumugam, P., Metson, J., Nasmyth, K. (2008).** The cohesin ring concatenates sister DNA molecules. *Nature* 454: 297–301.
- Haering, C. H., Löwe, J., Hochwagen, A., Nasmyth, K. (2002).** Molecular architecture of SMC proteins and the yeast cohesin complex. *Molecular cell* 9: 773–788.
- Haering, C. H., Schoffnegger, D., Nishino, T., Helmhart, W., Nasmyth, K., Löwe, J. (2004).** Structure and stability of cohesin's Smc1-kleisin interaction. *Molecular cell* 15: 951–964.
- Hara, K., Zheng, G., Qu, Q., Liu, H., Ouyang, Z., Chen, Z., Tomchick, D. R., Yu, H. (2014).** Structure of cohesin subcomplex pinpoints direct shugoshin-Wapl antagonism in centromeric cohesion. *Nature structural & molecular biology* 21: 864–870.
- Hauf, S., Waizenegger, I. C., Peters, J. M. (2001).** Cohesin cleavage by separase required for anaphase and cytokinesis in human cells. *Science (New York, N.Y.)* 293: 1320–1323.
- Hayes, M. J., Kimata, Y., Wattam, S. L., Lindon, C., Mao, G., Yamano, H., Fry, A. M. (2006).** Early mitotic degradation of Nek2A depends on Cdc20-independent interaction with the APC/C. *Nature cell biology* 8: 607–614.
- Heald, R., McKeon, F. (1990).** Mutations of phosphorylation sites in lamin A that prevent nuclear lamina disassembly in mitosis. *Cell* 61: 579–589.
- Heidinger-Pauli, J. M., Onn, I., Koshland, D. (2010).** Genetic evidence that the acetylation of the Smc3p subunit of cohesin modulates its ATP-bound state to promote cohesion establishment in *Saccharomyces cerevisiae*. *Genetics* 185: 1249–1256.
- Hellmuth, S., Gutiérrez-Caballero, C., Llano, E., Pendás, A. M., Stemmann, O. (2018).** Local activation of mammalian separase in interphase promotes double-strand break repair and prevents oncogenic transformation. *The EMBO journal* 37: e99184.
- Hellmuth, S., Pöhlmann, C., Brown, A., Böttger, F., Sprinzl, M., Stemmann, O. (2015).** Positive and negative regulation of vertebrate separase by Cdk1-cyclin B1 may explain why securin is dispensable. *The Journal of biological chemistry* 290: 8002–8010.
- Hellmuth, S., Rata, S., Brown, A., Heidmann, S., Novak, B., Stemmann, O. (2015).** Human chromosome segregation involves multi-layered regulation of separase by the peptidyl-prolyl-isomerase Pin1. *Molecular cell* 58: 495–506.

- Hellmuth, S., Gómez-H, L., Pendás, A. M., Stemmann, O.** (2020). Securin-independent regulation of separase by checkpoint-induced Shugoshin-MAD2. *Nature* 580: 536-541.
- Hellmuth, S., Stemmann, O.** (2020). Separase-triggered apoptosis enforces minimal length of mitosis. *Nature* 580: 542–547.
- Hertz, E. P. T., Kruse, T., Davey, N. E., López-Méndez, B., Sigurðsson, J. O., Montoya, G., Olsen, J. V., Nilsson, J.** (2016). A Conserved Motif Provides Binding Specificity to the PP2A-B56 Phosphatase. *Molecular cell* 63: 686–695.
- Higashi, T. L., Eickhoff, P., Sousa, J. S., Locke, J., Nans, A., Flynn, H. R., Snijders, A. P., Papageorgiou, G., O'Reilly, N., Chen, Z. A., O'Reilly, F. J., Rappsilber, J., Costa, A., Uhlmann, F.** (2020). A Structure-Based Mechanism for DNA Entry into the Cohesin Ring. *Molecular cell* 79: 917-933.e9.
- Hirano, M., Anderson, D. E., Erickson, H. P., Hirano, T.** (2001). Bimodal activation of SMC ATPase by intra- and inter-molecular interactions. *The EMBO journal* 20: 3238–3250.
- Hirano, T.** (2016). Condensin-Based Chromosome Organization from Bacteria to Vertebrates. *Cell* 164: 847–857.
- Ho, K. L., Ma, L., Cheung, S., Manhas, S., Fang, N., Wang, K., Young, B., Loewen, C., Mayor, T., Measday, V.** (2015). A role for the budding yeast separase, Esp1, in Ty1 element retrotransposition. *PLoS genetics* 11: e1005109.
- Holland, A. J., Böttger, F., Stemmann, O., Taylor, S. S.** (2007). Protein phosphatase 2A and separase form a complex regulated by separase autocleavage. *The Journal of biological chemistry* 282: 24623–24632.
- Holland, A. J., Taylor, S. S.** (2006). Cyclin-B1-mediated inhibition of excess separase is required for timely chromosome disjunction. *Journal of cell science* 119: 3325–3336.
- Holloway, S. L., Glotzer, M., King, R. W., Murray, A. W.** (1993). Anaphase is initiated by proteolysis rather than by the inactivation of maturation-promoting factor. *Cell* 73: 1393–1402.

- Hons, M. T., Huis in 't Veld, P. J., Kaesler, J., Rombaut, P., Schleiffer, A., Herzog, F., Stark, H., Peters, J.-M.** (2016). Topology and structure of an engineered human cohesin complex bound to Pds5B. *Nature communications* 7: 12523.
- Hornick, J. E., Bader, J. R., Tribble, E. K., Trimble, K., Breunig, J. S., Halpin, E. S., Vaughan, K. T., Hinchcliffe, E. H.** (2008). Live-cell analysis of mitotic spindle formation in taxol-treated cells. *Cell motility and the cytoskeleton* 65: 595–613.
- Hou, F., Zou, H.** (2005). Two human orthologues of Eco1/Ctf7 acetyltransferases are both required for proper sister-chromatid cohesion. *Molecular biology of the cell* 16: 3908–3918.
- Huis in 't Veld, P. J., Herzog, F., Ladurner, R., Davidson, I. F., Piric, S., Kreidl, E., Bhaskara, V., Aebersold, R., Peters, J.-M.** (2014). Characterization of a DNA exit gate in the human cohesin ring. *Science (New York, N.Y.)* 346: 968–972.
- Hwang, L. H., Lau, L. F., Smith, D. L., Mistrot, C. A., Hardwick, K. G., Hwang, E. S., Amon, A., Murray, A. W.** (1998). Budding yeast Cdc20: a target of the spindle checkpoint. *Science (New York, N.Y.)* 279: 1041–1044.
- Ivanov, D., Nasmyth, K.** (2005). A topological interaction between cohesin rings and a circular minichromosome. *Cell* 122: 849–860.
- Ivanov, D., Nasmyth, K.** (2007). A physical assay for sister chromatid cohesion *in vitro*. *Molecular cell* 27: 300–310.
- Ivanov, D., Schleiffer, A., Eisenhaber, F., Mechtler, K., Haering, C. H., Nasmyth, K.** (2002). Eco1 is a novel acetyltransferase that can acetylate proteins involved in cohesion. *Current biology* : CB 12: 323–328.
- Jäger, H., Herzig, A., Lehner, C. F., Heidmann, S.** (2001). *Drosophila* separase is required for sister chromatid separation and binds to PIM and THR. *Genes & development* 15: 2572–2584.
- Jäger, H., Herzig, B., Herzig, A., Sticht, H., Lehner, C. F., Heidmann, S.** (2004). Structure predictions and interaction studies indicate homology of separase N-terminal regulatory domains and *Drosophila* THR. *Cell cycle (Georgetown, Tex.)* 3: 182–188.

- Jallepalli, P. V., Waizenegger, I. C., Bunz, F., Langer, S., Speicher, M. R., Peters, J.-M., Kinzler, K. W., Vogelstein, B., Lengauer, C.** (2001). Securin Is Required for Chromosomal Stability in Human Cells. *Cell* 105: 445–457.
- Juan, G., Traganos, F., James, W. M., Ray, J. M., Roberge, M., Sauve, D. M., Anderson, H., Darzynkiewicz, Z.** (1998). Histone H3 phosphorylation and expression of cyclins A and B1 measured in individual cells during their progression through G2 and mitosis. *Cytometry* 32: 71–77.
- Kagey, M. H., Newman, J. J., Bilodeau, S., Zhan, Y., Orlando, D. A., van Berkum, N. L., Ebmeier, C. C., Goossens, J., Rahl, P. B., Levine, S. S., Taatjes, D. J., Dekker, J., Young, R. A.** (2010). Mediator and cohesin connect gene expression and chromatin architecture. *Nature* 467: 430–435.
- Kawashima, S. A., Yamagishi, Y., Honda, T., Ishiguro, K., Watanabe, Y.** (2010). Phosphorylation of H2A by Bub1 prevents chromosomal instability through localizing shugoshin. *Science (New York, N.Y.)* 327: 172–177.
- Kim, J., Ishiguro, K., Nambu, A., Akiyoshi, B., Yokobayashi, S., Kagami, A., Ishiguro, T., Pendas, A. M., Takeda, N., Sakakibara, Y., Kitajima, T. S., Tanno, Y., Sakuno, T., Watanabe, Y.** (2015). Meikin is a conserved regulator of meiosis-I-specific kinetochore function. *Nature* 517: 466–471.
- Kim, J.-S., Krasieva, T. B., LaMorte, V., Taylor, A. M. R., Yokomori, K.** (2002). Specific recruitment of human cohesin to laser-induced DNA damage. *The Journal of biological chemistry* 277: 45149–45153.
- Kim, Y., Shi, Z., Zhang, H., Finkelstein, I. J., Yu, H.** (2019). Human cohesin compacts DNA by loop extrusion. *Science (New York, N.Y.)* 366: 1345–1349.
- Kirchhofer, A., Helma, J., Schmidhals, K., Frauer, C., Cui, S., Karcher, A., Pellis, M., Muyldermans, S., Casas-Delucchi, C. S., Cardoso, M. C., Leonhardt, H., Hopfner, K.-P., Rothbauer, U.** (2010). Modulation of protein properties in living cells using nanobodies. *Nature structural & molecular biology* 17: 133–138.
- Kitajima, T. S., Kawashima, S. A., Watanabe, Y.** (2004). The conserved kinetochore protein shugoshin protects centromeric cohesion during meiosis. *Nature* 427: 510–517.

- Kitajima, T. S., Sakuno, T., Ishiguro, K., Iemura, S., Natsume, T., Kawashima, S. A., Watanabe, Y.** (2006). Shugoshin collaborates with protein phosphatase 2A to protect cohesin. *Nature* 441: 46–52.
- Kops, G. J. P. L., Weaver, B. A. A., Cleveland, D. W.** (2005). On the road to cancer: aneuploidy and the mitotic checkpoint. *Nature reviews. Cancer* 5: 773–785.
- Koshland, D., Hartwell, L. H.** (1987). The structure of sister minichromosome DNA before anaphase in *Saccharomyces cerevisiae*. *Science (New York, N.Y.)* 238: 1713–1716.
- Kosugi, S., Hasebe, M., Tomita, M., Yanagawa, H.** (2009). Systematic identification of cell cycle-dependent yeast nucleocytoplasmic shuttling proteins by prediction of composite motifs. *Proceedings of the National Academy of Sciences of the United States of America* 106: 10171–10176.
- Kraft, C., Herzog, F., Gieffers, C., Mechtler, K., Hagting, A., Pines, J., Peters, J.-M.** (2003). Mitotic regulation of the human anaphase-promoting complex by phosphorylation. *The EMBO journal* 22: 6598–6609.
- Kucej, M., Zou, H.** (2010). DNA-dependent cohesin cleavage by separase. *Nucleus (Austin, Tex.)* 1: 4–7.
- Kudo, N. R., Wassmann, K., Anger, M., Schuh, M., Wirth, K. G., Xu, H., Helmhart, W., Kudo, H., McKay, M., Maro, B., Ellenberg, J., Boer, P. de, Nasmyth, K.** (2006). Resolution of chiasmata in oocytes requires separase-mediated proteolysis. *Cell* 126: 135–146.
- Kueng, S., Hegemann, B., Peters, B. H., Lipp, J. J., Schleiffer, A., Mechtler, K., Peters, J.-M.** (2006). Wapl controls the dynamic association of cohesin with chromatin. *Cell* 127: 955–967.
- Ladurner, R., Kreidl, E., Ivanov, M. P., Ekker, H., Idarraga-Amado, M. H., Busslinger, G. A., Wutz, G., Cisneros, D. A., Peters, J.-M.** (2016). Sororin actively maintains sister chromatid cohesion. *The EMBO journal* 35: 635–653.
- Lafont, A. L., Song, J., Rankin, S.** (2010). Sororin cooperates with the acetyltransferase Eco2 to ensure DNA replication-dependent sister chromatid cohesion. *Proceedings of the National Academy of Sciences of the United States of America* 107: 20364–20369.

- Lange, A., McLane, L. M., Mills, R. E., Devine, S. E., Corbett, A. H.** (2010). Expanding the definition of the classical bipartite nuclear localization signal. *Traffic* (Copenhagen, Denmark) 11: 311–323.
- Lee, B.-G., Merkel, F., Allegretti, M., Hassler, M., Cawood, C., Lecomte, L., O'Reilly, F. J., Sinn, L. R., Gutierrez-Escribano, P., Kschonsak, M., Bravo, S., Nakane, T., Rappsilber, J., Aragon, L., Beck, M., Löwe, J., Haering, C. H.** (2020). Cryo-EM structures of holo condensin reveal a subunit flip-flop mechanism. *Nature structural & molecular biology* 27: 743–751.
- Lee, J., Kitajima, T. S., Tanno, Y., Yoshida, K., Morita, T., Miyano, T., Miyake, M., Watanabe, Y.** (2008). Unified mode of centromeric protection by shugoshin in mammalian oocytes and somatic cells. *Nature cell biology* 10: 42–52.
- Lehmann, A. R., Walicka, M., Griffiths, D. J., Murray, J. M., Watts, F. Z., McCready, S., Carr, A. M.** (1995). The rad18 gene of *Schizosaccharomyces pombe* defines a new subgroup of the SMC superfamily involved in DNA repair. *Molecular and cellular biology* 15: 7067–7080.
- Lengronne, A., McIntyre, J., Katou, Y., Kanoh, Y., Hopfner, K.-P., Shirahige, K., Uhlmann, F.** (2006). Establishment of sister chromatid cohesion at the *S. cerevisiae* replication fork. *Molecular cell* 23: 787–799.
- Li, M., York, J. P., Zhang, P.** (2007). Loss of Cdc20 causes a securin-dependent metaphase arrest in two-cell mouse embryos. *Molecular and cellular biology* 27: 3481–3488.
- Li, S., Yue, Z., Tanaka, T. U.** (2017). Smc3 Deacetylation by Hos1 Facilitates Efficient Dissolution of Sister Chromatid Cohesion during Early Anaphase. *Molecular cell* 68: 605-614.e4.
- Lin, Z., Luo, X., Yu, H.** (2016). Structural basis of cohesin cleavage by separase. *Nature* 532: 131–134.
- Lindqvist, A., Rodríguez-Bravo, V., Medema, R. H.** (2009). The decision to enter mitosis: feedback and redundancy in the mitotic entry network. *The Journal of cell biology* 185: 193–202.
- Liu, H., Rankin, S., Yu, H.** (2013). Phosphorylation-enabled binding of SGO1-PP2A to cohesin protects sororin and centromeric cohesion during mitosis. *Nature cell biology* 15: 40–49.

- Llano, E., Gómez, R., Gutiérrez-Caballero, C., Herrán, Y., Sánchez-Martín, M., Vázquez-Quiñones, L., Hernández, T., Alava, E. de, Cuadrado, A., Barbero, J. L., Suja, J. A., Pendás, A. M.** (2008). Shugoshin-2 is essential for the completion of meiosis but not for mitotic cell division in mice. *Genes & development* 22: 2400–2413.
- Lopez-Serra, L., Kelly, G., Patel, H., Stewart, A., Uhlmann, F.** (2014). The Scc2-Scc4 complex acts in sister chromatid cohesion and transcriptional regulation by maintaining nucleosome-free regions. *Nature genetics* 46: 1147–1151.
- Losada, A., Hirano, M., Hirano, T.** (1998). Identification of *Xenopus* SMC protein complexes required for sister chromatid cohesion. *Genes & development* 12: 1986–1997.
- Losada, A., Yokochi, T., Kobayashi, R., Hirano, T.** (2000). Identification and characterization of SA/Scc3p subunits in the *Xenopus* and human cohesin complexes. *The Journal of cell biology* 150: 405–416.
- Losada, A., Hirano, M., Hirano, T.** (2002). Cohesin release is required for sister chromatid resolution, but not for condensin-mediated compaction, at the onset of mitosis. *Genes & development* 16: 3004–3016.
- Losada, A., Yokochi, T., Hirano, T.** (2005). Functional contribution of Pds5 to cohesin-mediated cohesion in human cells and *Xenopus* egg extracts. *Journal of cell science* 118: 2133–2141.
- Luo, S., Tong, L.** (2018). Structural biology of the separase-securin complex with crucial roles in chromosome segregation. *Current opinion in structural biology* 49: 114–122.
- Luo, S., Tong, L.** (2021). Structure and Function of the Separase-Securin Complex. *Sub-cellular biochemistry* 96: 217–232.
- Maier, N. K., Ma, J., Lampson, M. A., Cheeseman, I. M.** (2020). Separase cleaves the kinetochore protein Meikin to direct the meiosis I/II transition. *bioRxiv*: 2020-11.
- Masui, Y., Markert, C. L.** (1971). Cytoplasmic control of nuclear behavior during meiotic maturation of frog oocytes. *The Journal of experimental zoology* 177: 129–145.

- Matsuo, K., Ohsumi, K., Iwabuchi, M., Kawamata, T., Ono, Y., Takahashi, M.** (2012). Kendrin is a novel substrate for separase involved in the licensing of centriole duplication. *Current biology* : CB 22: 915–921.
- McAleenan, A., Clemente-Blanco, A., Cordon-Preciado, V., Sen, N., Esteras, M., Jarmuz, A., Aragón, L.** (2013). Post-replicative repair involves separase-dependent removal of the kleisin subunit of cohesin. *Nature* 493: 250–254.
- McGuinness, B. E., Hirota, T., Kudo, N. R., Peters, J.-M., Nasmyth, K.** (2005). Shugoshin prevents dissociation of cohesin from centromeres during mitosis in vertebrate cells. *PLoS biology* 3: e86.
- McNicoll, F., Stevense, M., Jessberger, R.** (2013). Cohesin in gametogenesis. *Current topics in developmental biology* 102: 1–34.
- Melby, T. E., Ciampaglio, C. N., Briscoe, G., Erickson, H. P.** (1998). The symmetrical structure of structural maintenance of chromosomes (SMC) and MukB proteins: long, antiparallel coiled coils, folded at a flexible hinge. *The Journal of cell biology* 142: 1595–1604.
- Michaelis, C., Ciosk, R., Nasmyth, K.** (1997). Cohesins: chromosomal proteins that prevent premature separation of sister chromatids. *Cell* 91: 35–45.
- Mimura, S., Seki, T., Tanaka, S., Diffley, J. F. X.** (2004). Phosphorylation-dependent binding of mitotic cyclins to Cdc6 contributes to DNA replication control. *Nature* 431: 1118–1123.
- Minamino, M., Ishibashi, M., Nakato, R., Akiyama, K., Tanaka, H., Kato, Y., Negishi, L., Hirota, T., Sutani, T., Bando, M., Shirahige, K.** (2015). Esco1 Acetylates Cohesin via a Mechanism Different from That of Esco2. *Current biology* : CB 25: 1694–1706.
- Morales, C., Losada, A.** (2018). Establishing and dissolving cohesion during the vertebrate cell cycle. *Current opinion in cell biology* 52: 51–57.
- Muir, K. W., Li, Y., Weis, F., Panne, D.** (2020). The structure of the cohesin ATPase elucidates the mechanism of SMC-kleisin ring opening. *Nature structural & molecular biology* 27: 233–239.
- Murayama, Y., Uhlmann, F.** (2015). DNA Entry into and Exit out of the Cohesin Ring by an Interlocking Gate Mechanism. *Cell* 163: 1628–1640.

- Murray, A. W.** (1991). Chapter 30 Cell Cycle Extracts, pp. 581–605. *Methods in Cell Biology*, Elsevier. ISBN 9780125641364.
- Murray, A. W.** (2004). Recycling the Cell Cycle. *Cell* 116: 221–234.
- Musacchio, A.** (2015). The Molecular Biology of Spindle Assembly Checkpoint Signaling Dynamics. *Current biology : CB* 25: R1002-18.
- Nabti, I., Reis, A., Levasseur, M., Stemmann, O., Jones, K. T.** (2008). Securin and not CDK1/cyclin B1 regulates sister chromatid disjunction during meiosis II in mouse eggs. *Developmental biology* 321: 379–386.
- Nagao, K., Adachi, Y., Yanagida, M.** (2004). Separase-mediated cleavage of cohesin at interphase is required for DNA repair. *Nature* 430: 1044–1048.
- Nakamura, A., Arai, H., Fujita, N.** (2009). Centrosomal Aki1 and cohesin function in separase-regulated centriole disengagement. *The Journal of cell biology* 187: 607–614.
- Nasmyth, K.** (2002). Segregating sister genomes: the molecular biology of chromosome separation. *Science (New York, N.Y.)* 297: 559–565.
- Nasmyth, K., Haering, C. H.** (2009). Cohesin: its roles and mechanisms. *Annual review of genetics* 43: 525–558.
- Nishimura, K., Fukagawa, T., Takisawa, H., Kakimoto, T., Kanemaki, M.** (2009). An auxin-based degron system for the rapid depletion of proteins in nonplant cells. *Nature methods* 6: 917–922.
- Nishiyama, T., Ladurner, R., Schmitz, J., Kreidl, E., Schleiffer, A., Bhaskara, V., Bando, M., Shirahige, K., Hyman, A. A., Mechtler, K., Peters, J.-M.** (2010). Sororin mediates sister chromatid cohesion by antagonizing Wapl. *Cell* 143: 737–749.
- Nishiyama, T., Sykora, M. M., Huis in 't Veld, P. J., Mechtler, K., Peters, J.-M.** (2013). Aurora B and Cdk1 mediate Wapl activation and release of acetylated cohesin from chromosomes by phosphorylating Sororin. *Proceedings of the National Academy of Sciences of the United States of America* 110: 13404–13409.

- Onn, I., Aono, N., Hirano, M., Hirano, T.** (2007). Reconstitution and subunit geometry of human condensin complexes. *The EMBO journal* 26: 1024–1034.
- Orgil, O., Matityahu, A., Eng, T., Guacci, V., Koshland, D., Onn, I.** (2015). A conserved domain in the scc3 subunit of cohesin mediates the interaction with both mcd1 and the cohesin loader complex. *PLoS genetics* 11: e1005036.
- Ouyang, Z., Zheng, G., Song, J., Borek, D. M., Otwinowski, Z., Brautigam, C. A., Tomchick, D. R., Rankin, S., Yu, H.** (2013). Structure of the human cohesin inhibitor Wapl. *Proceedings of the National Academy of Sciences of the United States of America* 110: 11355–11360.
- Palecek, J., Vidot, S., Feng, M., Doherty, A. J., Lehmann, A. R.** (2006). The Smc5-Smc6 DNA repair complex. bridging of the Smc5-Smc6 heads by the KLEISIN, Nse4, and non-Kleisin subunits. *The Journal of biological chemistry* 281: 36952–36959.
- Panizza, S., Tanaka, T., Hochwagen, A., Eisenhaber, F., Nasmyth, K.** (2000). Pds5 cooperates with cohesin in maintaining sister chromatid cohesion. *Current biology : CB* 10: 1557–1564.
- Pauli, A., Althoff, F., Oliveira, R. A., Heidmann, S., Schuldiner, O., Lehner, C. F., Dickson, B. J., Nasmyth, K.** (2008). Cell-type-specific TEV protease cleavage reveals cohesin functions in *Drosophila* neurons. *Developmental cell* 14: 239–251.
- Pearlman, S. M., Serber, Z., Ferrell, J. E.** (2011). A mechanism for the evolution of phosphorylation sites. *Cell* 147: 934–946.
- Perera, D., Taylor, S. S.** (2010). Sgo1 establishes the centromeric cohesin protection mechanism in G2 before subsequent Bub1-dependent recruitment in mitosis. *Journal of cell science* 123: 653–659.
- Petela, N. J., Gligoris, T. G., Metson, J., Lee, B.-G., Voulgaris, M., Hu, B., Kikuchi, S., Chapard, C., Chen, W., Rajendra, E., Srinivisan, M., Yu, H., Löwe, J., Nasmyth, K. A.** (2017). Multiple interactions between Scc1 and Scc2 activate cohesin's DNA dependent ATPase and replace Pds5 during loading. *bioRxiv*: 205914.
- Petela, N. J., Gligoris, T. G., Metson, J., Lee, B.-G., Voulgaris, M., Hu, B., Kikuchi, S., Chapard, C., Chen, W., Rajendra, E., Srinivisan, M., Yu, H., Löwe, J., Nasmyth, K. A.** (2018). Scc2 Is a Potent Activator of Cohesin's ATPase that Promotes Loading by Binding Scc1 without Pds5. *Molecular cell* 70: 1134-1148.e7.

Pfleger, C. M., Kirschner, M. W. (2000). The KEN box: an APC recognition signal distinct from the D box targeted by Cdh1. *Genes & development* 14: 655–665.

Pfleghaar, K., Heubes, S., Cox, J., Stemmann, O., Speicher, M. R. (2005). Securin is not required for chromosomal stability in human cells. *PLoS biology* 3: e416.

Rankin, S., Ayad, N. G., Kirschner, M. W. (2005). Sororin, a substrate of the anaphase-promoting complex, is required for sister chromatid cohesion in vertebrates. *Molecular cell* 18: 185–200.

Riedel, C. G., Katis, V. L., Katou, Y., Mori, S., Itoh, T., Helmhart, W., Gálová, M., Petronczki, M., Gregan, J., Cetin, B., Mudrak, I., Ogris, E., Mechtler, K., Pelletier, L., Buchholz, F., Shirahige, K., Nasmyth, K. (2006). Protein phosphatase 2A protects centromeric sister chromatid cohesion during meiosis I. *Nature* 441: 53–61.

Roig, M. B., Löwe, J., Chan, K.-L., Beckouët, F., Metson, J., Nasmyth, K. (2014). Structure and function of cohesin's Scc3/SA regulatory subunit. *FEBS letters* 588: 3692–3702.

Roief Ben-Shahar, T., Heeger, S., Lehane, C., East, P., Flynn, H., Skehel, M., Uhlmann, F. (2008). Eco1-dependent cohesin acetylation during establishment of sister chromatid cohesion. *Science (New York, N.Y.)* 321: 563–566.

Rosen, L. E., Klebba, J. E., Asfaha, J. B., Ghent, C. M., Campbell, M. G., Cheng, Y., Morgan, D. O. (2019). Cohesin cleavage by separase is enhanced by a substrate motif distinct from the cleavage site. *Nature communications* 10: 5189.

Rothbauer, U., Zolghadr, K., Muyldermans, S., Schepers, A., Cardoso, M. C., Leonhardt, H. (2008). A versatile nanotrap for biochemical and functional studies with fluorescent fusion proteins. *Molecular & cellular proteomics : MCP* 7: 282–289.

Rowland, B. D., Roig, M. B., Nishino, T., Kurze, A., Uluocak, P., Mishra, A., Beckouët, F., Underwood, P., Metson, J., Imre, R., Mechtler, K., Katis, V. L., Nasmyth, K. (2009). Building sister chromatid cohesion: smc3 acetylation counteracts an antiestablishment activity. *Molecular cell* 33: 763–774.

Sánchez-Puig, N., Veprintsev, D. B., Fersht, A. R. (2005). Human full-length Securin is a natively unfolded protein. *Protein science : a publication of the Protein Society* 14: 1410–1418.

Schmitz, J., Watrin, E., Lénárt, P., Mechtler, K., Peters, J.-M. (2007). Sororin is required for stable binding of cohesin to chromatin and for sister chromatid cohesion in interphase. *Current biology* : CB 17: 630–636.

Schöckel, L., Möckel, M., Mayer, B., Boos, D., Stemmann, O. (2011). Cleavage of cohesin rings coordinates the separation of centrioles and chromatids. *Nature cell biology* 13: 966–972.

Schulman, B. A., Lindstrom, D. L., Harlow, E. (1998). Substrate recruitment to cyclin-dependent kinase 2 by a multipurpose docking site on cyclin A. *Proceedings of the National Academy of Sciences of the United States of America* 95: 10453–10458.

Schwartzman, J. B., Krimer, D. B., Van't Hof, J. (1984). The effects of different thymidine concentrations on DNA replication in pea-root cells synchronized by a protracted 5-fluorodeoxyuridine treatment. *Experimental cell research* 150: 379–389.

Shi, Y. (2002). Mechanisms of caspase activation and inhibition during apoptosis. *Molecular cell* 9: 459–470.

Shintomi, K., Hirano, T. (2009). Releasing cohesin from chromosome arms in early mitosis: opposing actions of Wapl-Pds5 and Sgo1. *Genes & development* 23: 2224–2236.

Shintomi, K., Takahashi, T. S., Hirano, T. (2015). Reconstitution of mitotic chromatids with a minimum set of purified factors. *Nature cell biology* 17: 1014–1023.

Silva, M. C. C., Powell, S., Ladstätter, S., Gassler, J., Stocsits, R., Tedeschi, A., Peters, J.-M., Tachibana, K. (2020). Wapl releases Scc1-cohesin and regulates chromosome structure and segregation in mouse oocytes. *The Journal of cell biology* 219 (4): e201906100.

Skibbens, R. V., Corson, L. B., Koshland, D., Hieter, P. (1999). Ctf7p is essential for sister chromatid cohesion and links mitotic chromosome structure to the DNA replication machinery. *Genes & development* 13: 307–319.

Skibbens, R. V. (2009). Establishment of sister chromatid cohesion. *Current biology*: CB 19: R1126-32.

- Srinivasan, M., Fumasoni, M., Petela, N. J., Murray, A., Nasmyth, K. A.** (2020). Cohesion is established during DNA replication utilising chromosome associated cohesin rings as well as those loaded de novo onto nascent DNAs. *eLife* 9: e56611.
- Srinivasan, M., Scheinost, J. C., Petela, N. J., Gligoris, T. G., Wissler, M., Ogushi, S., Collier, J. E., Voulgaris, M., Kurze, A., Chan, K.-L., Hu, B., Costanzo, V., Nasmyth, K. A.** (2018). The Cohesin Ring Uses Its Hinge to Organize DNA Using Non-topological as well as Topological Mechanisms. *Cell* 173: 1508-1519.e18.
- Stade, K., Ford, C. S., Guthrie, C., Weis, K.** (1997). Exportin 1 (Crm1p) is an essential nuclear export factor. *Cell* 90: 1041–1050.
- Stegmaier, M., Hoffmann, M., Baum, A., Lénárt, P., Petronczki, M., Krssák, M., Gürtler, U., Garin-Chesa, P., Lieb, S., Quant, J., Grauert, M., Adolf, G. R., Kraut, N., Peters, J.-M., Rettig, W. J.** (2007). BI 2536, a potent and selective inhibitor of polo-like kinase 1, inhibits tumor growth *in vivo*. *Current biology* : CB 17: 316–322.
- Stemmann, O., Zou, H., Gerber, S. A., Gygi, S. P., Kirschner, M. W.** (2001). Dual inhibition of sister chromatid separation at metaphase. *Cell* 107: 715–726.
- Stratmann, R., Lehner, C. F.** (1996). Separation of sister chromatids in mitosis requires the *Drosophila* pimples product, a protein degraded after the metaphase/anaphase transition. *Cell* 84: 25–35.
- Ström, L., Karlsson, C., Lindroos, H. B., Wedahl, S., Katou, Y., Shirahige, K., Sjögren, C.** (2007). Postreplicative formation of cohesion is required for repair and induced by a single DNA break. *Science (New York, N.Y.)* 317: 242–245.
- Ström, L., Lindroos, H. B., Shirahige, K., Sjögren, C.** (2004). Postreplicative recruitment of cohesin to double-strand breaks is required for DNA repair. *Molecular cell* 16: 1003–1015.
- Sullivan, M., Lehane, C., Uhlmann, F.** (2001). Orchestrating anaphase and mitotic exit: separase cleavage and localization of Slk19. *Nature cell biology* 3: 771–777.
- Sullivan, M., Hornig, N. C. D., Porstmann, T., Uhlmann, F.** (2004). Studies on substrate recognition by the budding yeast separase. *The Journal of biological chemistry* 279: 1191–1196.

- Sumara, I., Vorlaufer, E., Gieffers, C., Peters, B. H., Peters, J. M.** (2000). Characterization of vertebrate cohesin complexes and their regulation in prophase. *The Journal of cell biology* 151: 749–762.
- Sun, Y., Kucej, M., Fan, H.-Y., Yu, H., Sun, Q.-Y., Zou, H.** (2009). Separase is recruited to mitotic chromosomes to dissolve sister chromatid cohesion in a DNA-dependent manner. *Cell* 137: 123–132.
- Sun, Y., Yu, H., Zou, H.** (2006). Nuclear exclusion of separase prevents cohesin cleavage in interphase cells. *Cell cycle (Georgetown, Tex.)* 5: 2537–2542.
- Sundin, O., Varshavsky, A.** (1981). Arrest of segregation leads to accumulation of highly intertwined catenated dimers: dissection of the final stages of SV40 DNA replication. *Cell* 25: 659–669.
- Sutani, T., Kawaguchi, T., Kanno, R., Itoh, T., Shirahige, K.** (2009). Budding yeast Wpl1(Rad61)-Pds5 complex counteracts sister chromatid cohesion-establishing reaction. *Current biology : CB* 19: 492–497.
- Tang, Z., Shu, H., Qi, W., Mahmood, N. A., Mumby, M. C., Yu, H.** (2006). PP2A is required for centromeric localization of Sgo1 and proper chromosome segregation. *Developmental cell* 10: 575–585.
- Tang, Z., Sun, Y., Harley, S. E., Zou, H., Yu, H.** (2004). Human Bub1 protects centromeric sister-chromatid cohesion through Shugoshin during mitosis. *Proceedings of the National Academy of Sciences of the United States of America* 101: 18012–18017.
- Tarin, D.** (1968). Normal Table of *Xenopus laevis* (Daudin). *Journal of Anatomy* 103: 578.
- Tóth, A., Ciosk, R., Uhlmann, F., Galova, M., Schleiffer, A., Nasmyth, K.** (1999). Yeast cohesin complex requires a conserved protein, Eco1p(Ctf7), to establish cohesion between sister chromatids during DNA replication. *Genes & development* 13: 320–333.
- Tsou, M.-F. B., Stearns, T.** (2006). Mechanism limiting centrosome duplication to once per cell cycle. *Nature* 442: 947–951.

Tsou, M.-F. B., Wang, W.-J., George, K. A., Uryu, K., Stearns, T., Jallepalli, P. V. (2009). Polo kinase and separase regulate the mitotic licensing of centriole duplication in human cells. *Developmental cell* 17: 344–354.

Uhlmann, F., Lottspeich, F., Nasmyth, K. (1999). Sister-chromatid separation at anaphase onset is promoted by cleavage of the cohesin subunit Scc1. *Nature* 400: 37–42.

Uhlmann, F., Wernic, D., Poupart, M. A., Koonin, E. V., Nasmyth, K. (2000). Cleavage of cohesin by the CD clan protease separin triggers anaphase in yeast. *Cell* 103: 375–386.

Unal, E., Arbel-Eden, A., Sattler, U., Shroff, R., Lichten, M., Haber, J. E., Koshland, D. (2004). DNA damage response pathway uses histone modification to assemble a double-strand break-specific cohesin domain. *Molecular cell* 16: 991–1002.

Unal, E., Heidinger-Pauli, J. M., Kim, W., Guacci, V., Onn, I., Gygi, S. P., Koshland, D. E. (2008). A molecular determinant for the establishment of sister chromatid cohesion. *Science (New York, N.Y.)* 321: 566–569.

Unal, E., Heidinger-Pauli, J. M., Koshland, D. (2007). DNA double-strand breaks trigger genome-wide sister-chromatid cohesion through Eco1 (Ctf7). *Science (New York, N.Y.)* 317: 245–248.

Vaur, S., Feytout, A., Vazquez, S., Javerzat, J.-P. (2012). Pds5 promotes cohesin acetylation and stable cohesin-chromosome interaction. *EMBO reports* 13: 645–652.

Viadiu, H., Stemmann, O., Kirschner, M. W., Walz, T. (2005). Domain structure of separase and its binding to securin as determined by EM. *Nature structural & molecular biology* 12: 552–553.

Waizenegger, I. C., Hauf, S., Meinke, A., Peters, J. M. (2000). Two distinct pathways remove mammalian cohesin from chromosome arms in prophase and from centromeres in anaphase. *Cell* 103: 399–410.

Wang, Y., Ng, T.-Y. (2006). Phosphatase 2A negatively regulates mitotic exit in *Saccharomyces cerevisiae*. *Molecular biology of the cell* 17: 80–89.

Ward, G. E., Kirschner, M. W. (1990). Identification of cell cycle-regulated phosphorylation sites on nuclear lamin C. *Cell* 61: 561–577.

- Weitzer, S., Lehane, C., Uhlmann, F.** (2003). A model for ATP hydrolysis-dependent binding of cohesin to DNA. *Current biology* : CB 13: 1930–1940.
- Wendt, K. S.** (2017). Resolving the Genomic Localization of the Kollerin Cohesin-Loader Complex. *Methods in molecular biology* (Clifton, N.J.) 1515: 115–123.
- Wheeler, G. N., Brändli, A. W.** (2009). Simple vertebrate models for chemical genetics and drug discovery screens: lessons from zebrafish and *Xenopus*. *Developmental dynamics* : an official publication of the American Association of Anatomists 238: 1287–1308.
- Wirth, K. G., Wutz, G., Kudo, N. R., Desdouets, C., Zetterberg, A., Taghybeeglu, S., Seznec, J., Ducos, G. M., Ricci, R., Firnberg, N., Peters, J.-M., Nasmyth, K.** (2006). Separase: a universal trigger for sister chromatid disjunction but not chromosome cycle progression. *The Journal of cell biology* 172: 847–860.
- Wolf, P. G., Cuba Ramos, A., Kenzel, J., Neumann, B., Stemmann, O.** (2018). Studying meiotic cohesin in somatic cells reveals that Rec8-containing cohesin requires Stag3 to function and is regulated by Wapl and sororin. *Journal of cell science* 131: jcs212100.
- Wu, F. M., Nguyen, J. V., Rankin, S.** (2011). A conserved motif at the C terminus of sororin is required for sister chromatid cohesion. *The Journal of biological chemistry* 286: 3579–3586.
- Yamada, T., Tahara, E., Kanke, M., Kuwata, K., Nishiyama, T.** (2017). *Drosophila* Dalmatian combines sororin and shugoshin roles in establishment and protection of cohesion. *The EMBO journal* 36: 1513–1527.
- Yamagishi, Y., Honda, T., Tanno, Y., Watanabe, Y.** (2010). Two histone marks establish the inner centromere and chromosome bi-orientation. *Science (New York, N.Y.)* 330: 239–243.
- Yang, C., Hamamura, Y., Sofroni, K., Böwer, F., Stolze, S. C., Nakagami, H., Schnittger, A.** (2019). SWITCH 1/DYAD is a WINGS APART-LIKE antagonist that maintains sister chromatid cohesion in meiosis. *Nature communications* 10: 1755.
- Zhang, J., Shi, X., Li, Y., Kim, B.-J., Jia, J., Huang, Z., Yang, T., Fu, X., Jung, S. Y., Wang, Y., Zhang, P., Kim, S.-T., Pan, X., Qin, J.** (2008). Acetylation of Smc3 by Eco1 is required for S phase sister chromatid cohesion in both human and yeast. *Molecular cell* 31: 143–151.

References

Zhang, N., Coutinho, L. E., Pati, D. (2021). PDS5A and PDS5B in Cohesin Function and Human Disease. *International journal of molecular sciences* 22: 5868.

Zhang, N., Pati, D. (2012). Sororin is a master regulator of sister chromatid cohesion and separation. *Cell cycle (Georgetown, Tex.)* 11: 2073–2083.

7 Danksagung

Vielen Dank an:

- Prof. Dr. Olaf Stemmann für die Möglichkeit in seiner Arbeitsgruppe forschen zu dürfen. Für den unermüdlichen und ansteckenden wissenschaftlichen Enthusiasmus, für die stete Unterstützung im Labor, aber auch abseits der Wissenschaft und für die Freiheiten auch mal einfach ausprobieren zu dürfen. Manchmal erfolglos, manchmal umso erfolgreicher.
- allen aktuellen und ehemaligen Mitgliedern des Lehrstuhls für Ihre Unterstützung bei den kleinen und großen Herausforderungen der Wissenschaft, das zur Verfügung stellen von Reagenzien und Hilfsmitteln aller Art, sowie Erheiterungen im Alltag. Insbesondere Dr. Susanne Hellmuth und Dr. Peter Wolf für die Bereitstellung von Reagenzien, Zellen, Protokollen und Erfahrung.
- Prof. Dr. Stefan Heidmann und seinen „Fliegenschubsern“ (das sagt ihr selbst! ;) für zahlreiche lustige Momente und insbesondere Nina Vießmann für ihre Freundschaft, auch über das Labor hinaus.
- Markus Hermann für seine stete Geduld, unermüdliche (technische) Unterstützung und Freundschaft, auch nachts, am Wochenende und im Urlaub.
- ganz besonders Dr. Peter Wolf und Nina Vießmann für das Korrekturlesen dieser Arbeit
- alle ehemaligen Studenten für die gute Zusammenarbeit und häufig die Freundschaft über ihre Zeit an der Uni hinaus.
- Andreas Popp, dafür dass du immer für mich da bist und mich immer irgendwie zum Lachen bringst. Ich bin froh dich gefunden zu haben!

8 (Eidesstattliche) Versicherungen und Erklärungen

(§ 8 Satz 2 Nr. 3 PromO Fakultät)

Hiermit versichere ich eidesstattlich, dass ich die Arbeit selbstständig verfasst und keine anderen als die von mir angegebenen Quellen und Hilfsmittel benutzt habe (vgl. Art. 64 Abs. 1 Satz 6 BayHSchG).

(§ 8 Satz 2 Nr. 3 PromO Fakultät)

Hiermit erkläre ich, dass ich die Dissertation nicht bereits zur Erlangung eines akademischen Grades eingereicht habe und dass ich nicht bereits diese oder eine gleichartige Doktorprüfung endgültig nicht bestanden habe.

(§ 8 Satz 2 Nr. 4 PromO Fakultät)

Hiermit erkläre ich, dass ich Hilfe von gewerblichen Promotionsberatern bzw. –vermittlern oder ähnlichen Dienstleistern weder bisher in Anspruch genommen habe noch künftig in Anspruch nehmen werde.

(§ 8 Satz 2 Nr. 7 PromO Fakultät)

Hiermit erkläre ich mein Einverständnis, dass die elektronische Fassung der Dissertation unter Wahrung meiner Urheberrechte und des Datenschutzes einer gesonderten Überprüfung unterzogen werden kann.

(§ 8 Satz 2 Nr. 8 PromO Fakultät)

Hiermit erkläre ich mein Einverständnis, dass bei Verdacht wissenschaftlichen Fehlverhaltens Ermittlungen durch universitätsinterne Organe der wissenschaftlichen Selbstkontrolle stattfinden können.

.....
Ort, Datum, Unterschrift